To the Graduate Council:

I am submitting herewith a dissertation written by Sarita Rattanakunuprakarn entitled "Intermodal Freight Transportation Management: Life Cycle Benefit-Cost Analysis, Stochastic Facility Planning, and Reinforcement Learning for Container Movement." I have examined the final paper copy of this dissertation for form and content and recommend that it be accepted in partial fulfillment of the requirements for the degree of Doctor of Philosophy, with a major in Industrial and Systems Engineering.

Mingzhou Jin, Major Professor

We have read this dissertation
and recommend its acceptance:

Mingzhou Jin

Hugh Medal

Xueping Li

Hyun Kim

Accepted for the Council:

Dixie L. Thompson

Vice Provost and Dean of the Graduate School

To the Graduate Council:

I am submitting herewith a dissertation written by Sarita Rattanakunuprakarn entitled "Intermodal Freight Transportation Management: Life Cycle Benefit-Cost Analysis, Stochastic Facility Planning, and Reinforcement Learning for Container Movement." I have examined the final electronic copy of this dissertation for form and content and recommend that it be accepted in partial fulfillment of the requirements for the degree of Doctor of Philosophy, with a major in Industrial and Systems Engineering.

Mingzhou Jin, Major Professor

We have read this dissertation
and recommend its acceptance:

Mingzhou Jin

Hugh Medal

Xueping Li

Hyun Kim

Accepted for the Council:

Dixie L. Thompson

Vice Provost and Dean of the Graduate School

(Original signatures are on file with official student records.)

Intermodal Freight Transportation Management: Life Cycle Benefit-Cost Analysis, Stochastic Facility Planning, and Reinforcement Learning for Container Movement

A Dissertation Presented for the
Doctor of Philosophy
Degree
The University of Tennessee, Knoxville

Sarita Rattanakunuprakarn

May 2025

Acknowledgements

I would like to express my deepest gratitude to my advisor, Dr. Mingzhou Jin, for his continuous guidance and support throughout my Ph.D. journey. His mentorship has shaped not only my academic work but also the person I am today.

I would also like to sincerely thank my committee members—Dr. Xueping Li, Dr. Hugh Medal, and Dr. Hyun Kim—for their valuable insights and thoughtful feedback, which have been instrumental in shaping my dissertation.

I would like to extend my appreciation to the Thai government for granting me the opportunity and scholarship to pursue my graduate studies in the United States.

A special thank you to my family for raising me to be a strong, determined woman and for always believing in me, even from afar.

To Dr. Zeyu Liu, thank you for being by my side throughout all highs and lows. Your love, encouragement, and support have meant the world to me and given me the strength to keep going.

To all my supporters—my Thai friends in Knoxville, Ziwei Liu, Beau Groom, Samuel Affar, my labmates, roommates, and many others—thank you for filling my days with laughter, motivation, and companionship. You cheered me on, lifted me up, and made this journey so much more meaningful.

Abstract

This dissertation develops a comprehensive framework to study freight intermodal transportation, focusing on a holistic understanding of the interactions between trucks and railroads. The research is structured into three main chapters, dedicated to the following topics: life-cycle benefit-cost analysis, two-stage stochastic optimization of location-allocation problems, and stochastic optimization of container movement problems.

The first chapter conducts a comprehensive Life-Cycle Benefit-Cost Analysis (LBCA) comparison of highways and railroads to evaluate the nationwide impacts on economic, social, and environmental impacts across the life cycles of transport infrastructure and equipment. The study examines both actual and maximum capacity flows to identify cost-effective, sustainable investment options. This tool can support stakeholder-specific decision-making, depending on whether their goals prioritize specific impacts or broader impacts.

Chapter Two explores an important intermodal system case study of inbound freight in the U.S. Southwest region, which originates from California's San Pedro Bay port complex (SPPC). To improve system efficiency, we propose a strategy of expanding inland logistic centers for container classification across four states—California, Nevada, Arizona, and Utah. A two-stage mixed-integer stochastic programming model is developed to manage demand uncertainty, and sensitivity analyses are conducted to evaluate performance under varying cost and demand scenarios.

In Chapter Three, we extend the scope of the preceding model to capture the operational dynamics of inbound freight container movement within the SPPC intermodal system. This expanded model incorporates key factors such as container flow, mode selection, operational timing, and lead time considerations. The problem is formulated as a Markov Decision Process and solved using deep reinforcement learning techniques, including Deep Q-Learning and Advantage Actor-Critic. The goal is to minimize container dwell time at ports and warehouses, thereby increasing system efficiency, reducing transportation time and costs, and enhancing the overall resilience and adaptability of the intermodal logistics network. The trained models demonstrate the ability to learn effective container movement strategies, providing valuable decision support for planners seeking to optimize operations, reduce delays, and respond to fluctuating conditions.

Table of Contents

List of Tables

List of Figures

Chapter 1

Comparative Evaluation of Highways and Railroads Using Life-Cycle Benefit-Cost Analysis

This chapter is from a paper published in International Journal of Sustainable Transportation, authored by Sarita Rattanakunuprakarna, Mingzhou Jin, Michael Sussman, and Powell Felix (2024).

Abstract

The transportation sector significantly impacts our quality of life and the environment. Compared to rail transport, road transport has a higher likelihood of environmental and social problems. As increasing freight volume in the global supply chain grows the need for transportation activities, the current heavy reliance on road transport, combined with the under-utilization of the railway system, will prove inadequate to meet the escalating demand and exacerbate existing environmental and social concerns. Consequently, a complete comparison of transportation investment alternatives requires capturing these environmental and social, as well as economic, concerns in an interpretable and consistent way. This study develops a comprehensive Life-cycle Benefit-Cost Analysis and an accessible tool that captures overall nationwide impacts across various stages of transport infrastructure and equipment life cycles. We conduct a comparative evaluation of highways and railroads, considering both actual and theoretical maximum flows, to identify the most cost-effective and sustainable investment.

Keyword: Benefit-cost analysis, Life cycle assessment, Transportation cost, Railroads, Highways

1.1 Introduction

The highway system in the United States serves as the primary mode of transportation for freight and passengers. Currently, trucks handle a significant portion of domestic freight shipments, accounting for 72.2% in 2021 (Costello, 2022). However, the escalating issue of traffic congestion, driven by a multitude of factors such as urbanization, population expansion, insufficient infrastructure development, and the increasing dependence on personal vehicles and trucks, poses a critical challenge. This congestion results in extended travel times, elevated transportation expenses, reduced overall system dependability, and plays a substantial role in various environmental and social problems, particularly the emission of greenhouse gases and air pollution. The emissions released by these vehicles, such as carbon dioxide, nitrogen oxides, and particulate matter, significantly contribute to air pollution, leading to respiratory problems and environmental degradation. In addition to air quality issues, accidental spills of hazardous materials and improper waste disposal can contaminate water bodies, threatening aquatic ecosystems and potentially affecting drinking water supplies. Additionally, the increased use of trucks results in a higher accident rate on the roads, causing injuries and fatalities. The noise pollution emitted by these vehicles can also significantly impact the well-being of individuals living near major transportation routes. Research by Link et al. (2016) showed that noise pollution, road accidents, and wear and tear can be more significant than global warming, particularly during peak hours. Moreover, the growing demand for vehicles often prompts the expansion of the transportation network, leading to the destruction of natural habitats and ecosystems, including deforestation, habitat fragmentation, and loss of biodiversity.

Addressing these environmental concerns requires concerted efforts to promote sustainable transportation alternatives and reduce reliance on trucks. One sustainable and efficient alternative to highways is the rail system. Due to its considerable capacity and relatively consistent timetable, railroads contribute less to environmental and social impacts on a per-ton-mile basis. However, implementing such a system requires substantial investments in rail infrastructure, including constructing new tracks, upgrading existing ones, expanding the rail network for better coverage and accessibility, and establishing efficient handling facilities. Despite these challenges, the advantages of the rail system make it an attractive option for certain situations. For example, it can accommodate large volumes of goods and passengers, making it ideal for transporting heavy or bulk items over long distances. Additionally, it can effectively handle projected increases in freight volumes, which are anticipated to grow by 50% by 2050 (Solomon and Singer, 2021). In contrast, relying on trucks as the primary transportation mode would be inadequate to meet predicted demand while also exacerbating congestion and the existing shortage of 78,000 truck drivers, which is only slightly lower than the peak of 81,258 in 2021 (Premack, 2022). As an added benefit, the rail system maintains a more predictable schedule and ensures greater reliability for shippers and travelers than highways.

As previously discussed, the dominance of the highway system in the United States raises substantial concerns, underscoring the urgency of exploring alternatives, such as the rail system. When comparing transportation investment alternatives, it is crucial to consider not only the capital investment, operating, and maintenance costs, but also the environmental and social impacts of each mode. To evaluate these impacts, we propose a Life-Cycle Benefit-Cost Analysis (LBCA) method, which combines the Benefit-Cost Analysis (BCA) approach with life-cycle analysis. The LBCA method enables an interpretable and consistent evaluation of the economic efficiency of highway and railroad projects, capturing impacts across different stages of the transport infrastructure and equipment lifecycles. Our LBCA method encompasses a wide range of metrics, including land value, initial construction, operations, maintenance, traffic safety, congestion, greenhouse gas emissions, water quality, noise pollution, and wildlife vitality. By considering these metrics, we provide a comparative evaluation of highways and railroads in terms of their economic efficiency, measured in 2020 US dollar value per thousand ton-miles. We analyze two scenarios, actual flows and theoretical maximum flows, allowing for a comprehensive understanding of the potential benefits and costs of each mode. To facilitate the adoption of LBCA as a decision-making tool, we create a user-friendly Excel spreadsheet for interested parties. Our research highlights the importance of considering the full range of impacts associated with transportation investment alternatives. By utilizing the LBCA approach, decision-makers can make informed choices about sustainable and efficient transportation solutions. The integration of economic, environmental, and societal factors through LBCA ensures that transportation investments align with long-term sustainability goals while maximizing benefits and minimizing negative impacts.

1.2 Literature review

BCA is a powerful and extensively used tool for assessing the economic efficiency of various investment projects and policies in terms of their advantages and disadvantages. Benefits refer to the positive outcomes or advantages that result from implementing the project or policy. These can include increased productivity, improved safety and public health, enhanced environmental quality, or any other positive impacts. Costs, on the other hand, represent the expenses or sacrifices incurred in implementing the project or policy, such as construction costs, operational costs, or foregone opportunities. The BCA process typically involves several key steps. Firstly, the analyst identifies all relevant benefits and costs associated with the project or policy. This may require extensive data collection and analysis. Next, the analyst assigns monetary values to these benefits and costs, accounting for both short-term and long-term impacts. This step often involves estimating future costs and benefits and discounting them to present values. Once the benefits and costs are quantified, they are compared to determine the net benefits. One common application is assessing the economic returns associated with transportation infrastructure projects and determining preservation strategies for existing transportation assets. In addition to the financial impact, this standardized, systemic approach can also consider the environmental and social impacts of the project by quantifying these potential economic losses as monetary values. There are several BCA methodologies established by many organizations. The examples of BCA process guidelines include Puget Sound Regional Council BCA, Federal Aviation Authority Airport (FAA) BCA guidance, Transportation Investment Generating Economic

Recovery grants program, Washington State Department of Transportation freight rail benefit cost (Goodchild et al., 2014), the new Better Utilizing Investments to Leverage Development transportation discretionary grants program, Federal Highway Administration (FHWA) fright benefit cost, The American Association of State Highway and Transportation Officials benefit analysis for highways, The National Center for Fatality Review and Prevention freight transport BCA (Lee and Jin, 2020). **Table 1.1** summarizes factors commonly considered in BCA methodology.

Based on the literature review, it is clear that BCA has been used in infrastructure projects to make decisions regarding single transportation modes, to compare segregated transportation modes, and to evaluate multimodal transport. Various factors have been commonly evaluated for both rail and truck transportation modes, including capital cost, operational costs, transport time savings, reduction in the number of miles, traffic safety, reliability, maintenance cost, and environmental effects, such as air pollutant emission, noise emission, and climate endangerment. While BCA offers a valuable decision-making framework, it is important to acknowledge its limitations. Challenges in BCA arise at various stages of the methodology, starting with metric selection, which often varies significantly across research projects. Some papers only partially consider impacts across the economic, environmental, and social categories, and even among those papers, they tend to focus on specific phases of the lifecycle rather than adopting a holistic approach. Several factors contribute to this variation, including the inapplicability of certain metrics to certain projects and the unavailability of necessary data. For instance, when examining upstream activities in a product's lifecycle, such as raw material extraction and production, assessing associated impacts like environmental effects or financial costs can be intricate and challenging to determine. Time and budget also limit the scope of the analysis, as collecting the necessary data requires significant resources. BCA can be heavily dependent on predictive data, such as transportation patterns, traffic forecasts, project lifespan assessments, freight demands, and discount rates, all of

Table 1.1: Summary of BCA metrics.

Reference	Method	Categories	B/C Components
Bohmhold and Weiss (2015)	BCA	IC, ENV, LV, SO, ECON	Labor, materials, energy, labor and admin of assets, maintenance of assets and equipment, air pollution, pavement, safety, mobility, reliability
Dharmadhikari et al. (2016)	BCA	IC, OP, SO, ECON	Labor, materials, contractor, ROW, maintenance of assets and equipment, safety, congestion, mobility
Federal Railroad Administration (1990)	BCA	OP, ENV, SO, ECON	Maintenance of assets, end of life value, air pollution, employment, price of service, tax revenue, profit and revenues
Federal Railroad Association (2016)	BCA	IC, OP, ENV, SO, ECON	Capital cost, labor and admin of assets, maintenance of assets and equipment, air pollution, safety, connectivity, mobility
Goodchild et al. (2014)	BCA, Scorecard	IC, OP, ENV, LV, SO, ECON	Labor, materials, contractor, ROW, labor and admin of assets, maintenance of assets and equipment, energy sustainability, air pollution, noise, water, Land use changed the reduce VMT, safety, congestion, accessibility, employment, mobility, reliability, price of service, revenue
Gühnemann et al. (2012)	BCA, MCA	ENV, SO	Air pollution, noise, accessibility
Khattak et al. (2018)	BCA, ROI	OP, ENP, SO, ECON	Energy, energy sustainability, air pollution, noise, water, wildlife vitality, safety, congestion, accessibility, equity, property value, mobility, price of service
Korytárová and Papežíková (2015)	BCA	OP, ENV, SO, ECON	Labor and admin of assets, maintenance of assets and equipment, air pollution, noise, safety, congestion, employment, mobility
Lee and Jin (2020)	BCA, WEB	SO, ECON	Connectivity, accessibility, reliability

Table 1.1 Continued

Reference	Method	Categories	B/C Components
Leleur et al. (2007)	BCA, MCA	OP, ENV, SO, ECON	Labor and admin of assets, maintenance of assets and equipment, air pollution, noise, safety, connectivity, accessibility, mobility
Mascoop (2017)	BCA	IC, ENV, SO, ECON	Materials energy, labor and admin of assets, maintenance of assets, insurance, air pollution, safety, congestion, employment, capacity, mobility, tax revenue
Rezvani et al. (2015)	BCA	IC, OP, ENV, SO	Construction costs, maintenance of assets, air pollution, noise, safety, congestion
Siciliano et al. (2016)	BCA	IC, OP, ENV, SO, ECON	Labor, materials, energy, labor and admin of assets, maintenance of assets and equipment, insurance, air pollution, noise, water, wildlife vitality, nature and land scape (now in env), safety, congestion, urban effect, capacity, mobility
Spasovic et al. (2018)	BCA, Demand models	OP, ENV, SO, ECON	Energy, air pollution, safety, mobility
Tolliver and Lindamood (1993)	BCA	OP, LV, SO, ECON	Energy, labor cost, maintenance of assets, opportunity of investment, congestion, property value, mobility, price of service, profit and revenue, user profit
Walther et al. (2015)	BCA	IC, OP, ENV, SO, ECON	Materials, labor and admin of assets, air pollution, noise, safety, connectivity, accessibility, mobility, reliability, price of service

which could reduce the efficiency and accuracy of the project (Dharmadhikari et al., 2016; Korytárová and Papežíková, 2015). In addition, the performance of BCA can be affected by analyst decision criteria, especially when attempting to quantify metrics that are not easily monetized. In such cases, analysts may resort to qualitative descriptions or employ simpler calculations to quantify these metrics, such as willingness to pay, the extent of displeasure, and mitigation costs. As a result, personal judgment and experience play a significant role in these approaches, leading to a considerable dependence on them and making them susceptible to bias, uncertainty, and human error. Finally, another challenge is the tendency to overlook transparency after decisions are already made. It is crucial for the infrastructure options selected by evaluators to be publicly disclosed, recognized, and accepted to prevent potential opposition that could cause delays or rejections (Leleur et al., 2007). As a result, the outcomes of such research may not be interpretable, comparable, accessible, or applicable to new transportation systems or different scenarios.

To address all the above issues, it is necessary to develop a rigorous and structured LBCA that can better estimate the long-term impacts of a project while maintaining the attainability and robustness of the analysis. Our approach involves analyzing the life cycle of transportation infrastructure and equipment while identifying a comprehensive range of metrics that need to be considered to evaluate the overall impacts (such as economic, environmental, and financial) during various stages of the project's lifespan. In the next subsection, life cycle graphs and details will be provided to further explain the methodology and results of this analysis. By conducting a comprehensive LBCA, we can ensure that the impacts of transportation projects are accurately estimated and can be effectively compared to other potential projects or scenarios.

1.3 Proposed LBCA framework and calculation procedures

In attempting to embrace all potential benefits and costs that can emerge over the life cycles of transportation projects, we sort the components into two different graphs: the life cycle of the asset and the life cycle of the transportation equipment. LCA of the asset consists of five stages: 1) extraction, processing, or manufacturing, 2) construction, 3) operation, 4) maintenance and upgrading, and 5) end-of-life and recycling. For the LCA of transportation equipment, the stages are 1) extraction or processing, 2) manufacturing or construction, 3) operation, 4) maintenance and upgrading, and 5) end-of-life and recycling. The definition of infrastructure can cover several things, such as road surfaces, foundations, bridges, tunnels, tracks, stations, electrification, signaling, communication systems, and so on. For freight transportation equipment, highway transport systems include tractors and trailers while railroad transportation systems include locomotives and railcars.

To estimate the national benefits and costs for transportation projects, our value-based year is 2020. To better see the investment needs annually which align with the annual budget, we will evaluate life-cycle benefits and costs over a 35-year analysis period of highways and railroads using annual worth which is called the equivalent uniform annual cost (EUAC). Therefore, whenever we use present value we need to convert it using a 3% discount rate according to the Department of Transportation (DOT) recommends a 3% real discount rate for long-term analyses like this, deviating from the standard 7% rate (USDOT, 2022). Since this work is nationwide scale, we multiply the cost per mile by the total mileages of each transportation mode and then divide by the annual 2020 freight ton-miles carried by each transportation mode as represented in equation 1. Equation 1 will be used throughout this paper to estimate the EUAC of all the metrics.

$$\text{Equivalent Uniform Annual Cost (EUAC)} = \frac{\text{unit cost per mile} \times \text{mileage of the systems}}{\text{ton-miles of freight}}$$

Due to the factors discussed above in the literature review and defined life cycle stages, we have researched and assessed the currently available data, and we propose the following five LBCA metrics, including land use, initial construction, operating, environment, and social metrics.

1.3.1 Land use metric

This metric compares the highway and rail surface land acreage and the right-of-way needed by either mode to meet their transportation requirements. If no right-of-way exists for transportation infrastructure construction, land and right-of-way need to be acquired. The land use cost can be quantified using the land value factor up by the size of the area required for each project. The recent land value estimation published by the Bureau of Economic Analysis was conducted by Larson (2015), using data from 2000 to 2009. The total land values in 2009 were estimated to be worth $23 trillion for approximately 1.89 billion acres across the United States, which equals $12,169.31 per acre. This includes ecosystems (root systems such as alfalfa), basic siting improvements (fencing, irrigation, and land clearing), property value (households, businesses, and government), and land natural resources (timber, water, hunting, and fishing rights) (Larson, 2015). This estimated value is parcel-level data (at the census tract), which allows analysis of land areas by ownership sectors. The 2009 land value corresponds to a more recent study conducted by Nolte (2020), which introduces high-resolution maps depicting private land value. This study not only incorporates parcel-level data on ownership, price, and demographics, as previous research has done, but also factors in additional elements such as building footprints, terrain, accessibility, land cover, hydrography, and flood risk and protection. Since the values from both years are consistent and similar, we can assume that the 2009 land value estimated by Larson (2015) at $12,169.31 per acre remains valid for the year 2020, without the need for adjustment due to inflation rates.

The cost of right-of-way is shared among road users, including passenger cars, public transportation, and commercial transport vehicles, as they all utilize the same road space. This means that the cost will be divided and shared based on the space taken by each vehicle, which is measured in PCE (Passenger Car Equivalent). We based the cost responsibility of trucks on the case study of North Carolina's highway infrastructure, as outlined in the research of Hasnat et al. (2021). Starting from this juncture in the research, we will denote this concept as "truck cost allocation", encompassing vehicles ranging from Class 8 (i.e., 4AST or fewer axles with a single trailer) to Class 13 (i.e., 7AMT for seven or more axles with multi-trailers), in accordance with the FHWA vehicle classification system. After applying the truck cost allocation of 7.08% for right-of-way costs (Hasnat et al., 2021) to the present land value of $12,169.31 per acre, we obtained the land value of $862 per acre for the highway system.

In estimating the Equivalent Uniform Annual Cost (EUAC) over a 35-year analysis period for highways and railroads, we begin by converting the present land value of $862 per acre. For this long-term analysis, the DOT suggests a 3% real discount rate, differing from the standard 7% rate (USDOT, 2022).This results in an EUAC of $40.10 per acre per year across the 35-year lifecycle. Moving forward, we determine the required right-of-way area for each mode of transport. Assuming a standard width of 75 feet per lane (equivalent to 0.0142 miles per lane) for highways, we calculate an area requirement of 9.09 acres per lane mile by converting 0.0142 miles to space using a factor of 640. This estimation doesn't encompass auxiliary facilities like parking and gas stations; we consistently account for such aspects across research metrics. Consequently, the annual land cost is computed at $364.5 per lane mile or $729.05 per mile for a two-lane, single-way highway. Extending this assessment to the nation's freight volume, we multiply the $729.05 per mile by the total length of the U.S. national highway system of 161,188 miles (Federal Highway Administration, 2000) and divide by the total ton-miles transported by trucks in 2020 of 2,233,588,364,732 ton-miles (Bureau of Transportation Statistics, 2022a). This yields an EUAC of \$0.00005 per ton-mile for a two-lane, single-way highway and \$0.00011 per ton-mile for the four-lane, two-way national highway system.

In scenario two, with the U.S. highway freight system at its peak capacity of 12,943,396,400,000 ton-miles, as computed in A, the allocation of truck costs for the right-of-way expenditure would increase from 7.08% to 30.63%. This shift is based on the premise of escalating the annual highway volume from 2,233,588,364,732 to 12,943,396,400,000 ton-miles while retaining the passenger vehicle volume at its existing level. Consequently, the annual cost of land value per mile for a two-lane highway surges to \$3,154.03. Analogous to the scenario involving the actual freight volume, this cost is multiplied by the length of the national highway system and then by 2 to account for the transformation from a two-lane, single-way configuration to a four-lane configuration, after which it's divided by the estimated ton-mile of maximum flow. The resultant calculation yields an EUAC for land use in the context of maximum flow, amounting to \$0.000079 per ton-mile.

To estimate the EUAC attributed to land value for railroads, we employed the same national land value of \$12,169.31 per acre, while excluding train cost allocation considerations due to Class I railroads' ownership and operation of their freight railroad infrastructure. Assuming a 100-foot-wide railroad right-of-way (equivalent to 0.0189 miles), we determined a requirement of 12.12 acres per mile, excluding considerations for auxiliary facilities, terminals, bridges, and the like. After converting the national land value to an EUAC, the resulting EUAC for railroad land value was calculated at \$566 over 35 years. By multiplying the 12.12-acre right-of-way area by the land value cost of \$566 per acre, the EUAC land value amounted to \$6,865 per mile. Extending this assessment to the nation's railroad freight volume, the \$6,865 per mile value was multiplied by the Class I network road mileage, 92,190 miles (Association of American Railroads, 2021) and divided by the total ton-miles moved by railroads in 2020, 1,439,814,000,000 ton-miles (Bureau of Transportation Statistics, 2022b), resulting in an estimated EUAC for land use specific to the mainline railroad context of approximately $0.00044 per ton-mile.

Similarly, the EUAC cost per ton-mile can be determined by calculating the land value cost of $6,865 per mile, multiplying it by the Class I network road mileage of 92,190 miles, and then dividing the result by the estimated maximum flow of 24,059,285,250,000 ton-miles as computed in A. Consequently, the EUAC for land use in the context of maximum flow is assessed at $0.00003 per ton-mile for the mainline.

1.3.2 Initial construction metric

This measures factors affecting the capital costs of building transportation infrastructure, including material, labor, equipment, energy, land transformation, and related construction activities. The Washington State Department of Transportation published the national average construction cost of $2.3 million per lane-mile of a 1.02-mile diamond interchange project (WSDOT, 2002). This cost captures new alignments of four-lane structures, surfacing, paving, barriers, and pavement striping. We converted this 2002-dollar value into a 2020-dollar value by using the National Highway Construction Cost Index (NHCCI) 2.0 provided by Federal Highway Administration (2020). The result is $4,713,047 per lane mile in 2020 dollars. Then, we account for the cost allocation for trucks according to Hasnat et al. (2021) that trucks account for 35.87% of interstate new pavement construction costs. It is worth noting that this cost allocation is much higher than the cost allocation for land value. The logic for this comes from the impacts that trucks and other vehicles have on the infrastructure. For right-of-way, the cost allocation is based only on space taken by vehicles (PCE). However, for construction cost allocation, Hasnat et al. (2021) also consider the fact that heavy-duty trucks have a higher rate of deterioration in highway conditions. After applying this percentage, we obtained $1,690,570 per lane-mile. Since we consider four-lane highways, the cost is doubled to $3,381,140 per mile. After distributing this cost over 35 years, the EUAC of initial construction is estimated to be $157,356 per mile. The EUAC of initial construction per ton-mile across the nation's freight volume for highways is estimated by multiplying this EUAC of initial construction of $157,356 per mile by the total length of national highways at 161,188 miles and dividing by the total ton-miles of fright transported by trucks of 2,233,588,364,732 in 2020. Then, we double this result to derive the EUAC of initial construction of $0.0227 ton-mile for a four-lane, two-way highway.

To calculate the initial construction cost for the estimated maximum flow case, we recalculated the cost allocation for trucks by proportioning it with the estimated maximum freight volume. We obtain the cost allocation for new pavement construction cost which is increased from 35.87% to 76.42% compared to the actual flow given passenger vehicle volume remains the same. Consequently, the EUAC of initial construction of $157,356 per mile increased to $335,252 per mile for the maximum flow. Then, we estimate the EUAC of initial construction under maximum flow by multiplying the cost of $335,252 per mile by the total mileage of 161,188 miles and divided by the estimated maximum flow of 12,943,396,400,000 ton-miles. Then, we double the result to account for a four-lane, two-way highway system, resulting in $0.0083 ton-mile.

In most cases, ongoing roadway construction results in a partial or full road closure, which will cause delays, travel route change, increased risk of accidents, etc. The road user costs (RUC) quantifies the impacts of the construction for road users, including the increase of fuel cost, maintenance cost, tire wear cost, crash cost, depreciation cost, and finance charges. In addition, it also leads to the local impact cost which includes reduced business revenue in surrounding areas, and increased congestion of linked road networks. However, this cost is considered an indirect cost and generally neglected by state DOTs because of the complexity and intensive use of resources. The Tennessee Department of Transportation (TDOT) suggested including RUCs in the calculation method instead of only focusing on direct construction costs while appraising the best bidder. To determine whether RUCs should be included in contracts, the following criteria are ranked in descending order of influencing decision-making: the location, duration, complexity, and dollar value of the project (Shrestha et al., 2021). State DOTs tend to calculate the RUCs for high-traffic urban projects and projects that need to be completed in a short time to minimize impacts on road users (Shrestha et al., 2021). They conclude the daily RUC of $50,162.27 per day based on a case study in Sullivan County in Tennessee with a Length of work zone of 0.75 miles and a total highway of 5.37 miles. Using A+B contract evaluation, the daily RUC times the number of days to complete the construction which is the RUC of this specific project added to the estimated construction cost is estimated to be 237.53% of the construction cost. However, we cannot integrate this cost in our initial construction cost metric due to the national scale of the project which makes us unable to identify the length of construction side across the US highway system. We suggest that when practitioners apply our construction cost to their project, they should calibrate for this RUC adding to the construction cost only if they consider the project of building a new highway. To derive RUC for a project, analysts need to provide specific information for their construction zone, speed limit, original route length, detour length, and other traffic characteristics. The calculation procedure and tool can be found in the research of Shrestha et al. (2021).

As for freight railroad infrastructure in the United States, construction costs have not been widely disclosed. Blaze (2020) reported a construction cost of $3.5 to $4.5 million per mile for a single-track main line and an additional $1 to $1.5 million per mile to build a parallel second main track. The cost is roughly estimated from the costs of rails, ties, ballast, sub-compaction, and grading. Note that building a completely new track has greater costs than the common case in real situations, which is building new parallel tracks beside the existing tracks. However, this study considers only single-track lines based on the assumption that our benefit-cost analysis compares new infrastructure construction projects. After distributing a single-track construction cost of $4 million over 35 years, the EUAC of mainline construction is estimated to be $186,157 per mile with an inflation rate of 3%. We multiply this cost by the class I miles of road, which is 92,190 miles, and divide it by the actual ton-miles or estimated ton-miles, which are 1,439,814,000,000 and 24,059,285,250,000, respectively, to calculate the EUAC for the initial construction, resulting in \$0.012 per ton-mile for actual flow and \$0.001 per ton-mile for estimated maximum flow.

1.3.3 Operating metrics

These metrics encompass factors that influence operating costs and have impacts on the utilization and upkeep of transportation infrastructure and equipment. We have segmented this metric into six elements encompassing both benefits and costs: energy, labor and administrative expenses, maintenance of transportation infrastructure, end-of-life asset valuation, equipment expenditures, and maintenance of transportation equipment.

Energy

The cost associated with diesel fuel or energy used for transporting goods is a significant factor. According to a Texas A&M Transportation Institute report (Kruse et al., 2022), average fuel efficiencies were reported as 151 ton-miles per gallon for freight trucks and 472 ton-miles per gallon for freight railroads in 2019 at the national level. The fuel efficiency for trucks is based on combination truck data at the national level, as indicated in the BTS report. This is under the assumption of a truckload weighing 25 tons and maintaining the same speed on the empty return trip. Rail efficiency is drawn from national-level data primarily derived from the R-1 reports of the Surface Transportation Board and partially from sources within the railroad industry and the Securities and Exchange Commission. For the analysis, the average weekly diesel price from the EIA was taken as \$4.5 per gallon in 2022 (U.S. Energy Information Administration, 2022). With these inputs, we can proceed to calculate the EUAC of energy per ton-mile as follows:

$$
\begin{aligned}
\text{EUAC}_{\text{HW}} \text{ of energy} &= \frac{\text{avg fuel efficiency}}{\text{fuel prices}} \\
&= \frac{4.5(\$/\text{gallon})}{151(\text{ton-miles/ gallon})} \quad = 0.0298(\$/\text{ton-mile})
\end{aligned}
$$

$$
\begin{aligned}
\text{EUAC}_{\text{RR}} \text{ of energy} &= \frac{\text{avg fuel efficiency}}{\text{fuel prices}} \\
&= \frac{4.5(\$/\text{gallon})}{472(\text{ton-miles/ gallon})} = 0.0095(\$/\text{ton-mile})
\end{aligned}
$$

For this metric, we cannot provide the estimation of EUAC for the maximum flow scenario due to the lack of resources. New fuel consumption under the maximum flow scenario needs to be identified because it will vary depending on new traffic and operating characteristics such as operating weight, moving speed, and the fuel efficiency of vehicles.

Labor and administration

This metric assesses the labor and administrative costs associated with delivering the necessary transportation service, encompassing employee salaries, wages, and benefits. According to the American Transportation Research Institute (Leslie and Murray, 2021), the average compensation for drivers, including wages and benefits, amounted to $0.737 per mile in 2020. Respondents were able to choose benefits from a range of categories, such as health insurance, paid vacation, 401K, dental insurance, paid sick leave, vision insurance, and per diems. Notably, this figure does not encompass performance-based bonuses designed to attract talent, enhance safety practices, and improve driver retention. In order to compute the EUAC of driver compensation per ton-mile, we multiply the mean driver compensation per mile of $0.737 by the total truck vehicle miles, thereby establishing the total costs for the year 2020. We then divide this result by the total truck freight ton-miles for the year 2020. Consequently, the average driver compensation per ton-mile for the specific scenario in 2020 stands at $0.0997. Moreover, for the scenario of maximum flow—assuming that truck flows reach highway capacity—the corresponding value is calculated to be \$0.0369. These numerical values are derived through the subsequent calculations:

$$
\begin{aligned}
&\text{Actual EUAC}_{\text{HW}} \text{ of L\&A for actual flow} \\
&\qquad = \frac{\text{driver compensation} \times \text{truck vehicle miles}}{\text{ton-miles}} \\
&\qquad = \frac{0.737(\$/\text{mile}) \times 302,141,000,000(\text{mile})}{2,233,588,364,732(\text{ton-miles})} \\
&\qquad = 0.0997(\$/\text{ton-mile})
\end{aligned}
$$

$$
\begin{aligned}
&\text{Estimated EUAC}_{\text{HW}} \text{ of L\&A for maximum flow} \\
&\qquad = \frac{\text{driver compensation} \times \text{estimated truck vehicle miles}}{\text{estimated ton-miles}} \\
&\qquad = \frac{0.737(\$/\text{mile}) \times 698,943,405,600(\text{mile})}{12,943,396,400,000(\text{ton-miles})} \\
&\qquad = 0.0369(\$/\text{ton-mile})
\end{aligned}
$$

The average L&A cost during maximum truck flows in 2020 is notably 63% lower compared to actual flows, primarily due to the significantly higher truckload of 20 tons in the maximum flow scenario as opposed to the actual 7.39 tons. Diverging from truck carriers, railroads exhibit distinct L&A cost dynamics stemming from their lack of infrastructure ownership, exempting them from direct highway management expenses. Instead, railroads are encumbered by covering train conductor labor outlays and infrastructure management expenditures, with the operating costs outlined in the R-1 report (Surface Transportation Board, 2022). Using the BNSF R-1 report as an exemplar for Class I railroads, the calculated annual L&A cost amounted to \$7,343,009,000 for 2020. Notably, depreciation costs were excluded from this figure due to their non-cash flow nature, having been estimated primarily for tax purposes. Similar to the highway cost methodology, the EUAC under actual flow conditions, denoted in dollars per ton-mile, is computed by dividing the total annual cost by the annual ton-miles:

$$\begin{aligned}
&\text{Actual EUAC}_{\text{RR}} \text{ of L\&A for actual flow} \\
&\qquad = \frac{\text{BNSF labor and administration cost}}{\text{BNSF ton-miles}} \\
&\qquad = \frac{7,343,009,000(\$/\text{year})}{588,919,405,000(\text{ton-miles})} \\
&\qquad = 0.0125(\$/\text{ton-mile})
\end{aligned}$$

If we assume the railroads flows reach the BNSF maximum capacity (estimated in A), the average L&A cost per ton-mile for railroads in 2020 is estimated at \$0.0369 based on the following calculation. Again, the average L&A cost under maximum flows for railroads is about 70.86% lower than that under actual flows in 2020 because each train carries more tons under the maximum flow scenario.

$$\begin{aligned}
&\text{Estimated EUAC}_{\text{RR}} \text{ of L\&A for maximum flow} \\
&\qquad = \frac{\text{BNSF labor and administration cost}}{\text{estimated BNSF ton-miles}} \\
&\qquad = \frac{7,343,009,000(\$/\text{year})}{5,841,664,400,000(\text{ton-miles})} \\
&\qquad = 0.0013(\$/\text{ton-mile})
\end{aligned}$$

Maintenance of transportation infrastructure

This metric quantifies the cost of maintenance necessary to ensure the continued viability and safety of freight transportation, encompassing both material purchases and labor during the maintenance process. According to the ADOT's Roadway Maintenance Costs Report (Maricopa Association of Governments, 2019), the national average maintenance cost stood at \$28,020 per lane mile in 2015. This nationwide cost encompasses maintenance activities on interstates, freeways, highways, bridges, landscaping, lighting, and more. We adjusted this 2015 cost to 2020 using a 4% inflation rate, resulting in an EUAC of \$34,091 per lane mile for highways. For truck in-house maintenance cost allocation based on load-related expenses, Class 8 to Class 13 trucks accounted for an estimated 88.33% of the total interstate maintenance costs (Hasnat et al., 2021). These total costs were gathered from 2014 to 2017 for maintenance work performed by the NCDOT, covering activities such as asphalt overlay, patching, grading, drainage, shoulder repair, pavement markings, landscaping, sealing, slope protection, traffic control devices, ITS setup, and more (Hasnat et al., 2021). It's crucial to note that this in-house maintenance cost does not encompass external maintenance for major projects that involve contractors. By multiplying the EUAC of maintenance, $34,091 per lane mile, by the 88.33% cost allocation for trucks, we obtain an EUAC of truck maintenance cost at $30,112 per lane mile or $60,224 per mile for a two-lane highway. To convert this per-mile cost into per-ton-mile cost, we must multiply it by the system's length and divide it by annual ton-miles:

$$\begin{aligned}
&\text{Actual EUAC}_{\text{HW}} \text{ of asset maintenance for actual flow} \\
&\qquad = \frac{\text{annual maintenance cost} \times \text{national highway system}}{\text{actual ton-miles in 2020}} \\
&\qquad = \frac{60,224(\$/\text{mile}) \times 2 \times 161,188(\text{miles})}{2,233,588,364,732(\text{ton-miles})} \\
&\qquad = 0.0087(\$/\text{ton-mile})
\end{aligned}$$

As with any calculations involving truck cost allocations, the cost allocation will be increased from 88.33% to 97.93% when using maximum flow highway volume, assuming passenger vehicle volume remains the same. Therefore, the annual maintenance of transportation asset cost per mile for a two-lane highway increased to $66,661 and EUAC of maintenance cost can be assessed as follows:

$$
\begin{aligned}
&\text{Estimated EUAC}_{\text{HW}} \text{ of asset maintenance for maximum flow} \\
&= \frac{\text{annual maintenance cost} \times \text{national highway system}}{\text{estimated ton-miles}} \\
&= \frac{66,661(\$/\text{mile}) \times 2 \times 161,188(\text{miles})}{12,943,396,400,000(\text{ton-miles})} \\
&= 0.0017(\$/\text{ton-mile})
\end{aligned}
$$

For railroad maintenance costs, we sourced the BNSF annual repair and maintenance expenditure, totaling \$2,788,492,000, from the 2020 R-1 report (Surface Transportation Board, 2022). Maintenance costs encompass various elements, including wages, materials, tools, supplies, and fuel. We then divided this figure by BNSF's ton-miles in 2020, which amounted to 588,919,405,000. This calculation yielded an EUAC of \$0.0047 per ton-mile for freight railroads. In the case of maximum capacity operations, we lack data regarding potential increases in maintenance costs as we handle higher loads. Consequently, we assume that railroad maintenance costs will remain consistent with those of the actual scenario, which stands at \$0.0047 per ton-mile.

$$
\begin{aligned}
\text{Actual EUAC}_{\text{RR}} \text{ of asset maintenance} &= \frac{\text{annual maintenance cost}}{\text{actual ton-miles}} \\
&= \frac{2,788,492,000(\$/\text{year})}{588,919,405,000(\text{ton-miles})} \\
&= 0.0047(\$/\text{ton-mile})
\end{aligned}
$$

End of life asset value

This metric assesses the remaining value of transportation infrastructure after a 35-year analysis period, based on their functional life. The Federal Highway Administration (FHWA) recommends a minimum 35-year life cycle cost analysis period for new and repaired pavement projects (Walls and Smith, 2018). However, the Department of Transportation's (DOT) BCA guidance suggests that analysts limit the analysis scope to no more than 30 years and consider the remaining useful life when assets have lifetimes exceeding 35 years (USDOT, 2022). This shorter threshold is recommended because, in later years, the present value diminishes significantly due to discount rates and long-term cash flow predictions carry greater uncertainty, potentially affecting analysis credibility. Considering both recommendations, we have chosen a 35-year useful life for transportation assets and determined the remaining useful life at the analysis period's end. FHWA suggests calculating the salvage value based on the assumption that the remaining life of a transportation asset reflects a prorated cost of the last rehabilitation expenses (Walls and Smith, 2018). FHWA's major rehabilitation costs, as reported by Transportation for America (2019), were \$471,071 per lane-mile for concrete and \$211,761 for asphalt in 2017 dollars, gathered from six states, including California, Kansas, Michigan, Minnesota, Texas, and Washington. According to Sullivan (2006), 60% of the US highway interstate system consists of concrete. However, this doesn't apply to other road types primarily paved with asphalt. Therefore, we have decided to utilize the average cost between these two road types, which is \$341,416 per lane-mile. Converting this value to 2020 dollars with a 4% inflation rate, we have an average rehabilitation cost of \$384,047. Assuming the last rehabilitation occurs in the 30th year, and the analysis period concludes at 35 years, the asset's remaining life is 10 years, assuming that rehabilitation extends the end-of-life period by 15 years. Consequently, the salvage value can be calculated as 10/15 of \$384,047, which equals \$256,031 per lane-mile at the end of the lifecycle. Calculating the EUAC of salvage value, we determine that the annual salvage value over 35 years is \$11,915.5 per lane-mile. Given that we are considering a four-lane, two-way highway system, we multiply this value per lane-mile by 4 to obtain the total salvage cost per mile for our analyzed system. Subsequently, we can evaluate the actual EUAC of salvage value in dollars per ton-mile using the following formula:

$$
\begin{aligned}
\text{Actual EUAC}_{\text{HW}} & \text{ of asset salvage value} \\
&= \frac{\text{annual salvage value} \times \text{national highway system}}{\text{actual ton-miles in 2020}} \\
&= \frac{11,915.5(\$/\text{lane-mile}) \times 4(\text{lane}) \times 161,188(\text{miles})}{2,233,588,364,732(\text{ton-miles})} \\
&= 0.00344(\$/\text{ton-mile})
\end{aligned}
$$

In the scenario of maximum capacity, there is a lack of data regarding deterioration rates or any potential increase in the frequency of rehabilitation when trucks carry heavier loads. Consequently, we assume that the salvage value will remain consistent with that of the actual scenario.

For determining railroad salvage value, we utilize annual rail depreciation data from the 2020 BNSF R-1 report (Surface Transportation Board, 2022). At the beginning of 2020, the depreciation cost was $55,643,790,000, and at the end of the year, it amounted to $57,024,412,000. The difference between these values is $1,380,622,000. Dividing this by BNSF's route-miles gives us $1,380,622,000/22,384 = $61,679 per route-mile per year. Employing the straight-line depreciation method, we calculate the initial construction cost minus the total salvage value over 35 years as $4,000,000 – ($61,679 x 35 years). Consequently, the salvage value of the railroad asset at the end of its lifecycle is $1,841,236 per route-mile. To determine the annual worth, considering the future worth (salvage value at the end of the 35th year), the EUAC of salvage value after 35 years amounts to $30,453 per route-mile in present value, with a 3% discount factor. Finally, we compute the EUAC of salvage value (SV) in dollars per ton-mile using the following formula:

$$
\begin{aligned}
&\text{Actual } \mathrm{EUAC}_{\mathrm{RR}} \text{ of asset salvage value} \\
&\qquad = \frac{\text{annual salvage value} \times \text{BNSF miles of road}}{\text{actual BNSF ton-miles}} \\
&\qquad = \frac{30,453(\$/\text{route-mile}) \times 22,384(\text{route-miles})}{588,919,405,000(\text{ton-miles})} \\
&\qquad = 0.0012(\$/\text{ton-mile})
\end{aligned}
$$

Similar to the scenario of maximum capacity described earlier, we lack data on the potential deterioration rate and increased rehabilitation frequency resulting from higher loads. Consequently, we assume that in the estimated maximum flow case, the depreciation cost remains constant, resulting in the same salvage value of \$0.0012 per ton-mile. It's important to note that the current depreciation cost is influenced by aging infrastructure and the operation of trains. Thus, BNSF's annual depreciation may appear higher compared to the calculation for a new project with fresh infrastructure and equipment. This assumption suggests that the additional payload does not significantly accelerate equipment deterioration and is primarily intended for rough estimations. Furthermore, the annual depreciation used here stems from the existing infrastructure currently in use, which may age over time, resulting in higher depreciation costs. An alternative perspective should consider market costs and the value of road and track materials, encompassing factors like sales commission, demolition activities, disposal, and environmental remediation. Asset value can be derived from recycling for on-site infrastructure reconstruction (e.g., recycling concrete, gravel, and sand as structural fill, reusing recycled asphalt for new roads, and re-laying unused rails) or considered as a market disposition value. In the latter case, the adaptability of end-of-life assets should be taken into account (e.g., repurposing ties as biomass fuel chips for waste-to-energy plants or using them as landscaping timbers, and converting scrap metal into new products). The promotion of reuse and recycling initiatives plays a crucial role in reducing environmental impacts, including waste in landfills, the extraction of new materials, pollution, energy consumption, and more.

Transport equipment

The transport equipment metric encompasses expenses related to leasing and purchasing various transportation assets such as trucks, containers, locomotives, rail cars, and more. These costs may involve license fees, registration, insurance, and taxes. Transportation services' insurance costs encompass essential coverage for injuries, property damage, and hazardous material spills, with rates influenced by factors like commodity type, shipment volume, susceptibility to loss, special transportation methods, and others. The cost breakdown for a truck includes lease or purchase expenses of \$0.271 per mile, truck insurance at \$0.087 per mile, truck permits and licenses amounting to \$0.016 per mile, and tolls totaling \$0.037 per mile, as reported by Leslie and Murray (2021). These figures were obtained from respondents to the American Transportation Research Institute's survey for for-hire fleets. By multiplying the \$0.411 per mile by the truck vehicle-miles of 302,141,000,000 in 2020 (Bureau of Transportation Statistics, 2022c) and subsequently dividing it by the total truck freight ton-miles of 2,233,588 million in 2020 (Bureau of Transportation Statistics, 2022a), we derive the EUAC transport equipment cost of \$0.056 per ton-mile as follows:

$$\begin{aligned}\text{Actual EUAC}_{\text{HW}}\text{ of equipment} &= \frac{\text{equipment costs} \times \text{truck VMT}}{\text{actual ton-miles}} \\ &= \frac{0.411(\$/\text{mile}) \times 302,141,000,000(\text{miles})}{2,233,588,364,732(\text{ton-miles})} \\ &= 0.056(\$/\text{ton-mile})\end{aligned}$$

In scenarios of maximum flow, we assume an increase in average truck loads to 20 tons, resulting in the following EUAC transport equipment cost:

$$
\begin{aligned}
\text{Estimated EUAC}_{\text{HW}}\text{ of equipment} &= \frac{\text{equipment costs} \times \text{estimated VMT}}{\text{estimated ton-miles}} \\
&= \frac{0.411(\$/\text{mile}) \times 698,943,405,600(\text{miles})}{12,943,396,400,000(\text{ton-miles})} \\
&= 0.021(\$/\text{ton-mile})
\end{aligned}
$$

The railroad transport equipment cost was determined using the total annual equipment cost of \$2,117,493,000 from the 2020 BNSF R-1 report (Surface Transportation Board, 2022). This cost was employed to calculate the EUAC transport equipment costs for railroads, considering both actual ton-miles and maximum flows, through the following equations:

$$
\begin{aligned}
\text{Actual EUAC}_{\text{RR}}\text{ of equipment} &= \frac{\text{annual equipment costs}}{\text{actual BNSF ton-miles}} \\
&= \frac{2,117,493,000(\$)}{588,919,405,000(\text{ton-miles})} \\
&= 0.0036(\$/\text{ton-mile})
\end{aligned}
$$

$$
\begin{aligned}
\text{Estimated EUAC}_{\text{RR}}\text{ of equipment} &= \frac{\text{annual equipment costs}}{\text{estimated BNSF ton-miles}} \\
&= \frac{2,117,493,000(\$)}{5,841,664,400,000(\text{ton-miles})} \\
&= 0.0004(\$/\text{ton-mile})
\end{aligned}
$$

Maintenance of transport equipment

This encompasses maintenance costs necessary for ensuring the viability and safety of freight transportation equipment. In 2020, the repair and maintenance cost for trucks was \$0.195 per mile, while tire costs amounted to \$0.043 per mile, as reported by Leslie and Murray (2021). Consequently, the total cost sum equaled \$0.238 per mile. The study included data from 138,930 truck-tractors, which collectively covered a distance of over 12 billion VMT and maintained an average fleet size of 1,130 power units nationwide. To calculate the EUAC for transport equipment costs, we multiplied this unit cost by the truck vehicle-miles of 302,141,000,000 in 2020 (Bureau of Transportation Statistics, 2022c) and then divided it by the total truck freight ton-miles of 2,233,588 million in 2020 (Bureau of Transportation Statistics, 2022a). Given the absence of data regarding truck deterioration rates under higher truckloads, we assume that the truck maintenance cost remains constant, matching the actual case at \$0.0322 per ton-mile.

$$\begin{aligned}
\text{Actual EUAC}_{\text{HW}} & \text{ of equipment maintenance} \\
&= \frac{\text{equipment maintenance costs} \times \text{truck VMT}}{\text{actual ton-miles}} \\
&= \frac{0.238(\$/\text{mile}) \times 302,141,000,000(\text{miles})}{2,233,588,364,732(\text{ton-miles})} \\
&= 0.0322(\$/\text{ton-mile})
\end{aligned}$$

Regarding railroads' equipment repair and maintenance cost, we rely on the value of \$630,353,000 calculated from the 2020 BNSF R-1 report (Surface Transportation Board, 2022). For the maximum flow scenario, we adopt a similar assumption to the truck maintenance cost, assuming that the value remains consistent with the actual flow case. The EUAC of equipment maintenance costs is estimated using the following equation:

$$\begin{aligned}
\text{Actual EUAC}_{\text{RR}} & \text{ of equipment maintenance} \\
&= \frac{\text{annual equipment maintenance costs}}{\text{actual BNSF ton-miles}} \\
&= \frac{630,353,000(\$)}{588,919,405,000(\text{ton-miles})} \\
&= 0.0011(\$/\text{ton-mile})
\end{aligned}$$

1.3.4 Environmental metrics

The environmental impact metric within transportation systems involves a thorough assessment that examines the ecological footprint of multiple factors. This encompasses the analysis of greenhouse gas emissions, criteria air pollutants, releases of toxic substances from hazardous materials, noise pollution, contamination of water and soil, as well as the repercussions for wildlife vitality.

Greenhouse gases

Greenhouse gases (GHGs) consist of emissions generated throughout the lifecycle of transport infrastructure, encompassing construction, operation, maintenance, disposal, and recycling processes. These emissions significantly contribute to global warming. The Interagency Working Group, a collaboration involving the EPA, DOE, and other agencies, conducted an assessment of the social costs associated with GHGs. They projected the monetized impacts of the three major GHGs—carbon dioxide (CO2), methane (CH4), and nitrous oxide (N2O)—from 2020 to 2050. These impacts include changes in agricultural productivity, health, property damages due to increased flood risk, and energy system costs. In 2020, the social costs were set at \$51 per metric ton for CO2, \$1,500 per metric ton for CH4, and \$18,000 per metric ton for N2O, considering a 3% discount rate for average impacts (Interagency Working Group, 2021). Fluorinated gases (e.g., HFCs, PFCs, SF6, and NF3) constitute the fourth GHG category according to U.S. Environmental Protection Agency (2021), yet they contributed only 3% of total GHG emissions in 2020 (U.S. Environmental Protection Agency, 2021). Due to limited research on their emission rates and social costs, we have excluded these gases from our analysis.

To calculate transportation emission costs, knowledge of emission rates is essential. Emission factors for medium- and heavy-duty trucks stand at 211 grams per ton-mile for CO2, 0.002 grams per ton-mile for CH4, and 0.0049 grams per ton-mile for N2O (EPA, 2021). Rail emissions factors are 22 grams per ton-mile for CO2, 0.0017 grams per ton-mile for CH4, and 0.0005 grams per ton-mile for N2O (U.S. Environmental Protection Agency, 2021). With this data, we determine the GHG costs for both transportation modes in 2020 using the following equations:

$$
\begin{aligned}
\text{GHGs cost}_{\text{HW}} =& \text{summation of (social costs} \times \text{emission rates)} \\
=& \Big[51(\$ \text{ / metric ton}) \times 211(\text{grams/ ton-miles}) \\
& +1,500(\$/ \text{ metric ton}) \times 0.002(\text{grams/ ton-miles}) \\
& +18,000(\$/ \text{ metric ton}) \times 0.0049(\text{grams/ ton-miles})\Big] \\
& /1,000,000(\text{grams/ metric ton}) \\
=& 0.0109(\$/\text{ton-mile})
\end{aligned}
$$

$$
\begin{aligned}
\text{GHGs cost}_{\text{RR}} =& \Big[51(\$ \text{ / metric ton}) \times 22(\text{grams/ ton-miles}) \\
& +1,500(\$/ \text{ metric ton}) \times 0.0017(\text{grams/ ton-miles}) \\
& +18,000(\$/ \text{ metric ton}) \times 0.0005(\text{grams/ ton-miles})\Big] \\
& /1,000,000(\text{grams/ metric ton}) \\
=& 0.0011(\$/\text{ton-mile})
\end{aligned}
$$

Criteria air pollutants

Criteria air pollutants constitute a group of air pollutants stemming from fuel emissions, known to contribute to smog, acid rain, and various health hazards. As estimated by Kruse et al. (2022), the emission rates of HC or VOC, NOx, PM10, and CO in grams per ton-mile are 0.0221, 0.4487, 0.0191, and 0.1898, respectively, for trucks, and 0.0083, 0.2181, 0.0053, and 0.0564, respectively, for rail transport. Emission factors for VOC, carbon monoxide, nitrogen oxides, and PM10 in locomotive exhaust are classified into eight tiers of emission standards. This categorization is based on the locomotive's original manufacturing year. The Bureau of Transportation Statistics (2021a) provides U.S. average emissions rates per vehicle for the years 2000, 2010, 2020, and 2030 (projected future year), encompassing HC, exhaust CO, exhaust NOx, and exhaust PM2.5, inclusive of brake wear PM2.5, tire wear PM2.5, and other PM2.5.

In terms of PM2.5 emission rates for 2020, heavy-duty vehicles, specifically diesel trucks with more than two axles or four tires, emitted PM2.5 at a rate of 0.106 grams per mile, encompassing brake wear at 0.009 grams per mile and tire wear at 0.004 grams per mile (Bureau of Transportation Statistics, 2021a). To convert the PM2.5 emission rate of 0.106 grams per mile to grams per ton-mile, we multiplied it by the total VMT in 2020 and then divided it by 2020 ton-miles, yielding a heavy-duty vehicle PM2.5 emission rate of 0.0143 grams per ton-mile. In comparison, the industry-average freight rail registered a PM2.5 emission rate of 0.0120 g/short ton-mile in 2018, according to the 2018 Technical Documentation of U.S. Environmental Protection Agency (2018).

The SOx emission rates, initially reported in tons per VMT, are converted to grams per ton-mile. Truck SOx emission is 2×10^{-8} tons per VMT, which is equivalent to 0.0025 grams per ton-mile. Meanwhile, rail SOx emission is recorded at 7.9×10^{-7} tons per VMT, equating to 0.0002 grams per ton-mile (Kruse et al., 2022). To facilitate this conversion from short tons to grams, a multiplier of 907,185 is applied. **Table 1.2** summarizes emission rates and associated damage costs.

The 2020 monetized damage costs for emissions in 2021 can be primarily derived from the DOT Benefit-Cost Analysis Guidelines. According to Kruse et al. (2022), these estimates include \$15,600 per metric ton for NOx, \$41,500 per metric ton for SOx, \$748,600 per metric ton for PM2.5, and \$2,138 per metric ton for VOC as specified in the DOT guidance. However, the DOT guidance does not provide an economic value for PM10 emissions (USDOT, 2022). As PM10 has relatively minimal health impacts and demands fewer resources for management and emissions control (Lee et al., 2021), it is inappropriate to apply the economic damage value of PM2.5 to PM10, in accordance with the DOT BCA Guidance (USDOT, 2022). To address the lack of data availability, the social cost factor for PM10 is derived from a case study by Song (2017) in China, which estimated a damage value of \$62,702 per metric ton for PM10, significantly lower than the PM2.5 cost recommended by the US DOT. Song (2017) cautioned that their evaluations of emissions' social costs, especially

Table 1.2: Emission rates and damage costs of criteria air pollutants

Mode	Parameters	HC/ VOC	SOx	PM2.5	PM10	CO	NOx
Truck	emission rates (g/ ton-mile)	0.0221	0.0025	0.0143	0.0191	0.1898	0.4487
Train	emission rates (g/ ton-mile)	0.0083	≈ 0	0.0120	0.0053	0.0564	0.2181
Both mode	damage costs ($/ metric ton)	2,138	41,500	748,600	170,663	1.5	15,600

health-related costs, would carry high uncertainties and advised policymakers and researchers to exercise caution when using these figures (Song, 2017). Researchers should also consider the specific socioeconomic circumstances and conditions of their study area, such as traffic conditions, population density, medical expenses, and policy factors. Additionally, Kuschel (2022) published the social cost of PM10 in a case study conducted in New Zealand, which encompassed public health, mortality, morbidity, and productivity loss. In 2019, the damage cost for PM10 was NZ$503,346 per metric ton in urban areas and NZ$38,480 in rural areas (Kuschel, 2022). Converting these values to US dollars using an exchange rate of one New Zealand Dollar (NZD) to 0.63 US Dollars, the damage cost for PM10 amounts to $317,085 per metric ton in urban areas and $24,241 in rural areas. Therefore, this study utilizes an average damage cost of $170,663 per metric ton for PM10 emissions. Kuschel (2022) also estimated the CO emission damage cost to be 4.52 NZ dollars per metric ton in urban areas and 0.35 NZ dollars in rural areas. These values equate to $2.85 per metric ton in urban areas and $0.22 in rural areas, or $1.535 per metric ton in US dollars. The damage cost associated with CO emissions is negligible in comparison to other pollutants and will not impact the total cost per ton-mile.

Using a similar approach as in the calculation of GHG social costs per ton-mile, these dollar values per metric ton are converted into dollars per gram and then multiplied by grams per ton-mile to determine the total social cost of criteria pollutants. In summary, the total social cost of criteria pollutants for trucks in 2020 amounts to $0.0213 per ton-mile, while for rail, it stands at $0.0133 per ton-mile in 2020.

Toxic releases

This metric evaluates both unintentional and intentional releases of environmentally harmful transported materials into the air. In 2020, incidents involving the transportation of hazardous materials in commerce resulted in three fatalities, 49 injuries, and property damage costs totaling $26,345,000 (Bureau of Transportation

Statistics, 2021b). The unit cost of a fatality was $11,295,400 per incident, while the cost of an injury was $198,500 per incident, as shown in **Table 1.3**. Consequently, the combined cost for fatalities and injuries in highway transportation of hazardous materials in commerce totaled $43,612,700. When considering property damage, fatalities, and injuries, the overall annual cost amounted to $69,957,700. To determine the cost per ton-mile in the actual flow case, we divided this total by the total freight ton-miles in 2020, which were 2,233,588,364,732 ton-miles (Bureau of Transportation Statistics, 2022a). The estimated cost of hazmat incidents and property damages per ton-mile in 2020 was $0.00003. For the maximum flow scenario, we assumed this cost rate would remain constant at $0.00003 per ton-mile for hazardous material transport by highways, as there is no available research estimating new emissions for new truckloads.

$$\begin{aligned}
\text{EUAC}_{\text{HW}} \text{ of toxic release} &= \frac{\text{annual incident cost}}{\text{actual ton-miles}} \\
&= \frac{69,957,700(\$)}{2,233,588,364,732(\text{ton-mile})} \\
&= 0.00003(\$/\text{ton-mile})
\end{aligned}$$

In 2020, for rail transport, there were six individuals injured, and no fatalities linked to the transport of hazardous materials. Additionally, the incurred costs for property damage totaled $27,945,000, as reported by Bureau of Transportation Statistics (2021b). By multiplying the number of incidents by the associated cost per case, we calculated the total cost of fatalities and injuries to be $1,191,000 for hazardous materials transported by rail. The overall cost, inclusive of property damage, totaled $29,136,000 in 2020. To determine the EUAC of total toxic release costs for railroads, we divided this overall cost by the 1,439,814,000,000 ton-miles of Class I transport in 2020. The resulting EUAC stood at $0.000021 per ton-mile in 2020, as demonstrated in the following equation. Similar to the highway toxic release cost, we presumed that the cost rate for the maximum flow scenario would persist at $0.00002 per ton-mile for hazardous material transport by rail.

Table 1.3: KABCO highway-related crash severity rating.

Code	Severity	Description	Unit costs ($2016)
K	Fatal	Any injury that results in death within 30 days	$11,295,400
A	Incapacitating (Suspected Serious Injury)	Any injury other than a fatal injury that prevents the injured person from walking, driving, or normally continuing the activities the person was capable of (e.g., severe laceration, broken or distorted limbs, damaged skull, significant burns, and paralysis)	$655,000
B	Evident Injury (Suspected Minor Injury)	Any injury other than code K and A that is evident to observers at the scene (e.g., abrasions, bruises, minor cuts, minimal bleeding)	$198,500
C	Possible Injury	Any injury reported that is less severe than non-incapacitating evident injury (e.g., pain, nausea, hysteria, limping, momentary loss of consciousness)	$125,600
O	Property Damage Only	Property damage that reduces the monetary value of that property without any bodily harm	$11,900

Source: adapted from Harmon et al. (2018) and Shrestha et al. (2021)

$$
\begin{aligned}
\text{EUAC}_{\text{RR}} \text{ of toxic release} &= \frac{\text{annual incident cost}}{\text{actual Class I ton-miles}} \\
&= \frac{29,136,000(\$)}{1,439,814,000,000(\text{ton-mile})} \\
&= 0.00002(\$/\text{ton-mile})
\end{aligned}
$$

Noise pollution, water and soil pollution, and wildlife vitality

These impacts encompass the influence of engines, rolling stock, and aerodynamics on the quality of life for both humans and animals residing in areas adjacent to transport infrastructure. They include factors such as annoyance, health issues, and biodiversity loss. Examples of water and soil pollution resulting from the transportation sector include microplastics from tires, copper emissions from brake pads and rail wear, asphalt wear, fuel contamination from oil drips and leaks, petroleum leaks from underground storage tanks, material spillage from vehicle exhaust, organic compounds, chemicals, radiation, biohazard materials, oil and gas, and certain infrastructure construction and maintenance activities like rock and soil excavation, painting, de-icing practices using substances like CaCl2 and NaCl, pesticide application to roadside and trackside vegetation, disposal practices, and solid waste impact on the water quality of adjacent streams and downstream areas. These issues are interlinked with roadside soil quality, involving contaminants washed into the surrounding soil, erosion of disturbed soils (e.g., excavation areas and impervious surfaces), and damage to soil structure. Concerning wildlife impacts, both construction and operational activities can influence the life expectancy, habitat, health, and reproduction of animals, creating physical barriers that restrict animals' access to their habitat and pose a threat to population stability.

A European case study conducted by Siciliano et al. (2016) quantified the costs associated with these impacts. In 2016, the costs of noise pollution were reported at 2.5 euros per 1,000 ton-km for highways and 1 euro per 1,000 ton-km for railroads. Water and soil pollution costs were documented at 1 euro per 1,000 ton-km for highways and 0.4 euros per 1,000 ton-km for railroads. Biodiversity losses were exclusively linked to highway transportation, with a cost of 0.5 euro per 1,000 ton-km. The standard rail in the case study maintained an average speed of approximately 60 km/hr, equivalent to the speed of a US Class 3 railroad. These values were originally expressed in euros per 1000 ton-km, and for conversion to dollars per ton-mile, we assumed an exchange rate of one EUR to 1.11 USD, considering one ton-km as equivalent to 0.684931507 ton-miles. Consequently, the resulting costs in 2016 US dollars per ton-mile were as follows:

$$\begin{aligned}\text{Noise pollution cost}_{\text{HW}} &= \frac{2.5(€) \times 1.11(\$/€)}{1000(\text{ton-km}) \times 0.684931507(\text{ton-mile/ ton-km})} \\ &= 0.0041(\$/\text{ton-mile})\end{aligned}$$

$$\begin{aligned}\text{Noise pollution cost}_{\text{RR}} &= \frac{1(€) \times 1.11(\$/€)}{1000(\text{ton-km}) \times 0.684931507(\text{ton-mile/ ton-km})} \\ &= 0.0016(\$/\text{ton-mile})\end{aligned}$$

$$\begin{aligned}&\text{Water and soil pollution cost}_{\text{HW}} \\ &\qquad = \frac{1(€) \times 1.11(\$/€)}{1000(\text{ton-km}) \times 0.684931507(\text{ton-mile/ ton-km})} \\ &\qquad = 0.0016(\$/\text{ton-mile})\end{aligned}$$

$$\begin{aligned}&\text{Water and soil pollution cost}_{\text{RR}} \\ &\qquad = \frac{0.4(€) \times 1.11(\$/€)}{1000(\text{ton-km}) \times 0.684931507(\text{ton-mile/ ton-km})} \\ &\qquad = 0.00065(\$/\text{ton-mile})\end{aligned}$$

$$\text{Wildlife vitality cost}_{\text{HW}} = \frac{0.5(€) \times 1.11(\$/€)}{1000(\text{ton-km}) \times 0.684931507(\text{ton-mile/ ton-km})}$$
$$= 0.0008(\$/\text{ton-mile})$$

$$\text{Wildlife vitality cost}_{\text{RR}} = \frac{0(€) \times 1.11(\$/€)}{1000(\text{ton-km}) \times 0.684931507(\text{ton-mile/ ton-km})}$$
$$= 0(\$/\text{ton-mile})$$

We additionally adjusted these values to 2020 US dollars, yielding noise pollution costs of $0.0047 per ton-mile for highways and $0.0019 per ton-mile for railroads. Water and soil pollution costs amounted to $0.0019 per ton-mile for highways and $0.0008 per ton-mile for railroads. Wildlife vitality costs were estimated at $0.0009 per ton-mile for highways and $0 per ton-mile for railroads.

Regarding noise pollution, the BCA guidance offered suggested costs in 2020 dollars: $0.0197 per VMT for buses and trucks in all locations, $0.0033 per VMT for buses and trucks in rural areas, and $0.0393 per VMT for buses and trucks in urban areas (USDOT, 2022). It's important to note that these values were specifically designed for projects involving modal shifts, implying their applicability when there are known reductions in VMTs on the highway following the implementation of a new project. Currently, there is a dearth of explicit guidance for independently estimating noise pollution costs in transportation projects. The BCA guidance proposes that researchers and practitioners can quantitatively evaluate this metric using clearly defined thresholds, such as decibel levels or specific times of operation (for example, nighttime or daytime) (USDOT, 2022).

1.3.5 Social metrics

Social costs in transportation comprise a broad range of factors, both tangible and intangible, that profoundly influence individuals' and communities' quality of life. These costs extend beyond financial considerations, delving into deeper, often less quantifiable aspects of well-being. In this study, we categorize social costs into three primary types: safety, travel congestion, and the enjoyment of natural landscapes and tranquility.

Safety

Safety costs pertain to the expenses associated with fatalities and injuries per ton-mile of freight transport. These expenses include medical treatment, property damage, lost productivity, insurance administration, emergency services, as well as non-monetary costs related to reduced quality of life and pain and suffering. In their 2016 analysis, Harmon et al. (2018) categorized highway crashes by severity, outlining their costs in 2016 dollars, as depicted in **Table 1.3**. These values represent comprehensive costs, including economic impacts such as medical expenses, property damage, and the costs of goods and services related to crash response. They also account for workplace costs stemming from employee absences, congestion-related impacts like increased fuel consumption and pollution for those not directly involved in the accident, and societal crash costs, which capture the monetized value of pain and suffering.

According to Kruse et al. (2022), they compiled data regarding fatalities and injuries per billion ton-miles of truck transport. In 2018, this data indicated a ratio of 2.2212 fatalities per billion ton-miles and a ratio of 55.1714 injuries per billion ton-miles, sourced from the Large Truck and Bus Crash Facts 2018 report by the Federal Motor Carrier Safety Administration. For railroads, data from 2019 was utilized, revealing a ratio of 0.4793 fatalities per billion ton-miles and a ratio of 4.6207 injuries per billion ton-miles. Utilizing these figures, we computed safety costs for both transportation modes using the following equations:

$$
\begin{aligned}
&\text{Annual Safety cost}_{\text{HW}} \\
&\quad = \left(\frac{\text{number of incidents}}{\text{billion ton-mile}} \times \frac{\text{billion ton-mile}}{\text{ton-mile}} \times \text{unit cost}\right) \\
&\quad = \left(\frac{2.2212 \times 11,295,400(\$)}{1,000,000,000(\text{ton-mile})}\right) + \left(\frac{55.1714 \times 198,500(\$)}{1,000,000,000(\text{ton-mile})}\right) \\
&\quad = 0.036(\$/\text{ton-mile})
\end{aligned}
$$

$$
\begin{aligned}
&\text{Annual Safety cost}_{\text{RR}} \\
&\quad = \left(\frac{0.4793 \times 11,295,400(\$)}{1,000,000,000(\text{ton-mile})}\right) + \left(\frac{4.6207 \times 198,500(\$)}{1,000,000,000(\text{ton-mile})}\right) \\
&\quad = 0.006(\$/\text{ton-mile})
\end{aligned}
$$

These values were subsequently adjusted to 2020 dollars, incorporating a 4% inflation rate. As a result, the safety cost was assessed at $0.042 per ton-mile for highways and $0.007 per ton-mile for railroads.

Travel congestion

There are two types of congestion: recurring and non-recurring. Recurring congestion refers to persistent disruptions in highway and railroad capacity, leading to time and fuel inefficiencies. Non-recurring congestion encompasses unforeseen events, such as accidents and severe weather, resulting in lost time and additional fuel consumption. According to a report by the American Transportation Research Institute (ATRI), Hooper (2018) estimated the national congestion cost for the trucking industry to be $74.493 billion in 2016. This comprehensive figure includes increased operating costs associated with wasted fuel, elevated labor expenses, safety expenditures, and vehicle wear and tear. To adjust this cost to its equivalent value in 2020 dollars, an inflation rate of 4% has been applied, resulting in an approximate cost of $87.146 billion. When this adjusted cost is divided by the total ton-miles of 2,060,780,000,000 in 2016, it equates to a congestion cost of \$0.0423 per ton-mile in 2020 dollars. Nevertheless, the congestion cost advised in the DOT's 2022 BCA Guidance stood at \$0.212 per vehicle mile traveled (VMT) in 2020. When we translate this value to a per ton-mile basis, considering the ratio between 2020 VMT and ton-miles in the US, it equates to approximately \$0.0287 per ton-mile. Notably, the congestion cost estimated by Hooper (2018) is approximately 1.47 times higher than the BCA guidance's value. Given the comprehensiveness of Hooper (2018)'s calculation, we opted to employ their congestion cost of \$0.0423 per ton-mile in 2020 dollars.

For freight railroad congestion costs, an estimate indicated that grade crossing congestion incurred an annual cost of \$465,137,996 in the year 2000 (Gorman, 2008). Given the total annual ton-miles of 1,465,960 million in 2000 (Bureau of Transportation Statistics, 2022b), the corresponding grade crossing congestion cost was computed at \$0.0003 per ton-mile in 2000, equivalent to \$0.0007 per ton-mile when adjusted to 2020 dollars. Additionally, in 2020, freight trains caused delays of 700,000 minutes to passenger trains, according to Amtrak (National Railroad Passenger Corporation, 2021). To determine the passenger rail traffic congestion cost, we utilized values of travel time savings, amounting to \$47.1 per person-hour in 2015-dollar value (U.S. Department of Transportation, 2016). This value represents a weighted average, considering 59.6% personal trips and 40.4% business trips, based on intercity travel via high-speed rail. Given an average occupancy of approximately 286 persons per Amtrak train in 2016 (National Railroad Passenger Corporation, 2016), the rail traffic congestion cost can be calculated as follows:

$$\begin{aligned}
&\text{Passenger rail congestion cost} \\
&\qquad\qquad = \frac{\text{value of time} \times \text{time} \times \text{number of passengers}}{\text{ton-miles}} \\
&\qquad\qquad = \frac{47.1(\$/\text{ person-hr}) \times 700,000(\text{min}) \times 286(\text{passengers})}{60(\text{min/hr}) \times 1,439,814,000,000(\text{ton-miles})} \\
&\qquad\qquad = 0.00011(\$/\text{ton-mile})
\end{aligned}$$

Subsequently, after adjusting this value to 2020 dollars, the estimated passenger rail traffic congestion cost was determined to be \$0.00013 per ton-mile. Consequently, the overall traffic congestion cost, encompassing both grade crossing and passenger rail congestion, amounted to \$0.00083 per ton-mile.

Peaceful enjoyment of nature and landscape

This metric evaluates the qualitative impacts on human land use near road and rail transportation corridors, with a specific emphasis on livability influenced by the frequency of vehicle movement and its impact on the natural and scenic beauty of the landscape. Siciliano et al. (2016) presented values of 0.7 euros per 1,000 ton-kilometers for highways and 0 euros per 1,000 ton-kilometers for railroads as the transportation cost associated with disrupting peaceful enjoyment. We converted these values into US dollars per ton-mile using the following equations and subsequently adjusted them to 2020-dollar values. As a result, the estimated cost for disrupting peaceful enjoyment was \$0.0013 per ton-mile for highways and \$0 per ton-mile for railroads.

$$\begin{aligned}\text{Peaceful enjoyment cost}_{\text{HW}} &= \frac{0.7(€) \times 1.11(\$/€)}{1000(\text{ton-km}) \times 0.6849315(\text{ton-mile/ ton-km})}\\ &= 0.0008(\$/\text{ton-mile})\end{aligned}$$

$$\begin{aligned}\text{Peaceful enjoyment cost}_{\text{RR}} &= \frac{0(€) \times 1.11(\$/€)}{1000(\text{ton-km}) \times 0.6849315(\text{ton-mile/ ton-km})}\\ &= 0(\$/\text{ton-mile})\end{aligned}$$

1.4 Computational results and discussions

Using the methods and data outlined in Section 1.3, this section presents a LBCA comparison between highways and railroads. **Table 1.4** provides a summary of the comparison results in 2020 dollars per thousand ton-miles for each mode, including

Table 1.4: Life-cycle benefit and cost comparison between highway and railroad projects in 2020 dollars per thousand ton-miles

Cost Element	Highway		Railroad	
	Actual Flow	Max Flow	Actual Flow	Max Flow
Land Use Metric				
Land value	$0.11	$0.08	$0.44	$0.03
Initial Construction Metrics				
Initial Construction	$22.71	$8.35	$11.92	$0.71
Operating Metrics				
Energy	$29.80	$29.80	$9.53	$9.53
Labor and Administration	$99.70	$36.85	$12.47	$1.26
Maintenance of Assets	$8.69	$1.66	$4.73	$4.73
End of Life Asset Value	($3.44)	($3.44)	($1.16)	($1.16)
Transport Equipment	$55.60	$20.55	$3.60	$0.36
Maintenance of Equipment	$32.19	$32.19	$1.07	$1.07
Environmental Metrics				
Greenhouse Gases	$10.85	$10.85	$1.13	$1.13
Criteria Pollutants	$21.27	$21.27	$13.31	$13.31
Toxic releases	$0.03	$0.03	$0.02	$0.02
Noise Pollution	$4.74	$4.74	$1.62	$1.62
Water and Soil Pollution	$1.90	$1.90	$0.65	$0.65
Wildlife Vitality	$0.95	$0.95	-	-
Social Metrics				
Safety	$42.16	$42.16	$7.41	$7.41
Congestion	$42.29	$42.29	$0.83	$0.83
Peaceful Enjoyment	$1.33	$1.33	-	-
Total	$370.88	$251.56	$67.57	$41.51

calculations for both actual 2020 flows based on the BTS and R1 report data and theoretical maximum flows as described in A.

Based on the computational results presented in **Table 1.4**, the total current cost of a highway project amounts to \$370.88 per thousand ton-miles, which is roughly 5.49 times higher than the total current cost of a railroad project, estimated at \$67.57 per thousand ton-miles. **Figure 1.1** visually illustrates all the benefits and costs associated with both modes of transportation, with the blue area representing the costs of the highway project and the orange area representing the costs of the railroad project.

When we group the metrics for the highway project, the largest proportion of expenses includes driver wage and benefit costs, transport equipment costs, traffic congestion costs, and safety costs, in order of significance. In comparison, for the railroad project, the largest group of metrics includes criteria pollutants, labor and administration costs, initial construction costs, energy costs, and safety costs, respectively. The remaining metrics, which have not yet been discussed, contribute minimally to the total cost, accounting for less than 10% each. It is important to highlight that although criteria pollutant costs may appear to be a substantial component of railroad expenses, they comprise only approximately 19.7% of the total cost of railroad projects. Additionally, when we analyze these criteria pollutant costs on a per-thousand-ton-mile basis, we find that the railroad's criteria pollutant costs represent just 62.6% of those incurred by highway projects. Regarding overall costs, the only area where railroads are more expensive than highways is land value. This cost disparity arises because the allocation of costs for trucks among highway users is solely based on the space taken up by vehicles (PCE). Since passenger cars occupy a larger proportion of space compared to trucks, they bear a greater responsibility for the land value cost.

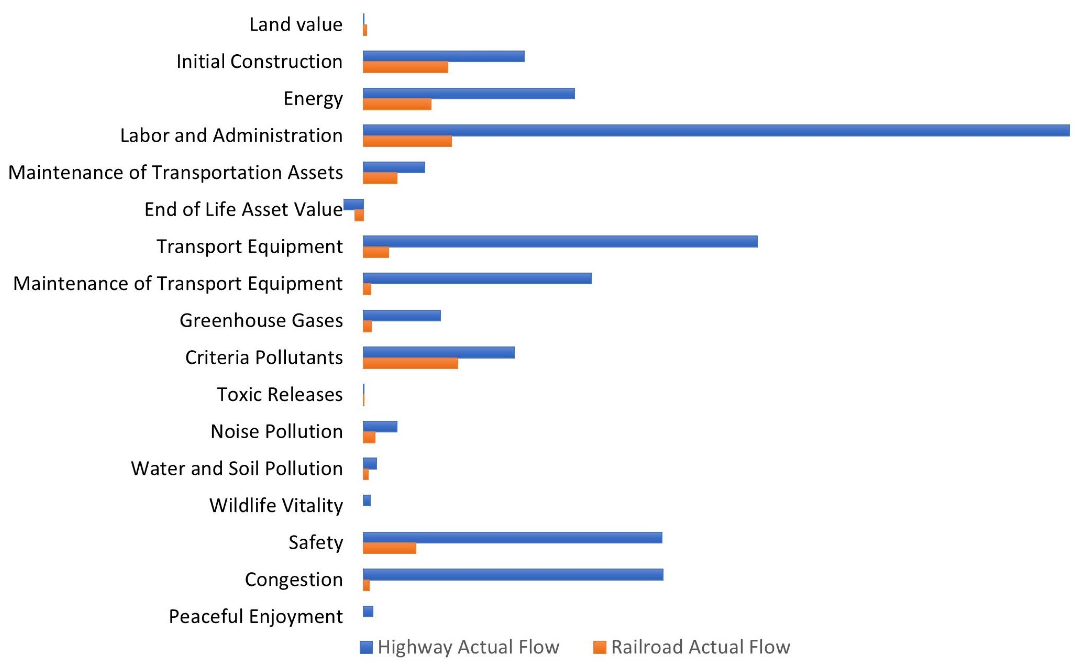

Figure 1.1: 2020 costs per ton-mile of highway and railroad projects

1.5 Conclusion, limitations and future research

This section discusses the applicability of the developed LBCA tool, its limitations, and future research needs, including metrics with insufficient quality data and the treatment of end-of-life values.

1.5.1 Applicability of the LBCA tool

Our tool evaluates the comprehensive benefits and costs associated with surface freight transportation, considering financial and non-financial dimensions, such as social and environmental factors, throughout their life cycle. Users have the flexibility to calculate metrics effortlessly using provided default values or opt to customize them for specific projects, requiring a certain level of effort and expertise. In terms of case-specific implementation, this tool may be more suitable for researchers or experts with experience working in the logistics and transportation industry than the general public. For the public, the tool offers a broad understanding of the differences between transportation modes, aiding projects seeking public support and promoting environment-conscious policies. Concerning the tool's performance, despite considerable efforts to collect and improve accuracy, certain data inconsistencies persist. These discrepancies arise from the utilization of data from diverse sources, encompassing different levels such as national, local, state, or international data, and are particularly notable in the assessment of environmental impacts. Furthermore, the scope of our tool is restricted to transportation infrastructure and equipment, excluding support infrastructure such as railroad yards, terminals, gas stations, and power stations. It also specifically targets conventional transport equipment such as diesel locomotives and trucks, omitting the inclusion of emerging technologies like electric or hydrogen trucks. In the next subsection, we will further discuss the limitation of this study caused by data availability in more detail.

1.5.2 Limitations of this study caused by data availability

The growing awareness of transportation's environmental impacts has spurred researchers to consider additional metrics for comparing transportation alternatives. These impacts encompass a range of factors, such as microplastic pollution, light pollution, water and soil pollution, noise and vibration damage, biodiversity loss, changes in environmental aesthetics, and the value of end-of-life assets and equipment. However, our LBCA tool does not incorporate some of these impacts due to a lack of high-quality data that would enable a meaningful comparison between the two transportation modes. For some included metrics, we acknowledge limitations in the calculations due to data constraints. In this subsection, we categorize these metrics into two groups. First, we discuss the metrics excluded from our LBCA tool because they lack associated monetized values. Subsequently, we address metrics included in our analysis, noting that caution should be exercised by U.S. users because the data primarily originate from other regions and may not be entirely applicable to U.S. scenarios. Additionally, we examine the concept of end-of-life asset versatility, which has gained prominence in the context of sustainability, yet has not been integrated into our calculations.

Environmental metrics that are not included

In our proposed life-cycle BCA, we have omitted several crucial environmental metrics, namely microplastic pollution, light pollution, and vibration, due to data limitations. In this subsection, we will discuss the significance of these metrics and the availability of relevant data.

Microplastic Pollution Tires, comprising 19% natural rubber and 24% plastic polymer, are a significant source of microplastic emissions (Root, 2019). They produce two types of road microplastics: tire wear particles (TWPs) and brake wear particles (BWPs). In 2014, global emissions of PM2.5 and PM10 TWPs amounted to 31,967 tons and 317,466 tons, respectively (Evangeliou et al., 2020). PM2.5 BWPs totaled

108,247 tons, and PM10 BWPs reached 160,937 tons in annual global emissions. North America contributed substantially, with 22% of TWPs and 17% of BWPs. Due to their airborne nature, these microplastics can travel long distances and deposit on land and in the ocean. TWPs and BWPs accounted for 43% - 46% of PM2.5 deposits on land and 53% - 57% in the oceans. PM10 TWPs and BWPs, larger particles, were primarily deposited on land (65% - 72%) and to a lesser extent in the ocean (28% - 35%) (Evangeliou et al., 2020). These pollutants have significant adverse effects on people, animals, and the environment. For example, they often contain toxic chemicals and microorganisms (Carrington, 2020) and damage marine animals and aquaculture. Lee (2015) evaluated the economic losses to UK shellfish, mollusk, and aquaculture in 2012 based on the microplastic density. While there's no specific research on their impact on human health, it's widely believed that microplastics may harm humans, particularly in densely populated regions where exposure to PM2.5 and PM10 can cause respiratory diseases (Evangeliou et al., 2020). Research by Goßmann et al. (2021) demonstrated that car tire wear significantly contributes to microplastic pollution in various samples, including road dust, sediments, marine salt, and mussels. Car-to-truck tire wear ratios were as high as 16:1 across all samples. In contrast, railroads, mainly composed of iron, steel, and metal, do not commonly emit microplastics, with only occasional synthetic rubber use in brake systems. Consequently, research on brake shoe microplastic release from railroads is lacking, and no data exists to quantify its environmental impact, precluding its inclusion in this study.

Light Pollution Artificial light pollution, emanating from diverse sources like buildings, public spaces, advertising, and transportation, poses a multifaceted threat. It disrupts animal habitats, mating behaviors, wildlife, human health, and astronomy. Research by Gallaway et al. (2010) estimated that poor lighting design contributes to nearly $7 billion in annual light pollution costs due to excessive energy consumption in the U.S. Numerous studies have explored the negative impacts of light pollution on ecosystems. For instance, it has been linked to a 47% reduction in moth caterpillar populations in hedgerows and disruptions in caterpillar development (Boyes et al., 2021), altered moths' abundance and their role in nocturnal pollen transport (Macgregor et al., 2017), sleep disturbances in birds (Aulsebrook et al., 2020), and changes in loggerhead turtle behavior during nesting and hatchling phases (Silva et al., 2017). However, the impact on human health remains a subject of debate. Svechkina et al. (2020) conducted a systematic review of seventy-four articles, revealing possible health issues like tumors, breast cancer, sleep disorders, and weight gain associated with light pollution. Yet, these findings are still tentative, and the reversibility of the impacts is uncertain (Svechkina et al., 2020). Moreover, some studies have assessed the economic aspects of light pollution, considering investment, maintenance, and energy costs (Narisada and Schreuder, 2004) and the benefits of reducing crime and accident rates (Bhagavathula et al., 2021; Narisada and Schreuder, 2004). Remarkably, no research has quantified the monetary toll of transportation-induced light pollution on humans and ecosystems. This represents a significant knowledge gap that merits further investigation.

Vibration Transportation system vibrations can negatively impact human well-being and health. Factors such as vibration intensity, frequency, distance from the source, and land use types all play a role. Federal Aviation Administration (2021) evaluated ground-borne vibrations of rail transit operations and constructions for the likelihood of annoyance using the FTA Manual. This evaluation focused on residential areas within 200 feet and institutional areas within 100 feet of the project alignment, as well as vibration-sensitive structures. If a new project's construction and operation vibrations increase by less than three vibration decibels (VdB) compared to existing levels, it won't contribute to vibration issues (Federal Aviation Administration, 2021). However, this may not apply to freight railroad transportation due to greater distances, lower operation frequency, and minimal incremental effects. Freight trucks produce less intense but more frequent vibrations. The vibration intensity of freight trucks is less than the vibration caused by the railroads, but its frequency could be much higher. There is no existing study quantifying the impacts on people associated with freight rails and trucks.

Environmental metrics that are included but require cautions

While European countries have extensively studied social and environmental costs, such research has been relatively limited in the United States. We include European data-based values for several impacts in our LBCA. It is important to note that when combining these European-derived values with U.S. costs for other impacts, it may compromise metric consistency, requiring caution from users. The environmental metrics in question encompass noise, water and soil pollution, biodiversity losses, and effects on nature and landscapes. For our analysis, we rely on more recent research conducted by Siciliano et al. (2016) that aligns with the BCA Guidelines of the European Commission and exclusively represents costs in Europe. Each of these metrics will be discussed in detail below.

Noise Pollution. The U.S. DOT's BCA Guidance suggests noise pollution costs of \$0.0197 per VMT for buses and trucks for all locations, \$0.0033 per VMT in rural areas, and \$0.0393 per VMT in urban areas in 2020(USDOT, 2022). These values are primarily intended for projects involving modal shifts, enabling the estimation of noise pollution cost savings through a reduction in VMT. Alternatively, analysts can provide a qualitative estimate of noise pollution in BCA when VMT reductions are unknown. If a quantitative approach is chosen, a clear explanation of the threshold (e.g., decibel levels, operation times) is required (USDOT, 2022). Notably, the guidance lacks specificity in calculating noise pollution costs for different transportation modes. The Federal Aviation Administration (FAA) does include noise costs in project evaluations, applying them to projects like commuter rail and bus realignments, and changes in operational frequency, following noise level prediction methods and screening analysis (Federal Aviation Administration, 2021). However, the focus has been primarily on mass transit sectors rather than freight transport. Beyond the U.S. studies, the Victoria Transport Policy Institute in Canada

(Litman, 2020) compiled traffic noise cost data from various countries for a wide range of land transport modes, including cars, electric cars, vans, mid-size trucks, heavy trucks, buses, motorcycles, and trains. The costs were also segregated into several categories depending on speed, different times of day, and characteristics of the area (i.e., urban, suburban, and rural). Most research they reviewed focuses on passenger transportation, with only CE Delft, the independent research and consultancy organization in the Netherlands, being a rare source of noise cost data for freight trains in 2008.

Water and Soil Pollution. Transportation has a direct impact on water and soil quality through hazardous material leaks resulting from operational activities and maintenance, such as fuel, lubricant, paint, brake fluid, road salt, hydraulic fluids, wooden tie preservation, and pesticide applications, as well as accidents. Chemicals from these incidents can either directly contaminate water sources or seep into the ground and eventually reach groundwater or downstream bodies of water. Moreover, chemicals, whether in particle or emission form, ultimately settle on land or water surfaces. Furthermore, the impermeable surfaces of transportation infrastructure can hinder the infiltration of surface water into the soil, heightening the risk of flooding and the transmission of pollutants to water sources far beyond adjacent areas. This issue is predominantly associated with dense road networks, influenced by the number of household vehicles and the preference for single-family homes, with limited consideration for highway traffic. This oversight may stem from the relatively small proportion of impervious surfaces linked to highway infrastructure (Hecht and Andrew, 1997). Victoria Transport Policy Institute (2015) reviewed articles on water pollution and hydrologic impacts resulting from transport facilities and vehicle usage. The cost categories include oil pollution, tanker spills, road salt contamination, cleanup of leaking tanks, highway runoff control, and stormwater management, among others.

Biodiversity Losses. The assessment of costs related to wildlife and traffic safety typically relies on statistical data regarding collisions between wildlife and vehicles

(National Highway Traffic Safety Administration, 2021). These costs are primarily focused on the impacts affecting humans, encompassing factors such as human fatalities and injuries, property damage, and time lost, without considering the impact on the animals involved. Additionally, expenses associated with mitigation efforts, such as the construction of road fences, wildlife crosswalks, and wildlife grids, should be considered (Seiler et al., 2016). However, the value of lost animals, while acknowledged in research, lacks standardized values and is often excluded from the analysis (Gren and Jägerbrand, 2019). Notably, existing research does not adequately address how the transportation sector impacts habitats and contributes to the loss of animal life, leaving this aspect uncertain.

Impact on Nature and Landscape. The development of expressways can lead to visual degradation and annoyance for those within sight. While some researchers acknowledge this issue, they argue that quantifying the cost of visual intrusion is not feasible (Lawson, 2007). In a more practical approach, the University of Karlsruhe in Germany and the Swiss Federal Office for Spatial Development recommended evaluating the cost of landscape degradation by estimating the expenditures needed to dismantle transportation structures and restore natural conditions. In our research, we derive the external cost of nature and landscape from the work of Siciliano et al. (2016), who utilized values from the European Commission's transport white paper. However, the methodology or factors used to estimate this cost are not explicitly identified.

Versatility of the end-of-life Value

The current life cycle cost analysis approach recommended by the FHWA primarily focuses on the remaining value of assets at the end of the analysis, typically based on the last rehabilitation. However, this method overlooks the condition of underlying pavement layers and neglects potentially costly reconstruction expenses beyond the analysis period. While they argue that these assumptions are considered feasible due to small salvage values at the end of the analysis (e.g., 30 years for pavement)

(Musselman et al., 2020), it is crucial to consider a broader perspective. In reality, the value of these residuals may remain significant or have the potential for recycling and reuse. In the context of road infrastructure, managing waste and by-products promotes the recycling and reutilization of secondary materials, given the continual growth in by-product volumes and disposal costs. When assessing the benefit-cost analysis of this metric, it is essential to benchmark the cost of utilizing recovered materials against conventional materials. Guidance provided by the Chesner et al. (2008) outlines the use of waste and by-product materials in six key highway construction applications, including Asphalt Concrete, Portland Cement Concrete, Granular Base, Embankment or Fill, Stabilized Base, and Flowable Fill. Despite this guidance, the incorporation of this concept into the BCA of transportation projects has not been realized. This broader aspect of the versatility of the end-of-life value still requires more attention in research.

1.5.3 Future research

In the preceding section, we identified three primary challenges hindering the inclusion of monetary values for factors in LBCA: data unavailability, limited metric scope, and computational method limitations. Some impacts are intangible and difficult to measure, for example, the annoyance and distraction of noise and distress from aesthetic degeneration of the environment. Additionally, certain metrics necessitate specialized personnel and equipment for measurement and analysis. When assessing human health impacts, attributing causation to a single factor is complex due to uncontrollable external variables. Consequently, it is more feasible to gauge factor impacts through controlled animal experiments, such as observing moth population reductions in response to artificial light exposure. This preference for ecosystem-focused research over human-centric studies has been observed in prior investigations. In this section, we will outline the future research direction for comprehensive comparisons of life-cycle benefits and costs in freight transportation systems. This will encompass input data, anticipated outcomes, and promising methodologies.

To evaluate the noise and vibration impact of freight transport in the U.S., we rely on European case studies as a guide for methodology. These studies emphasize gathering data related to operational factors (e.g., speed, operating hours), exposure duration, population density in affected areas, and existing noise and vibration levels. Several open-source software tools, such as SoundPLAN, openPSTD, and IMMI, aid in sound propagation estimation. These tools require input parameters like scheduling (duration and frequency), average train car counts, speeds, and infrastructure conditions. Notably, SoundPLAN, recommended by the FTA, offers insights into the costs and benefits of noise reduction measures, such as noise barriers. Identifying affected areas, such as hospitals, schools, and residential zones, is crucial, as the impact varies depending on land use functionality. The European Commission's handbook on transport's external costs provides data on noise impact cost per dB per person-year for road and rail transport, aligned with WHO guidelines. Analysts can derive annual total costs by multiplying these costs by appropriate weights, differentiating between road and rail sectors. Given the variation in population density across urban, suburban, and rural areas, adjusting the impact estimation is essential for accurate assessment. It is worth mentioning that while individual trains may produce higher noise levels than trucks, the lower frequency of freight trains compared to highway trucks results in slightly lower decibel levels per ton (Hecht and Andrew, 1997). Additionally, it is important to consider that railroads are often situated remotely from communities, while highways can run through them, potentially making highway noise impact more significant.

Assessing the versatility of end-of-life value in transportation infrastructure is vital, especially in the current circular economy trend. For road infrastructure, asphalt finds reuse in new pavement projects, while railroad steel and wood have broader applications. Calculating costs for using reclaimed materials in pavement construction involves three aspects: material cost, installation cost, and life-cycle cost

(Chesner et al., 2008). Material costs encompass six elements: 1) raw material price with disposal fee, 2) processing costs such as screening and crushing, 3) stockpiling expenses, 4) material loading, 5) transportation costs, and 6) producer profit. Installation costs are considered when using reclaimed materials with different design, construction, testing, or inspection needs compared to conventional materials. Lastly, life-cycle costs assess whether reclaimed materials alter maintenance requirements or the infrastructure's expected service life (Chesner et al., 2008). When using reused materials, a BCA should compare these costs with conventional materials. For railroad end-of-life value, similar considerations and cost elements apply. However, these scraps can be recycled into various products such as landscaping timbers, substructures, automotive parts, cans, and more. To simplify calculations, we can use scrap prices from the Scrap Price Bulletin offered by rail companies instead of considering varied recycled material values. Furthermore, the utilization of recycled materials has far-reaching effects, notably diminishing landfill waste, greenhouse gas emissions, energy consumption, resource extraction, production, and transportation. Nevertheless, estimating associated costs and end-of-life values based on these benefits demands substantial time and expertise. Multidisciplinary teams, including logistics, civil and environmental engineering, environmental science, geology, and materials science, are essential for future research in this area.

In the assessment of the cost of environmental aesthetics, future research could explore two critical dimensions: firstly, quantifying the value of dissatisfaction arising from diminishing beauty, and secondly, evaluating the expenses associated with restoring natural aesthetics. The calculation of the latter is relatively straightforward, as various European studies have already undertaken this task, involving the estimation of costs for dismantling transportation structures and reinstating natural conditions. Concerning the evaluation of the cost of dissatisfaction, despite its subjective nature and susceptibility to personal opinions, a rough estimate can be derived using the willingness-to-pay method. This involves conducting surveys to gauge how much residents are willing to invest in residing near transportation infrastructures. Alternatively, analysts can examine land values or asset values in proximity to these areas to determine any correlation with price fluctuations following the introduction of transportation infrastructures.

Another critical metric that demands increased attention for the successful implementation of the proposed LBCA in the U.S. is the impact on biodiversity. Currently, the costs associated with wildlife have predominantly focused on the valuation of human casualties and injuries resulting from collisions with road vehicles, as evidenced in existing literature. Some researchers approach this by framing it as the expense of restoring the previous environmental state, akin to the evaluation of environmental aesthetics costs. This consists of mitigation expenditures, including the construction of road fences, wildlife crosswalks, wildlife grids, and the like. Further research is imperative to holistically assess the effects of transportation systems on biodiversity.

In the realm of water and soil pollution's societal costs, three distinct impacts are discerned in the literature: transport construction spills, operational spills, and stormwater management. The proposed LBCA already factors in hazardous material spills through the toxic release metric, including cleanup expenses, mitigation outlays, and property damage. Nevertheless, the intricacies of water and soil pollution extend beyond this scope. Accidents resulting in spills are quantifiable due to their evident impact scale, whereas maintenance and operational spills, though smaller, endure for longer periods and present monitoring challenges. The gradual accrual of pollutants in surface and underground waters complicates source attribution. Common pollution indicators encompass organic compounds and metals (Trumbull and Bae, 2000). In addition, detection and measurement, particularly for underground water, incur significant costs. Regarding stormwater management, impervious surfaces heighten pollutant deposition in remote areas and increase corrosion severity. Assessing this impact and its costs involves predicting the risk of inadequate space for stormwater drainage systems or the expenses associated with constructing retention basins to compensate for reduced natural drainage basins.

In recent years, research has increasingly focused on understanding the ecological impact of transportation. Key areas of investigation include microplastic pollution and light pollution. Regarding microplastic pollution, studies have examined the emissions of microplastics (i.e., TBPs and BWPs) from vehicles, distinguishing between emissions from cars and trucks, as well as the subsequent deposition of microplastics in both terrestrial and aquatic environments. Economic losses to the UK's aquaculture industry have also been analyzed. However, future research should investigate the impacts on humans and the adverse effects on marine life. The assessment of the costs associated with these consequences should encompass various aspects, including aquaculture, fisheries, human health, and property devaluation in regions marked by high pollution. This challenge necessitates a multidisciplinary approach, encompassing various fields such as behavioral mechanisms, the ingestion of microplastics by marine organisms, pollution levels in humans from water and seafood consumption, and the toxicity threshold for marine life and allergic reactions in humans. Collaborative research involving marine sciences, ecology, biology, chemical engineering, food science, epidemiology, and other disciplines is essential to comprehensively address this issue.

Turning to light pollution, current research is less comprehensive compared to microplastic pollution. Studies have predominantly focused on specific animal species (e.g., moths, birds, turtles) in proximity to light sources like lamp posts and port areas. There is a need to expand the scope and differentiate between transportation-induced light pollution and other sources of artificial light, such as buildings, public spaces, and advertising. Assessing the impact on human health is challenging due to the numerous factors influencing our quality of life. While some researchers suggest a link between artificial light and health issues like tumors, cancer, and sleep disorders, conducting controlled experiments across diverse living conditions and gathering sufficient data for conclusive results is difficult. Moreover, there is a lack of research quantifying the economic value of light pollution on both humans and ecosystems. Utilizing methods like the willingness-to-pay approach offers a promising means to assess associated costs to society.

Furthermore, as people increasingly prioritize environmental concerns and quality of life, it is imperative to conduct extensive research that keeps pace with technological advancements and socioeconomic shifts. Freight transportation is rapidly evolving with the emergence of various new technologies and operational improvements, including electric trucks and trains, hydrogen-powered trucks, autonomous driving, connected vehicles, automatic material handling, innovative pavement materials, lighter vehicles, increasing carload, and advancements in middle-mile and last-mile delivery, along with the use of drones, among others. Evaluating the impacts of new freight infrastructure projects now requires careful consideration of the development and adoption of these cutting-edge technologies and practices. However, unlike rail and waterway transportation, the energy intensity for trucks has not yet exhibited a clear downward trend (Vanek, 2019). The urgency for fast shipping trucks highlights an example where the push for small truck shipments impedes the adoption of new technologies and current best practices. Future research needs to facilitate the changes and make more comprehensive comparisons between different transportation modes. We anticipate that this report will serve as a valuable resource for academics, industry practitioners, and the general public, enabling them to make informed comparisons among different freight transportation options. Additionally, we hope that this report will inspire further research in this ever-evolving field.

Chapter 2

Stochastic Optimization of Intermodal Freight Transportation: A Case Study of the U.S. Southwest Supply Chain

Abstract

The growing complexities of global trade have intensified pressures on port operations and the intermodal transportation systems that support them. Despite advancements, the U.S. logistics sector continues to grapple with congested highways, extended transportation times, elevated costs, and increased greenhouse gas emissions. California's San Pedro Bay Port Complex (SPPC), the nation's busiest, is particularly impacted by these challenges. This study addresses logistical inefficiencies in the U.S. Southwest region, focusing on optimizing the inbound freight supply chain network originating from the SPPC. A two-stage mixed-integer stochastic programming model is developed to capture demand uncertainties across U.S. states and support informed decision-making under unpredictable conditions. The proposed system expands container classification beyond the port area to include potential hinterland warehouses in California, Utah, Arizona, and Nevada. By utilizing inland facilities, the system enables more cost-effective rail usage even for shorter distances, reducing truck reliance, alleviating highway congestion, lowering transportation costs, and improving resource balance in the port complex. Computational results reveal that the proposed system offers significant cost-saving potential, with a projected reduction of $1.611 billion over a 10-year period compared to current operations. Additionally, it improves rail transport cost-effectiveness and environmental performance by reducing greenhouse gas emissions, pollutants, congestion, and safety risks. Sensitivity analysis confirms the system's robustness under varying installation costs and warehouse capacity allocations. Overall, the study provides valuable insights into the trade-offs between transportation modes and demonstrates that strategic adjustments in warehouse capacities and logistics costs can optimize freight distribution while enhancing sustainability and system resilience.

2.1 Introduction

Intermodal transportation, characterized by the integration of multiple transport modes such as trucks, trains, and ships, plays a critical role in facilitating efficient and sustainable freight movement. By utilizing standardized containers across different modes, intermodal systems offer potential cost reductions of up to 40% compared to road-only transport solutions (CSX, 2023). Additional advantages of intermodal transportation include enhanced flexibility, increased throughput, and reduced environmental and social impacts. Despite these benefits, the U.S. freight transportation landscape remains dominated by trucking, which poses challenges for optimizing logistics networks and managing congestion at major transportation hubs.

A critical area where intermodal transportation is essential is port operations, particularly at major facilities such as the San Pedro Bay Port Complex (SPPC), which encompasses the Port of Los Angeles (POLA) and the Port of Long Beach (POLB). SPPC accommodated 29% of U.S. containerized international waterborne trade in 2023, representing 75% of such trade in the West Coast region (POLA, 2024). POLA has consistently ranked as the leading U.S. container port for the past 23 years. However, this strategic position also comes with significant operational challenges, including congestion, capacity constraints, and fluctuating demand patterns.

The port faces significant challenges due to a lack of workforce and equipment, which have led to extended waiting periods for vessels and trucks. On January 19, 2022, about 100 container vessels experienced considerable delays, waiting between 17.6 and 28 days for clearance to berth at the SPPC (Western Overseas Corporation, 2022). In some instances, these vessels were forced to reroute to other ports for unloading, requiring further transportation to return the freight to its intended port (McKenzie, 2023). The shortage of truck drivers has also contributed to the 81,258 delays recorded in 2021, with forecasts suggesting this figure could increase to approximately 160,000 by 2031 (American Trucking Associations, 2022). Labor shortages have further exacerbated container congestion, prompting Union Pacific to halt services at all inland rail ramps servicing the complex in June 2023 (LaRocco, 2023). This decision aimed to prompt shippers to reroute their cargo to alternative ports and ensure smooth rail operations to and from terminals. Additionally, slow productivity at terminals has led to trucks being denied access. Beyond these labor-related challenges, transportation bottlenecks are compounded by factors such as surging e-commerce demand, globalized supply chains, pandemic impacts, congested highways, aging infrastructure, environmental regulations, and insufficient public-private collaboration among ports, warehouses, and railroads, as well as among private-sector stakeholders such as different railroad ownerships.

In response to these challenges, researchers actively strive to comprehend and enhance port operations and associated transportation systems, aiming to facilitate smoother international trade. As a result, there is a strong emphasis on developing advanced optimization methods to manage these systems more effectively. Among these methods, stochastic programming has gained prominence for its ability to model the inherent uncertainties within these intricate systems, such as fluctuating demand, varying shipping times, and unpredictable external factors such as natural disasters, which collectively contribute to operational inefficiencies and increased costs.

While existing literature extensively examines port operations and associated transportation systems, this research presents a novel perspective by investigating the expansion of inland locations for the classification process in the context of demand uncertainty (see Section 2.3). Our objective is to optimize the cost of inbound container freight distribution by relocating the classification process to facilities such as distribution centers and warehouses, while also upgrading these traditional facilities to intermodal capabilities when they lack rail accessibility. This approach involves transporting containers directly from the port to these upgraded intermodal facilities across four states—California (CA), Utah (UT), Arizona (AZ), and Nevada (NV)—diverging from traditional practices where classification typically occurs at the port, on-dock rail terminals, near-dock rail terminals, or near-port satellite rail terminals (see Section 2.2 for further elaboration).

In addition to the financial aspects, we evaluate the ancillary benefits of our system by considering social and environmental factors. Implementing our proposed system is expected to significantly reduce environmental impacts, such as greenhouse gas emissions and criteria pollutants, while also addressing social concerns like overwhelmed sorting tasks and congestion in port areas. Furthermore, it will decrease dependence on truck transportation, thereby alleviating highway congestion and promoting more balanced resource utilization. By addressing these challenges, this research aims to contribute to the development of more resilient and cost-effective strategies for managing containerized freight within intermodal systems. Additionally, we conduct a sensitivity analysis to thoroughly assess the efficiency and impacts of the proposed system, taking into account variations in costs, demand levels, intermodal equipment installation costs, warehouse capacity, and other relevant factors. The findings are anticipated to support both academic and industry stakeholders in enhancing the efficiency and sustainability of logistics operations at major port complexes.

This paper is structured as follows: First, in Section 2.3, we provide a comprehensive literature review. Next, Section 2.4 offers a detailed description of the model we generated and the assumptions we made. In Section 2.5, we describe the data collection process and how we justified and finalized our parameters. Section 2.6 defines the parameter variables and presents the mathematical modeling. We then proceed to Section 2.7, where we discuss the outcomes of the model applied to the SPPC case. Lastly, in Section 2.8, we summarize our work, present our findings, and consider potential directions for future research.

2.2 Problem description

In this section, we provide a brief overview of the operations and current practices related to handling inbound containers. As illustrated in **Figure 2.1**, after being unloaded from vessels at the ports, containers are transferred to either the container

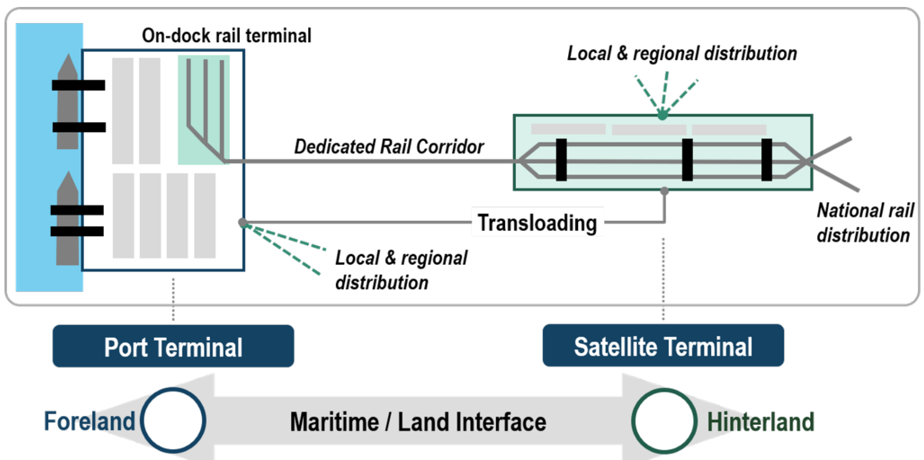

Figure 2.1: The insertion of a satellite terminal in port operations, adopted from Rodrigue et al. (2022).

terminal yard, rail terminal, classification yard, near-dock facility, or satellite terminal before being further transported via alternative modes to inland distribution areas. This process involves several activities, including determining container movement and placement within those locations, temporary storage until sufficient quantities for a unit train are met, container sorting, transferring cargo into domestic containers, consolidation, deconsolidation, transloading, or occasionally providing value-added services.

The container classification, also known as the sorting process, involves categorizing railcars based on various criteria such as railroad company, loaded or unloaded status, destination, car type, and the need for repairs (IntelliTrans, 2020). Subsequently, railcars are grouped to compose trains. Ideally, organizing railcars according to their destination enables trains to optimize efficiency by avoiding unnecessary stops at multiple intermediary rail yards. However, this efficiency is often hindered by limited space and overactivities at and around the port area, resulting in congestion and bottlenecks that increase costs.

Considering that conventional approaches to expanding capacity, such as enlarging port facilities or upgrading equipment for efficiency, may face limitations due to development constraints, the utilization of nearby facilities emerges as the favored solution. Specifically in the U.S., container unit trains frequently exceed the length of container port terminals. Consequently, cargo segments are consolidated at on-dock rail facilities and subsequently transported to nearby satellite rail terminals for complete unit train assembly (Rodrigue et al., 2022). Satellite rail terminals are connected to port terminals via either rail shuttle services or, more commonly, truck drayage services (Rodrigue, 2020) as depicted in **Figure 2.1**.

The current practice of employing satellite rail terminals as complementary to on-dock facilities at ports for classification aims to alleviate congestion, improve throughput, and facilitate the expansion of operational zones by diverting some freight traffic, cargo storage, and sorting activities to less crowded regions. Two primary shipment sorting methods are utilized at on-dock facilities: block swap and no-sort shuttle trains. In the block swap process, container car blocks are initially sorted at the on-dock facility for inland destinations, forming full-length trains. These trains are then transported to inland facilities to assemble destination-specific unit trains. Conversely, in the no-sort shuttle trains method, unsorted full-length trains are formed at the on-dock rail terminal and then transported to inland facilities for sorting into destination-specific unit trains. Both methods necessitate ample yard space for sorting operations.

To complement rail transport for non-local distribution, trucks are also utilized to retrieve containers from port terminals and transport them to distribution centers for cargo transfer into domestic containers. Subsequently, the trucks proceed to satellite rail terminals, where the cargo is transferred onto freight trains (Rodrigue et al., 2022). Regarding containers designated for local and regional distribution, typically assigned to trucks rather than railroads, they often linger at the port for prolonged durations, awaiting de-stuffing and restuffing into domestic containers. This process can take place at on-dock terminals or distribution centers. Once completed, trucks transport the containers to their destinations.

Despite the alteration in the sorting process, congestion persists predominantly due to all operations still being conducted close to the port area. In addition, this extensive process consumes significant time and resources and exacerbates shortages of drivers and port operators.

2.3 Literature review

The study of inland port locations, operational improvements, and related transportation enhancements to boost port efficiency has a long history. Operational optimization typically focuses on equipment, inventory levels, facility relocation, and resource scheduling within the port or its immediate vicinity. Molnar et al. (2018) examined the selection of a warehouse and its storage capacity to facilitate material transport through a reloading terminal and the seaport. Jula and Leachman

(2011) developed a mixed-integer non-linear programming model to optimize the supply chains for importers of waterborne containerized goods from Asia to the USA. Their goal is to minimize handling and inventory costs by determining the most suitable ports for inbound freight and selecting the appropriate land transportation modes. Chen et al. (2022) concentrated on regional empty container inventory management at inland freight stations. Cao et al. (2023) developed an integer linear programming model to analyze the impact of inland container depots on the efficiency of Yangshan Port, considering inter-terminal connections from the offshore port to satellite terminals. This research also focused on optimizing truck drayage operations within the port area.

Next, we will discuss the inland facility location problem, which is the focus of our study. This topic has been extensively studied using various approaches and focuses. For example, Rahimi et al. (2008) focused on the inland port for intermodal freight movement, particularly for the Ports of Los Angeles and Long Beach, with location choices restricted to five counties within 100 miles of the ports. Halim et al. (2016) used a multi-objective, multi-actor optimization approach to simultaneously optimize total logistics costs and client regions for European port-hinterland freight distribution networks. They formulated the problem as a Network Design Problem to optimize the location of distribution centers and demand allocation, restricting each demand region to be served by only one DC facility. Osorio-Mora et al. (2020) proposed a mixed-integer linear programming (MILP) model for capacitated multimodal, multi-commodity hub location problems (HLPs) that allows direct shipments between origins and destinations. Their model, however, does not account for uncertainties or externalities such as pollution and social costs. Shang et al. (2021) advanced the field by developing a stochastic multi-modal hub location problem that incorporates multiple capacity levels and mode-specific hubs within a hybrid hub-and-spoke (H&S) model, including direct links between spokes. However, this study limits each spoke to being served by a single, mode-specific hub, unlike ports where hubs can serve multiple modes and routes.

Sarmadi (2021) developed a stochastic programming approach to handle uncertain container demands, focusing on both strategic decisions (number and location of dry ports) and operational decisions (intermodal transportation of laden and empty containers, empty container repositioning, leasing, and inventory planning). They applied their model to a hypothetical dry port network design in North Carolina, assuming equal capacity for all destinations and constant unit transportation costs between location pairs. Zhang et al. (2022) addressed the stochastic incomplete multimodal hub location problem with multiple assignments and delivery-time restrictions. Their work considers mode-specific hubs and links, incomplete inter-hub connectivity, multiple assignment patterns for demand nodes, and two types of uncertainties. They conducted numerical experiments based on the Turkish network and AP dataset, evaluating both transportation costs and travel times, though the model does not include direct links between spokes.

In our research, we employ two-stage stochastic programs to address uncertain demand scenarios. Our study makes contributions in two main areas. Firstly, from a modeling perspective, we integrate several elements that are typically considered separately. We consider multiple warehouse locations with two transportation mode choices for multiple demand allocations at each destination. This allows multiple warehouses to serve each destination, rather than restricting each destination to be supplied by only one intermediate warehouse. Additionally, we allow direct flow from the source to destinations. The stochastic aspect of our problem captures the uncertainty of demand. We extend the existing models in the literature by situating container sorting warehouses in hinterland regions to obtain a new network design solution.

Secondly, regarding model implications, we offer insights into the design of inbound intermodal systems, using a real-world case study of the SPPC that utilizes more distant inland ports. We perform sensitivity analysis to compare various installation costs and probabilities of demand scenarios. Our cost considerations encompass a broad spectrum, including drayage, transloading, demurrage, storage at ports and warehouses, operating and administrative costs, and variable shipping costs. Additionally, we evaluate the performance of our proposed system by considering the impacts on greenhouse gas (GHG) emissions, alongside the financial aspects related to operations and transportation. This contributes to the field of sustainable supply chain and logistics, which requires more attention in the context of intermodal and marine transportation. Adopting our proposed system can reduce total costs, make rail transport profitable for shorter distances, and lower GHG emissions.

2.4 Problem statement

We chose the San Pedro Port Complex (SPPC) as our real-world case study, aiming to minimize the transportation impacts and costs of the inbound freight distribution system. Our strategy involves installing intermodal capability at potential locations to reduce dependence on the port's classification yard and minimize train assembly time. To address fluctuating demands, we develop a two-stage stochastic model. The process begins when containers arrive at the SPPC, from where they are dispatched by rail or truck to their final destinations or to intermediate nodes such as rail terminals, near-dock terminals, logistics centers, distribution centers, warehouses, and rail yards located in California and neighboring states, including Nevada, Utah, and Arizona. Traveling through multiple intermediate facilities is allowed. For instance, cargo could be initially transported by truck to a classification yard, then further moved to logistics center(s) before reaching the final destination as depicted in **Figure 2.2**. Solid lines indicate connectivity by rail systems, while dashed lines signify connectivity solely by truck systems. Orange nodes represent ports, logistics centers, and destinations with intermodal facilities, while grey nodes denote those without such facilities. Clear nodes represent final consumer destinations, which may or may not be equipped with intermodal facilities. Each node represents a distinct U.S. state. The dimly drawn lines and nodes form complete networks that extend beyond the scope of our decision problems.

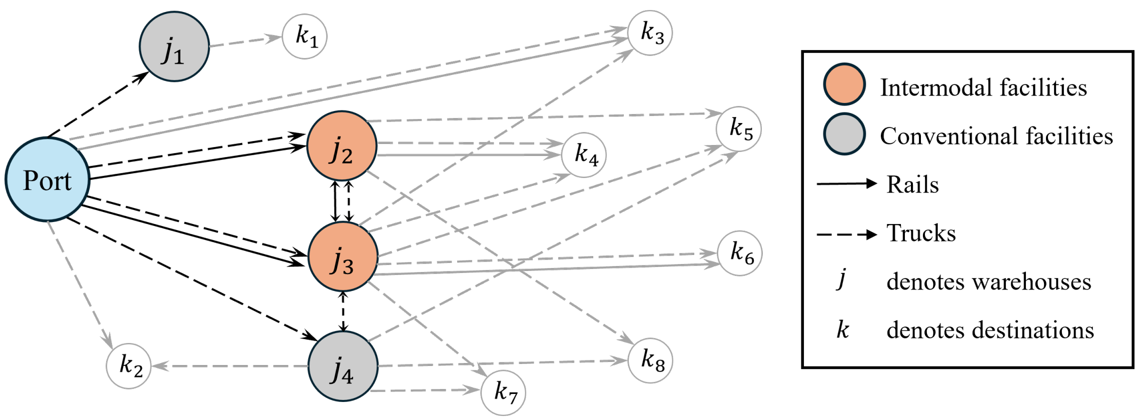

Figure 2.2: Proposed network of southwest supply chain.

To manage inbound containerized shipment flow and mitigate congestion, containers are loaded onto trucks or unsorted full-length trains at port areas. These trains are subsequently expedited to available warehouses regardless of their final destination. Once sorted at those warehouses, containers are transported to their destinations by trucks for shorter distances and railroads for longer distances. We make the following set of assumptions:

- The classification process in our proposed handling strategy is carried out at intermodal logistics centers. This approach relocates portions of the classification process that require significant time and space to less congested areas, thereby reducing congestion around the port.
- Traditional high fixed costs associated with railroads are also reduced. For example, the loading process no longer requires extra steps, such as unloading from ships and storing goods in container yards for extended periods until they can be grouped with others destined for the same location. Additionally, the steps of loading sorted containers onto railcars and sorting railcars to form a unit train are eliminated. Consequently, the process is expected to be faster and more cost-effective as explained in 2.6.1.
- Exclusively assembling full trains for transportation, while trucks manage both full truckload (FTL) and less-than-truckload (LTL) shipments. FTL shipments fill an entire truck, whereas LTL shipments combine smaller shipments from various customers into a single truck.
- In the first stage of decision-making, at the strategic level, the selection of warehouses to be equipped with intermodal capabilities will be made annually. Once installed, these capabilities will remain in place until the end of our 10-year analysis period. The second stage involves annual flow allocation. All parameters associated with the decision variables, including costs, capacity,

and demand, are calculated on a per-year basis. This stage does not reflect operational behaviors but is intended to provide a strategic overview.

- As mentioned previously, the connections between warehouses and destinations are not within our decision-making scope. Therefore, the mode of transportation and the percentage of freight sent to each destination are predefined. For distances over 500 miles, transportation will be designated to rail, while for distances less than 500 miles, trucks will be used.

2.5 Parameter justification

In this section, we describe the parameters used in this study and our approach to determining them, including annual demand, logistics centers' capacity, intermodal capability installation costs, transportation costs, and the costs associated with environmental and social impacts. The predicted commodity data and flow for U.S. freight are based on the Analysis Framework Version 5.6 (FAF5) dataset (Bureau of Transportation Statistics, 2022a). We filtered the dataset to include only import-related shipments that enter the U.S. through California and then used the distribution data to track the flow of these imports to 49 destinations, covering all U.S. states plus Washington, D.C., excluding Alaska and Hawaii, which have minimal ground transportation and no direct rail access from California. FAF5.6 provides forecasts up to 2050, with data available every five years (e.g., 2025, 2030, ...).

We then estimate the delivery flow proportions for each destination k at time t, denoted as α_{kt} in the model, using baseline values derived from the 2022 GDP data reported in U.S. Bureau of Economic Analysis (2023), as shown in **Table 2.1**, then vary this α_{kt} for year 2025 to 2034 based on scenarios generating explaining in section 2.6.3). This parameter regulates the flows from warehouses to multiple destinations, reflecting the mixed nature of cargo arriving at each warehouse. This characteristic aligns with our proposed classification system, where cargo is not classified before

Table 2.1: Real gross domestic product for 2022-2023 (adopted from U.S. Bureau of Economic Analysis (2023)), with the additional parameter estimated by the authors

	Real GDP (Millions of Chained 2017 Dollars)				Percent Change from Preceding Period[1]				α_k
Area	**2022**	**Q1 2023**	**Q2 2023**	**Q3 2023^p**	**2022**	**Q2 2023**	**Q3 2023^p**	**Rank Q3**	
United States	21,822,037	22,112,329	22,225,350	22,490,692	1.9	2.1	4.9	–	-
New England	1,140,308	1,148,112	1,153,162	1,166,373	2.2	1.8	4.7	–	-
Connecticut	276,669	279,910	280,440	283,694	2.9	0.8	4.7	27	0.01277
Maine	72,414	73,053	73,165	74,048	2.2	0.6	4.9	19	0.00334
Massachusetts	604,358	607,175	611,515	618,655	2.1	2.9	4.8	25	0.02789
New Hampshire	90,150	90,448	90,610	91,607	0.3	0.7	4.5	31	0.00416
Rhode Island	62,191	62,656	62,758	63,363	2.3	0.7	3.9	40	0.00287
Vermont	34,609	34,940	34,777	35,114	2.2	-1.9	3.9	39	0.00160
Mideast	3,814,224	3,829,133	3,841,282	3,879,022	1.9	1.3	4.0	–	-
Delaware	75,173	73,902	73,770	74,362	1.0	-0.7	3.3	45	0.00347
District of Columbia	144,030	144,558	145,118	145,996	0.9	1.6	2.4	–	0.00665
Maryland	412,283	417,983	419,681	422,486	1.6	1.6	2.7	48	0.01903
New Jersey	646,731	648,549	652,278	659,893	2.8	2.3	4.8	26	0.02984
New York	1,763,525	1,765,091	1,766,900	1,781,963	2.3	0.4	3.5	44	0.08138
Pennsylvania	772,336	778,915	783,389	794,150	1.0	2.3	5.6	14	0.03564
Great Lakes	2,825,277	2,832,060	2,841,882	2,871,316	1.3	1.4	4.2	–	-
Illinois	864,171	868,023	870,491	879,379	1.3	1.1	4.1	35	0.03988
Indiana	396,009	397,045	398,426	403,085	3.1	1.4	4.8	23	0.01827
Michigan	539,898	542,892	545,802	549,715	1.6	2.2	2.9	47	0.02491
Ohio	689,681	690,707	693,891	701,714	0.5	1.9	4.6	29	0.03183
Wisconsin	335,688	333,601	333,496	337,598	0.4	-0.1	5.0	18	0.01549
Plains	1,335,232	1,353,681	1,360,688	1,377,878	1.1	2.1	5.1	–	-
Iowa	197,846	198,852	199,355	201,358	-0.3	1.0	4.1	37	0.00913
Kansas	174,795	177,763	180,967	185,207	1.1	7.4	9.7	1	0.00807
Minnesota	379,112	380,654	381,281	385,131	1.2	0.7	4.1	36	0.01749
Missouri	336,626	341,789	341,731	345,061	2.0	-0.1	4.0	38	0.01553
Nebraska	137,078	141,330	143,365	145,983	2.7	5.9	7.5	3	0.00633
North Dakota	54,799	57,327	57,848	58,267	-1.1	3.7	2.9	46	0.00253
South Dakota	54,959	55,771	55,910	56,629	-0.3	1.0	5.2	15	0.00254
Southeast	4,735,643	4,829,724	4,846,562	4,904,756	2.7	1.4	4.9	–	-
Alabama	235,807	239,693	239,849	242,299	1.7	0.3	4.1	34	0.01088
Arkansas	137,356	140,575	140,438	140,678	1.3	-0.4	0.7	50	0.00634
Florida	1,218,430	1,260,692	1,267,911	1,286,673	4.6	2.3	6.1	8	0.05623
Georgia	655,827	655,663	656,155	663,389	2.6	0.3	4.5	30	0.03026
Kentucky	217,568	222,364	223,822	226,517	1.4	2.6	4.9	21	0.01004
Louisiana	231,262	234,459	236,325	240,105	-1.2	3.2	6.6	5	0.01067
Mississippi	114,153	114,987	114,474	114,691	0.0	-1.8	0.8	49	0.00527
North Carolina	609,058	619,470	621,116	628,133	2.0	1.1	4.6	28	0.02811
South Carolina	250,873	256,422	257,600	261,199	2.5	1.8	5.7	12	0.01158
Tennessee	412,101	421,438	422,195	427,540	3.9	0.7	5.2	16	0.01902
Virginia	576,964	585,051	587,013	593,102	2.5	1.3	4.2	32	0.02663
West Virginia	76,526	79,007	79,711	80,446	1.3	3.6	3.7	41	0.00353
Southwest	2,620,457	2,701,729	2,730,403	2,777,533	2.5	4.3	7.1	–	-
Arizona	403,474	409,514	411,009	415,961	3.2	1.5	4.9	20	0.01862
New Mexico	101,315	103,746	104,692	106,161	1.8	3.7	5.7	11	0.00468
Oklahoma	191,583	198,201	200,415	203,343	-1.0	4.5	6.0	9	0.00884
Texas	1,924,007	1,989,852	2,013,780	2,051,491	2.7	4.9	7.7	2	0.08879
Rocky Mountain	812,969	824,637	829,993	841,966	2.3	2.6	5.9	–	-
Colorado	416,114	422,277	424,981	430,996	2.2	2.6	5.8	10	0.01920
Idaho	91,684	93,570	93,775	95,386	4.2	0.9	7.0	4	0.00423
Montana	53,983	54,538	54,856	55,424	1.9	2.4	4.2	33	0.00249
Utah	213,898	215,856	217,161	220,396	1.9	2.4	6.1	7	0.00987
Wyoming	37,294	38,359	39,167	39,713	1.0	8.7	5.7	13	0.00172
Far West	4,385,658	4,439,121	4,468,462	4,521,933	1.0	2.7	4.9	–	-
Alaska	50,315	52,167	52,779	53,246	-1.4	4.8	3.6	43	0.00232
California	3,167,461	3,191,531	3,213,435	3,251,275	0.7	2.8	4.8	22	0.14617
Hawaii	85,211	86,337	86,472	87,268	1.3	0.6	3.7	42	0.00393
Nevada	187,226	189,320	190,176	193,114	3.4	1.8	6.3	6	0.00864
Oregon	254,708	257,380	258,495	261,516	1.8	1.7	4.8	24	0.01175
Washington	641,144	662,661	667,408	675,813	1.6	2.9	5.1	17	0.02959

Note: ^{p} is preliminary. [1] Quarterly percent changes shown are annualized—that is, they are a percent change from the preceding period at annual rates.

reaching the warehouses. α_{kt} defines the assignment of freight to various destinations, ensuring that each warehouse sends a diverse mix of freight that is subsequently classified for distribution to its assigned destinations, thus capturing the dynamic behaviors of the model.

The data collection challenge involves obtaining warehouse capacity data and locations. We gather real-world GIS data to capture capacity and functionality of 249 locations, including warehouses, distribution centers, logistic centers, and rail terminals spread across four states: CA, NV, AZ, and UT. Given that this data is not publicly accessible, we justified our estimates by considering various factors, such as warehouse space, number of rail doors, storage capacity, and annual lift. In cases where details were unavailable, we assumed the warehouse was relatively small with a space of 10,000 sq. ft, based on the data available from similar warehouses, resulting in an estimated annual capacity of 45,590 tons. This assumption is designed to ensure that the cumulative capacity of all our warehouses aligns closely with the total amount of inbound freight. When rail capability data is unavailable, we utilize Google Maps to determine whether there is a rail track leading to the location. Additionally, for all warehouses' capacity data, we assume that only 40% of each warehouse's capacity will be used to handle the inbound freight in our system, leaving the remaining 60% for other activities such as serving domestic shipments, outbound freight, or engaging in value-added activities.

To evaluate the total cost, we included the following operational costs per ton-mile: \$0.2225 for trucks and \$0.0302 for rails, based on data generated from the research conducted by Rattanakunuprakarn et al. (2024). These numbers are presented in 2020 dollars per ton-mile, encompassing costs solely related to operating metrics, such as energy, labor and administration, maintenance of transportation assets, end-of-life asset value, transport equipment, and maintenance of transport equipment.

For tonnage and vehicle capacity parameters, we base our assumptions on 16 tons per TEU. This figure is calculated based on data published by the Port of Long Beach (2024) including total tonnage of containerized commodity, number of loaded TEU, and number of empty TEU. Additionally, for Class I railroads, we consider an average ton loaded per railcar of 52.9 tons per railcar (Rattanakunuprakarn et al., 2024).

2.6 Mathematical formulation

This section presents a detailed mathematical model for optimizing transportation costs under demand uncertainty. The model is designed to identify the optimal allocation of containers across a network of warehouses, on-dock terminals, and destination points while minimizing overall transportation costs. The approach integrates long-term strategic decisions with short-term operational considerations to ensure robust and cost-efficient logistics planning under varying demand conditions.

2.6.1 Model assumptions and scope

The model is built on several key assumptions that define its scope, structure, and practical applicability. One central assumption is that decisions regarding network upgrades, such as converting existing warehouses into intermodal facilities, are made annually. Any upgrades decided upon in a given year will take effect in the following year. Once a warehouse is upgraded to an intermodal facility at time t, it will maintain this intermodal status from time $t+1$ onward, and continue serving as an intermodal hub for the remainder of the analysis period, which spans the next decade.

Truck movement. Trucks can pick up containers from the port after they have been classified at the on-dock facility and then proceed directly to their destination. This direct flow to the destination, utilizing on-dock facilities, is represented by our (Z_{ikts}) variable. Alternatively, trucks can pick up unclassified containers and stop at near-dock or off-dock locations before heading to their destination. This flow from the port to the warehouse corresponds to our ($Y_{jts}^{m=1}$) variable. Additionally, trucks can stop at multiple immediate near-dock and off-dock locations. For instance, a truck carrying international containers—commonly 40-foot containers, which account for approximately 90% of waterborne containers (Bureau of Transportation Statistics, 2024)—might first deliver these to a warehouse for transloading into domestic containers (53 feet) before proceeding to a second intermediate location, such as a rail terminal, where the domestic containers are loaded onto rail for later delivery to the final destination. This flow between two intermediate warehouses is represented by our ($W_{jbts}^{m=1}$) variable.

Classification of facilities. Warehouses, rail terminals, and distribution centers are classified into three categories based on their proximity to the port: on-dock facilities, which are located within the port area; near-dock facilities, positioned close to the port; and off-dock facilities, situated farther away. In our proposed system, each transportation route from the port to a destination is exclusive in its use of these facilities. For example, Direct Shipment (Z_{ikts}) involves cargo classification taking place at the on-dock facility at the port. In contrast, Indirect Flow (Y_{jts}^{m}) bypasses the on-dock facility, with cargo being transferred from vessels to rail without classification at the port. Instead, this flow proceeds to near-dock or off-dock facilities, where the classification occurs.

Transportation mode for last connection to destinations. For both direct flow from the port to destinations (Z_{ikts}) and flow from warehouses to destinations (V_{jkts}), the decision variables (Z_{ikts}) and (V_{jkts}) will only determine the amount of tonnage freight traveling to each destination for each location pair; they will not specify the transportation mode. The mode of transportation will be assigned based on the distance between each location pair: distances of less than 500 miles will utilize trucks, while distances of 500 miles or more will rely on rail transport. For freight transported by rail to the destination, we assume a drayage cost of \$35.667 per ton (71.334/2) associated with using trucks for the final delivery service.

Variable shipping costs. Variable shipping costs are influenced by several factors, including distance traveled, weight carried, mode of transportation, and specific activities required at each network connection. For instance, flow Z_{ikts} transported by rail will incur drayage costs, which cover the transportation of cargo by truck from the final rail destination to the end consumers. Additionally, storage costs, loading/unloading costs, and warehouse operation costs are assumed to depend solely on the weight carried and the mode of transportation selected.

Freight proportion. α_{kt} is the proportion of freight from each warehouse to the destination that captures the model's dynamic behaviors and facilitates the unclassified operations at the port to form a train to an intermodal logistic center. α_{kt} remains constant for each transfer train, regardless of which intermodal logistic center that train serves. For more details on how to define α_{kt}, please refer to Section 2.5.

Next, we will outline the assumptions governing current practices and those proposed for our system. The model distinguishes between the current logistics practices and those proposed for the upgraded system, incorporating various parameter changes to reflect improvements in processing efficiency and the introduction of additional connections to intermediate locations. These assumptions encompass different sets of parameter, different sets of nodes, and different transportation connecttions. We explain the assumptions we made and how the costs are different.

Current practice assumptions

In the current transportation system, freight is primarily transported to on-dock or near-dock rail terminals via drayage trucks. We estimated Demurrage/storage (D/S) costs at the port at $1.552 per ton, calculated based on an average dwell time of 4.3 days (Biggar, 2023). Notably, the initial 4 days do not incur charges, but any fraction of a day is treated as a full day, the charge is $24.83 per container per day (Los Angeles Harbor Department, 2023). Given that one TEU averages 16 tons, the resulting cost per ton is $1.552. Containers assigned to warehouses via truck transport incur no D/S costs due to their shorter average dwell time of 3.2 days (Biggar, 2023). However, exceptions exist for truck-assigned containers transported directly from the port to final destinations, which are subject to D/S costs due to container sorting and waiting time for truck pickup. For containers sorted at the port and assigned to rail for final destinations, loading/unloading (L&UL) costs are incurred in addition to D/S costs, amounting to \$17.01 per ton. This figure is derived from L&UL costs of \$900 per railcar divided by 52.9 tons per railcar.

The assumption of rail fixed costs, i.e., L&UL, at \$900 per railcar is based on railcar equipment costs, indicating that using rail or multi-modal transit adds about \$900 per railcar shipment (RSI Logistics, 2024). Regarding D/S costs at rail terminals, the cost for railcars at Barstow, CA BNSF terminals was estimated at \$9.375 per ton. This figure is based on an average dwell time at rail terminals of 42.3 hours (BNSF, 2024c), with the charge for one day calculated from the difference between the free time of 24 hours (BNSF, 2024a) and the dwell time of 42.3 hours, amounting to \$150 per container. When divided by 16 tons, the resulting cost is \$9.375 per ton. For inbound containers initially handled by trucks, we have assumed that D/S costs at rail terminals are not applicable. This assumption is based on the understanding that the processing time of trucks is relatively short compared to rail operations. Therefore, we assume that the dwell time for trucks at warehouses and rail terminals will be less than the free time of 24 hours, only slightly shorter compared to the average rail dwell time of all rail terminals at 28.1 hours (BNSF, 2024c).

Warehouses accumulate operating and administrative (O&A) expenses averaging \$2.62 per ton. This calculation is derived from the combined O&A costs across all warehouses, divided by their annual freight-handling capacity. The total O&A costs for all warehouses are estimated based on the square footage allocated to inbound freight in our system and the average cost per square foot. The average annual cost to rent warehouse space is \$7.96 per square foot, with additional operating expenses ranging from \$2 to \$5 per square foot (Warehouse and Fulfillment, 2024). These operating expenses include electricity, janitorial services, water, internet, taxes, and insurance. For the 122 warehouses with unknown capacity, we assumed a standard size of 10,000 square feet. Furthermore, the L&UL cost at the warehouses is assumed to be equivalent to that of the port and rail terminal, set at \$17.01. This estimate is based on the assumption of a \$900 cost per railcar, consistent with the port, due to the lack of updated cost data for performing L&UL operations at intermediate warehouses in the proposed system. These cost assumptions will be varied in the sensitivity analysis to assess the impact of potential changes. These costs will be varied for the impact change in sensitivity analysis. Additionally, warehouse operating costs encompass D/S costs, adopting the same cost as D/S at rail terminals, which is \$9.375 per ton for warehouses in proximity to the port area. For off-dock warehouses farther away, we assume a cost of \$0.3776. This figure was calculated using data from the BNSF 2020 R-1 report in Schedule 410 (Surface Transportation Board, 2022). BNSF recorded an operating income of \$193,279,000 from demurrage charges associated with freight-related revenue and expenses. We divided this D/S cost by the total tons handled, 511,801,000 in 2020, as per the R-1 report in Schedule 755. Consequently, on average, demurrage costs at rail facilities amounted to \$0.3776 per ton.

Proposed system assumptions

In the proposed system, with a presumed reduction of 6.98% in dwell time for containers assigned to rail at the port, the average dwell time falls below 4 days. This effectively eliminates D/S costs at the port associated with rail transportation. Additionally, D/S costs at the port remain at zero for trucks, assuming the new system does not increase dwell times for containers designated for truck transportation. However, if both trucks and rails are assigned to pick up cargo destined for the final destination, they must wait for the sorting process at the port, thus incurring D/S costs at the port as per the current practice (\$1.552 per ton for trucks and \$17.01 per ton for rails).

The key distinction of the proposed system is that it allows cargo to be transloaded directly from vessels to trains at the port without considering the final destination during the train formation process. This approach reduces the need for additional truck movements to store cargo at port facilities or rail terminals before transferring to rail, thereby lowering the associated L&UL costs. As a result, the L&UL cost for rail at the port is assumed to decrease to \$3.78 per ton, calculated from \$200 per rail car with an average capacity of 52.9 tons. This assumption is consistent with the Chargeable Events Demurrage rates published by Union Pacific Railroad (2024a), where charges range from \$105 to \$3,150 depending on factors such as freight type, L&UL locations, and other conditions. It is important to note that, in this context, Chargeable Events Demurrage—as defined by Union Pacific—refers specifically to the costs associated with the loading and unloading of railcars (Union Pacific Railroad, 2024b).

Comparison of truck and rail transportation costs

For trucking, the shipping cost per ton is competitive for short hauls up to approximately 500 miles, priced at \$0.2225 per ton-mile, based on the operating metric in the research by Rattanakunuprakarn et al. (2024), with an additional initial cost of \$19.268 per ton, estimated by Fayek (2021), where a comparison graph between rail and truck transportation indicates that the total cost at a distance of 0 for a TEU container is approximately \$180 for trucks. To convert this cost per TEU to cost per ton, we used data from the Port of Houston, as this study collected data based on a case study of the port. In 2023, the port handled 50,323,264 tons of all kinds of commodities (Port Houston, 2024a), with 71% being containerized cargo (Port Houston, 2024b), equivalent to 35,729,517.44 tons. Dividing this number by the 3,824,600 TEUs handled that year (Port Houston, 2024a) gives an average of 9.342 tons per TEU. Therefore, dividing \$180 per TEU by 9.342 tons per TEU yields an initial cost of \$19.268 per ton for using trucks.

On the other hand, rail shipping costs are relatively low at \$0.03 per ton-mile. Nevertheless, there are three additional initial costs associated with rail transportation even before the rail journey commences. These include: 1) Drayage costs at origin and destination, totaling \$71.334 per ton. 2) Transloading costs, amounting to \$17.01 per ton each time, for loading and unloading railcars at both origin and destination. 3) D/S costs at rail terminals, totaling \$9.375 per ton each time.

The drayage cost of \$71.334 per ton was derived from a drayage cost of \$666.4 per TEU based on the research by Fayek (2021), which indicates that the total cost at a distance of 0 for a TEU container is approximately \$680 for rail. According to the research, drayage accounts for 98% of this cost, resulting in \$666.4 per TEU. To determine the drayage cost per ton, we use the same method as for trucks, dividing by the average of 9.342 tons per TEU based on Port of Houston data (Port Houston, 2024a). Therefore, the drayage cost of \$666.4 per TEU translates to \$71.334 per ton. The transloading costs of \$17.01 per ton and D/S costs at rail terminals of \$9.375 per ton were previously explained in the Current Practice Assumptions and Parameters section.

The cumulative sum of these three costs is \$124.104. The interplay between these expenses indicates that rail transportation becomes cost-competitive at distances exceeding 645.367 to 545.169 miles. This distance is consistent with the general ranges established by researchers (Hu and Zhang, 2020; Rodrigue, 2024). The initial cost of the proposed system \$92.218 comes from $71.334\ /2 + 17.01 \times 2 + 3.781 + 9.375 \times 2$. as shown in **Figure 2.3**

According to Azimi et al. (2021), a 15 percent reduction in drayage costs would make rail intermodal competitive with trucks for hauls over 400 miles. With a 25 percent reduction, rail intermodal could be feasible even for distances under 400 miles. Furthermore, if issues related to drayage, terminal capacity, location, and configuration can be addressed, rail intermodal could compete with with trucking over distances as short as 150 miles.

2.6.2 Parameters and decision variables

The problem formulation uses a variety of parameters and decision variables, capturing aspects such as transportation costs, warehouse capacities, rail accessibility, and demand levels. A comprehensive list of notations and definitions is provided in **Table 2.2**, **Table 2.3**, and **Table 2.4**.

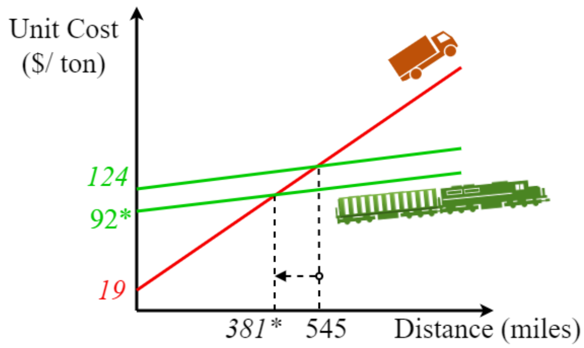

Figure 2.3: Rail and truck transportation costs.

Table 2.2: Definition of sets and indices

Sets	Definitions	Indices	Definitions
I	set of on-dock facilities	i	index for on-dock facilities, $i \in I$
J	set of candidate logistic warehouses	j	index for logistic warehouse $j \in J$
K	set of destinations	k	index for destination $k \in K$
T	number of planning horizon periods	t	index for time $t \in \{1, 2, ..., T\}$
S	set of expected demand scenarios	s	index for scenarios $s \in S$
		m	index for modes $m \in \{0, 1\}$ where 0 is trucks and 1 is rails

Table 2.3: Definition of parameters

Parameters	**Definitions**
c_j	one-time fixed infrastructure investment cost associated intermodal capability installation at warehouse $j \in J$
μ_j^m	variable costs per ton for mode $m \in \{0,1\}$ from the port to warehouse $j \in J$
γ_{jb}^m	variable costs per ton for mode $m \in \{0,1\}$ from warehouse $j \in J$ to warehouse $b \in J \setminus \{j\}$
δ_{jk}	variable costs per ton for the most cost-effective mode from warehouse $j \in J$ to destination $k \in K$
σ_k	variable costs per ton for the most cost-effective mode from the port to destination $k \in K$
e_j	capacity of warehouse $j \in J$
e_i	capacity of on-dock facilities $i \in I$
d_{kts}	annual demand at destination $k \in K$ at time $t \in T$ under scenario $s \in S$
B_t	budgets for intermodal capability installation at time $t \in \{1, 2, ..., T\}$
$a_{j1} \in \{0,1\}$	indicate whether warehouse $j \in J$ initially has the intermodal capability at the beginning of time $t \in \{1\}$
$\alpha_{kt} \in [0,1]$	percentage of containers shipped to destination $k \in K$ at time $t \in \{1, 2, ..., T\}$
$\rho_s \in [0,1]$	probability of the occurrence of scenario $s \in S$
$M = 10^6$	Big M value used for logical constraints

Table 2.4: Definition of decision variables

Variables	**Definitions**
$X_{jt} \in \{0,1\}$	1, if intermodal capability is installed at warehouse $j \in J$ at year $t \in \{1,2,...,T\}$; 0, otherwise. The warehouses will become intermodal facilities at time $t = t+1$
$a_{jt} \in \{0,1\}$	1, if warehouse $j \in J$ has the intermodal capability at the beginning of year $t \in \{2,3,...,T\}$; 0, otherwise
$Y^m_{jts} \in \mathbb{R}^+$	annual amount of freight shipped from the port to facility $j \in J$ by transportation mode $m \in M$ at time $t \in \{1,2,...,T\}$ under scenario $s \in S$
$W^m_{jbts} \in \mathbb{R}^+$	annual amount of freight shipped from facility $j \in J$ to facility $b \in J \setminus \{j\}$ by transportation mode $m \in M$ at time $t \in \{1,2,...,T\}$ under scenario $s \in S$
$V_{jkts} \in \mathbb{R}^+$	annual amount of freight shipped from warehouse $j \in J$ to destination $k \in K$ by the most efficient transportation mode at time $t \in \{1,2,...,T\}$ under scenario $s \in S$
$Z_{ikts} \in \mathbb{R}^+$	annual amount of freight shipped directly from on-dock facility i to destination $k \in K$ by the most efficient transportation mode at time $t \in \{1,2,...,T\}$ under scenario $s \in S$

2.6.3 Scenario generation and representation

To account for inherit uncertainties influencing transportation costs within our intermodal freight transportation problem, we consider two key aspects: potential demand variability, which reflects fluctuations in the total annual cargo volume, and destination allocation dynamics, representing changes in the percentage of cargo distributed to each destination. These factors capture the variability in both the overall demand and the shipping patterns. Effectively capturing these uncertainties is crucial for developing robust decision-making frameworks. This section describes the methodologies used to generate multiple demand scenarios (d_{kts}) and destination distribution scenarios (α_{kts}), forming possible scenarios used in our stochastic model.

Historical data analysis, a common approach in forecasting, was employed to capture the uncertainty associated with freight demand (d_{kts}) and derive probable future demand scenarios. For identifying annual fluctuations and long-term demand trends, We utilized data from FAF5.6 (Bureau of Transportation Statistics, 2022a), which records the weight of commodities shipped in thousand ton-miles by origin-destination pairs in the State-Level Annual Data. Our analysis specifically focuses on import freight arriving in the U.S. via California by waterway, filtering out domestic and export shipments. For the distribution of these imported goods from California to destinations within California and other states, we excluded domestic transportation modes of Pipeline, Water, Air, Other, and Unknown, retaining only data for domestic transportation by Truck, Rail, and Multiple Modes & Mail. This dataset includes actual figures for 2022, with demand projections available in five-year intervals from 2025 to 2050. We applied linear interpolation to estimate annual tonnage and forecast demand from 2025 to 2034 in the low, medium and high demand projections. The annual tonnage across these years is summarized in **Table 2.5**. To account for variability, the low demand projection was adjusted to be 0.8 times the anticipated low demand, while the high demand projection was set to 1.2 times the expected high demand.

Table 2.5: Demand projections by year for Low, Medium, and High scenarios

Year	Lo Demand	Mid Demand	Hi Demand
2025	67806.34025	85638.27521	108386.3877
2026	69487.67291	87738.74282	110456.2786
2027	71169.00556	89839.21042	112526.1695
2028	72850.33822	91939.67802	114596.0604
2029	74531.67088	94040.14563	116665.9513
2030	76213.00353	96140.61323	118735.8422
2031	77815.08078	98289.97142	121863.5635
2032	79417.15803	100439.3296	124991.2848
2033	81019.23527	102588.6878	128119.0061
2034	82621.31252	104738.046	131246.7274

To capture destination distribution scenarios (α_{kts}), we applied heuristic approaches to generate scenarios based on two years of historical GDP data. We utilized data from the Bureau of Economic Analysis (BEA), specifically the Gross Domestic Product by State reports released in 2023 and 2024 (U.S. Bureau of Economic Analysis, 2023, 2024). Comparing these two releases reveals significant unpredictability in GDP changes. For instance, in Oklahoma, GDP decreased by 1% in 2020 compared to the previous year; however, it increased by 7.2% in 2023, marking the third-largest increase among all states. In contrast, Kansas experienced a GDP increase of 1.1% in 2022, followed by a 3.6% rise in 2023, but then saw a decline of 6% in the first quarter of 2024 compared to the preceding period. Given that historical data alone do not reveal clear trends in GDP behavior, we developed multiple potential destination allocation cases, assuming variations in GDP changes for each year t and each destination k (comprising U.S. states and Washington, DC, excluding Hawaii and Alaska).

Destination allocation cases in the stochastic model are structured systematically to enable meaningful interpretation. We consider potential demand allocation trends, including random variability and the creation of case groups that reflect specific changes. This organization facilitates the assessment of the impact of individual or combined changes on distribution patterns. The cases are categorized as follows:

1. **Baseline Scenario**: Represents the current or expected distribution.

2. **Perturbation Scenarios**: Adjust cargo allocations for specific states while keeping others proportional. For example, increase California's allocation by 20% while proportionally decreasing the allocations for other states.

3. **Stress Scenarios**: Simulate extreme conditions, such as a significant 50% increase in allocation for one state or region, to test the effects of over-concentration. Region classification includes five regions: Northeast, Southeast, Midwest, Southwest, and West.

4. **Random Variations**: Apply random fluctuations within the range of $\pm 10\%$ to all states in base case.

Due to the computational memory limitations of our Gurobi running mode, we generate a total of 16 types of destination allocation scenarios, which, when combined with three demand projection ranges, yield a total of 48 scenarios. The 16 destination allocation scenarios consist of one baseline case, six perturbation cases, six stress cases—targeting stress on California (CA) and five other regions—and three random variation cases with a variation range of $\pm 10\%$. To maintain consistency across all scenarios, the total demand across all states (destinations) is preserved by re-normalizing the demand values to ensure they sum to the annual demand. The random variation ranges are defined based on historical fluctuations in Gross Domestic Product (GDP) reported by the Bureau of Economic Analysis (BEA).

Together, the 16 destination allocation scenarios combined with the three demand projection ranges constitute a comprehensive set of 48 scenarios that address model uncertainties. As summarized in **Table 2.6**, this scenario set captures uncertainties arising from both demand variability and destination allocation.

2.6.4 Two-stage stochastic programming

To effectively capture the complexity of logistics planning under uncertainty, the model is formulated as a two-stage stochastic program. In the first stage, long-term strategic decisions are made to identify optimal locations for logistics centers equipped with intermodal facilities, improving accessibility to railroad systems and reducing transportation costs. This strategic design serves as a foundation for the second-stage problem, which deals with the operational aspects of transporting containers through the network over an extended period.

The second stage is formulated as a network flow problem, addressing annual transportation operations over a ten-year planning horizon. It determines the most efficient routing strategies and allocates the optimal quantities of containers to be

Table 2.6: Scenario table with detailed changes and expected effects.

No	Scenario Name	Change Description	Expected Effect
1-3	Baseline 1, 2, & 3	Original distribution across different levels of annual demand (i.e., low, medium, and high).	Control scenario for comparison
4-6 7-9 10-12 13-15 16-18 19-21	Perturbation CA Perturbation Northeast Perturbation Southeast Perturbation Midwest Perturbation Southwest Perturbation West	+10% increases in the allocations for California . with other states adjusted proportionally across different levels of annual demand (i.e., low, medium, and high)	Examines incremental allocation impacts per state and region
22-24 25-27 28-30 31-33 34-36 37-39	Stress CA Stress Northeast Stress Southeast Stress Midwest Stress Southwest Stress West	+30% allocation increase for California or all states in the selected region, others adjusted proportionally across different levels of annual demand (i.e., low, medium, and high).	Identifies sensitivity to allocation spikes per state and region
40-42 43-45 46-48	RandomVariation 1 RandomVariation 2 RandomVariation 3	3 different random demand allocation changes within a continuous range of $\pm10\%$, maintaining sum-to-one constraint.	Simulates unstructured small-scale deviations to assess robustness

transported via rail and truck to each designated location. This hierarchical approach ensures that the model balances strategic planning with tactical and operational decision-making.

First-stage problem: strategic network design

The first-stage problem focuses on long-term strategies for network design. This includes selecting logistic centers that should be upgraded with intermodal facilities to enhance connectivity to railroad systems. The objective function, defined in equation (2.1a), aims to minimize the overall costs associated with utilizing existing logistic centers or upgrading them to intermodal facilities. The first-stage constraint in equation (2.1b) ensures that upgrade decisions are made only at the beginning of the planning horizon. The solution of the first-stage problem provides a blueprint for the second-stage problem, where operational decisions are made based on the network configuration established in the first stage.

$$\min \sum_{j \in J} \sum_{t \in T} c_j X_{jt} + \sum_{s \in S} \rho_s \mathbb{Q}(X, s) \tag{2.1a}$$

$$s.t. \sum_{j \in J} c_j X_{jt'} \leq 0, \quad t' \in \{2, 3, \ldots, T\} \tag{2.1b}$$

$$X_{jt} \in \{0, 1\} \tag{2.1c}$$

Second-stage problem: operational planning under uncertainty

The second-stage problem addresses the operational aspects of the logistics network over a ten-year period, considering the network configuration established in the first stage. It is formulated as a multi-period network flow problem, where annual transportation operations are optimized. This stage determines the most efficient routing strategies and allocates optimal quantities of goods to be transported via rail and truck to each location. The solution provides robust operational plans that are resilient to variability and disruptions, ensuring that the network operates efficiently under different demand patterns.

The objective functions of both stages aim to minimize the total transportation and facility upgrade costs. Equation (2.2a) and (2.2b) represent the objective function, which is the sum of the following transportation costs: from SPPC to warehouse j (first term), from warehouse j to warehouse b (second term), from warehouse j to destination k (third term), and from SPPC to destination k (fourth term). The distribution costs include fixed costs at each location associated with transportation mode m such as loading/unloading costs, and variable costs related to the respective unit costs for inflow, inter-warehouse flow, and outflow to destinations.

$$\mathbb{Q}(X,s) = \min \sum_{j\in J}\sum_{m\in\{0,1\}}\sum_{t\in T}\mu_j^m Y_{jts}^m + \sum_{j\in J}\sum_{b\in J\setminus\{j\}}\sum_{m\in\{0,1\}}\sum_{t\in T}\gamma_{jb}^m W_{jbts}^m \tag{2.2a}$$

$$+\sum_{j\in J}\sum_{k\in K}\sum_{t\in T}\delta_{jk}V_{jkts} + \sum_{i\in I}\sum_{k\in K}\sum_{t\in T}\sigma_k Z_{ikts} \tag{2.2b}$$

$$s.t. \sum_{m\in\{0,1\}} Y_{jts}^m - \sum_{b\in J\setminus\{j\}}\sum_{m\in\{0,1\}} W_{jbts}^m + \sum_{b\in J\setminus\{j\}}\sum_{m\in\{0,1\}} W_{bjts}^m \leq e_j, \quad \forall j\in J, \forall t\in\{1,2,...,T\}, \forall s\in S \tag{2.3}$$

$$Y_{jts}^1 + \sum_{b\in J\setminus\{j\}} W_{jbts}^1 + \sum_{b\in J\setminus\{j\}} W_{bjts}^1 \leq M\cdot a_{jt}, \quad \forall j\in J, \forall t\in\{1,2,...,T\}, \forall s\in S \tag{2.4}$$

$$X_{jt} + a_{jt} = a_{j,t+1}, \quad \forall j\in J, \forall t\in\{1,2,...,T\} \tag{2.5}$$

$$\sum_{k\in K} Z_{ikts} \leq e_i, \quad \forall j\in J, \forall t\in\{1,2,...,T\}, \forall s\in S \tag{2.6}$$

$$\sum_{b \in J \setminus \{j\}} W^1_{jbts} \leq Y^1_{jts} + \sum_{b \in J \setminus \{j\}} W^1_{bjts}, \qquad \forall j \in J, \forall t \in \{1, 2, ..., T\}, \forall s \in S \tag{2.7}$$

$$\sum_{b \in J \setminus \{j\}} W^m_{jbts} \leq Y^m_{jts} + \sum_{b \in J \setminus \{j\}} W^m_{bjts}, \qquad \forall j \in J, \forall m \in \{0, 1\}, \forall t \in \{1, 2, ..., T\}, \forall s \in S \tag{2.8}$$

$$Z_{kts} + \sum_{j \in J} V_{jkts} = d_{kts}, \qquad \forall k \in K, \forall t \in \{1, 2, ..., T\}, \forall s \in S \tag{2.9}$$

$$\alpha_{kt}\left(\sum_{m \in \{0,1\}} Y^m_{jts} - \sum_{b \in J \setminus \{j\}} \sum_{m \in \{0,1\}} W^m_{jbts} + \sum_{b \in J \setminus \{j\}} \sum_{m \in \{0,1\}} W^m_{bjts} \right) = V_{jkts}, \qquad \forall j \in J, \forall k \in K, \forall t \in \{1, 2, ..., T\}, \forall s \in S \tag{2.10}$$

$$a_{jt} \in \{0, 1\}, Y^m_{jts} \geq 0, W^m_{jbts} \geq 0, Z_{kts} \geq 0, V_{jkts} \geq 0 \tag{2.11}$$

Equation (2.3) represents the warehouse capacity constraint, ensuring that the total amount of inflows from the port minus the outflow that passes through without being handled at that warehouse, do not exceed the capacity of each warehouse at time t. Equation (2.4) defines the rail accessibility constraint, allowing rail inflows to warehouse j only when access is available at time t (i.e., $a[j, t] = 1$). If access is unavailable (i.e., $a[j, t] = 0$), no rail inflows are permitted at that time. Equation (2.5) updates the rail capability of each warehouse for each time period. If a warehouse is upgraded to an intermodal facility at time t, it will retain intermodal status from time $t + 1$ onward, continuing until the end of the analysis period. Equation (2.6) represents the on-dock facility capacity constraint, ensuring that the total number of containers handled at the port by on-dock facility i does not exceed the capacity of the facility at time t. Equation (2.7) reflects our assumption that when a train carries containers out of the port, it can only drop those containers at warehouses and may only pick up containers from a warehouse if those containers were previously dropped off by another train. This approach prevents the scenario where a truck transports freight from the port to a warehouse and a train later picks up the cargo. The aim is to ensure that trains always start their routing at the port, rather than facilitating shipments solely between warehouses, which could otherwise occur if trains pick up cargo that was initially carried by truck from the port to a warehouse. However, once a train has dropped cargo at an intermodal warehouse, we allow trucks to transport that freight to other warehouses, whether they are traditional or intermodal facilities. This approach enables the first intermodal warehouse to function as a hub, receiving rail service and reducing the number of warehouses that need to be upgraded to intermodal facilities. While this strategy reduces the need for intermodal upgrades, it may increase truck activity, possibly necessitating a constraint on the number of trucks operating at the hub facility. Equation (2.9) represents the demand constraint, ensuring that all containers transported to destination k at time t under scenario s, whether they go directly from the port or pass through warehouses first, must equal the demand at destination k. Equation Equation (2.10) defines the delivery flow constraint, ensuring that each warehouse j distributes its available freight to multiple destinations k according to the specified proportions α_{kt} at each time period t. Equation (2.11) is non-negativity constraints to ensure that all flow variables are non-negative.

2.6.5 Model simplification

In this study, we undertook parameter scale reduction to enhance the efficiency and effectiveness of our model. Our original model included a broad range of matrix values, specifically between [2e-03, 2e+08], which exceeded the maximum parameter settings available in Gurobi, particularly the Integer Feasibility Tolerance (IntFeasTol), which has a minimum value of $1e^{-9}$. Additionally, the model encountered warnings such as max constraint violation exceeds tolerance.

To address these challenges, we modified the scale of our flow decision variables. Instead of having each unit represent 1 ton of freight, we adjusted our decision variables $Y^m_{jts}, W^m_{jbts}, V_{jkts},$ and Z_{ikts} such that each unit now represents 100 or 1000 tons of freight. By doing so, the cost parameters related to these second-stage decision variables are multiplied by 100 or 1000 to accommodate the change in unit for our decision variables. Consequently, the total cost remains consistent and is compatible with the cost for the installation of our first-stage decision variable X_{jt}, which does not change as it is a binary variable representing the installation of intermodal capability. Therefore, the total transportation cost will accurately represent the original model's costs for allocating freight.

This change not only reduced the complexity of the model but also enhanced computational performance and accuracy without altering the core essence of the problem. By scaling each unit of the decision variables to represent 1,000 tons, the matrix range is narrowed down to $[2e^{-03}, 1e^{+04}]$. If we instead scale each unit to represent 100 tons, the matrix range will be reduced to $[2e^{-03}, 1e^{+05}]$. Additionally, we have a large right-hand side (RHS) range of $[1e^{+00}, 1e^{+08}]$, with the maximum value derived from the warehouse capacity parameter, representing the annual amount of freight that a warehouse can handle. This warehouse capacity will also be reduced by a factor of either 100 or 1,000, depending on our parameter scaling, thus reducing the maximum RHS to either $1e + 06$ or $1e + 05$ or 1×10^5 or $1e^{+05}$.

The results for both deterministic and stochastic models are very similar when the parameter scaling factor is reduced to either 100 or 1000. Furthermore, identical results are obtained when the Numerical Focus parameter of Gurobi is set to at least 1. However, the computational time is slightly better with a scaling factor of 100 compared to 1000. This difference could be attributed to the fact that some warehouses have relatively small capacities, and scaling by dividing by 1000 may result in overly fragmented flows. Specifically, using the parameter α_{kt} to divide the total container flow in small-capacity warehouses into numerous smaller flows can lead to the smallest flow to a destination representing only 1.5% of the warehouse's size. This excessive fragmentation may introduce challenges for the model in achieving an optimal solution efficiently. Therefore, in our model, we adopt a parameter scaling factor of 100.

2.7 Results and discussion

The optimization was implemented using the Gurobi Optimizer (version 10.0.2) through its Python interface (version 3.10.6). To enhance numerical precision and solution quality, specific solver parameters were set: the NumericFocus parameter was set to 1, and the integer feasibility tolerance (IntFeasTol) was tightened to 1e-9. These settings help improve numerical stability and ensure higher precision in integer feasibility during optimization. All computations were performed on a Linux server equipped with two 2.80 GHz AMD EPYC 7573X CPUs and 512 GB of memory.

2.7.1 Performance evaluation

The computational analysis evaluates the performance of the current and proposed systems across various scenarios, considering the following metrics: costs (including objective value, intermodal setup cost, track setup cost, environmental impacts, and social impacts) and freight flows (tonnages and ton-miles by modes and states). The objective is to assess how the use of intermediate warehouses as intermodal facilities affects these metrics under different scenarios and parameter variations. This will help analysts determine whether upgrading existing warehouses to intermodal facilities with rail access is beneficial, and how changes in transportation modes and patterns may influence overall performance. The results, summarized in **Table 2.7** and **Table 2.8**, reveal significant differences in cost-effectiveness and freight distribution patterns between the two systems. **Figure 2.4** illustrates these freight distribution patterns.

Table 2.7: Computational results comparing the current and proposed systems across various scenarios. Costs are reported in millions of dollars, and freight is measured in million tons.

Scenario	Cost (millions of dollars)			Freight Flow (millions of tons)						
	Total Cost	Intermodal Setup Cost	Track Setup Cost	Port to Whs		Whs to Whs	Whs to Dest.		Port to Dest.	
				By Trucks	By Rails	By Rails	By Trucks	By Rails	By Trucks	By Rails
Current system	129,343.85918	Not allowed	Not allowed	264.99693	111.65843	-	66.91156	309.74381	143.37028	667.56162
Proposed system (Here-and-now)	127,732.56109	14.71711 [20]	3.90000	248.88795	127.76742	-	67.31756	309.33781	143.37028	667.56162
(Wait-and-see)	127,723.21465	-	-	-	-	-	-	-	-	-
Deterministic										
Baseline Low	98,352.69157	0	0	1.52812	0	100.00000	0.26668	1.26144	131.13068	620.27201
Perturbation California Low	97,614.47041	0	0	1.52812	0	100.00000	0.28843	1.23969	141.82723	609.57546
Perturbation Northeast Low	98,900.03797	0	0	1.52812	0	0	0.25998	1.26814	127.83718	623.56551
Perturbation Southeast Low	98,708.38195	0	0	1.52812	0	100.00000	0.25916	1.26896	127.43389	623.96881
Perturbation Midwest Low	98,468.57939	0	0	1.52812	0	100.00000	0.26029	1.26783	127.99046	623.41223
Perturbation Southwest Low	98,224.27924	0	0	1.52812	0	100.00000	0.26624	1.26188	130.91688	620.48582
Perturbation West Low	97,369.11212	0	0	1.52812	0	100.00000	0.28960	1.23852	142.40316	608.99953
Stress California Low	96,145.22925	1.48641 [2]	2.00000	0	1.52812	100.00000	0.32689	1.20123	163.22033	588.18236
Stress Northeast Low	99,994.93819	0	0	1.52812	0	100.00000	0.24659	1.28154	121.25019	630.15251
Stress Southeast Low	99,420.00119	0	0	1.52812	0	100.00000	0.24413	1.28400	120.04030	631.36239
Stress Midwest Low	98,700.55516	0	0	1.52812	0	100.00000	0.24752	1.28060	121.71003	629.69267
Stress Southwest Low	97,967.53997	0	0	1.52812	0	100.00000	0.26538	1.26275	130.48926	620.91343
Stress West Low	95,409.15712	1.48641 [2]	2.00000	0	1.52812	0	0.33658	1.19155	164.94812	586.45458
Random Variation 1 Low	98,481.63035	0	0	1.52812	0	100.00000	0.26256	1.26556	128.90689	622.49581
Random Variation 2 Low	97,889.52947	0	0	1.52812	0	100.00000	0.28287	1.24525	136.86153	614.54117
Random Variation 3 Low	98,224.51601	0	0	1.52812	0	100.00000	0.27289	1.25523	133.60787	617.79483
Baseline Mid	125,898.85299	8.40145 [11]	2.70000	125.09299	15.36781	100.00000	24.51859	115.94220	141.51939	669.41251
Perturbation California Mid	124,975.38900	8.40145 [11]	2.70000	111.24047	29.22033	100.00000	26.52491	113.93589	153.06337	657.86853
Perturbation Northeast Mid	126,584.86629	8.40145 [11]	2.70000	125.09299	15.36781	0	23.90278	116.55801	137.96497	672.96693
Perturbation Southeast Mid	126,342.49813	8.40145 [11]	2.70000	125.09299	15.36781	200.00000	23.82737	116.63342	137.52973	673.40218
Perturbation Midwest Mid	126,039.91621	8.40145 [11]	2.70000	125.09299	15.36781	100.00000	23.93144	116.52935	138.13040	672.80151
Perturbation Southwest Mid	125,737.01419	8.40145 [11]	2.70000	125.09299	15.36781	100.00000	24.47387	115.98692	141.28865	669.64325
Perturbation West Mid	124,665.53739	8.40145 [11]	2.70000	111.24047	29.22033	100.00000	26.65982	113.80098	153.68493	657.24698

Table 2.7 Continued

Scenario	Cost (millions of dollars)			Freight Flow (millions of tons)						
	Total Cost	Intermodal Setup Cost	Track Setup Cost	Port to Whs		Whs to Whs	Whs to Dest.		Port to Dest.	
				By Trucks	By Rails	By Rails	By Trucks	By Rails	By Trucks	By Rails
Stress California Mid	123,127.62933	7.50116 [10]	2.70000	109.28434	31.17645	100.00000	30.52422	109.93657	176.15132	634.78058
Stress Northeast Mid	127,955.64519	7.52792 [10]	1.90000	125.18061	15.28019	100.00000	22.70907	117.75173	130.85613	680.07578
Stress Southeast Mid	127,227.78888	7.52792 [10]	1.90000	125.18061	15.28019	100.00000	22.48247	117.97833	129.55039	681.38151
Stress Midwest Mid	126,320.87408	7.52792 [10]	1.90000	125.18061	15.28019	100.00000	22.79519	117.66561	131.35240	679.57951
Stress Southwest Mid	125,409.93243	6.91504 [9]	0.70000	122.27465	18.18615	100.00000	24.38443	116.07636	140.82716	670.10475
Stress West Mid	122,198.93693	8.40145 [11]	2.70000	109.28434	31.17645	0	30.93251	109.52829	178.01599	632.91592
Random Variation 1 Mid	125,505.12628	8.40145 [11]	2.70000	119.17229	21.28851	100.00000	25.42020	115.04059	145.59628	665.33563
Random Variation 2 Mid	125,743.47696	0	0	122.52356	17.93724	100.00000	24.56815	115.89264	143.19074	667.74116
Random Variation 3 Mid	125,903.22268	8.40145 [11]	2.70000	116.06700	24.39379	100.00000	24.42777	116.03303	141.62184	669.31006
Baseline High	159,788.47140	13.44217 [18]	3.90000	248.88795	127.76742	100.00000	66.38037	310.27500	141.51939	669.41251
Perturbation California High	158,662.86064	13.44217 [18]	3.90000	248.88795	127.76742	350.00000	71.70814	304.94723	153.06337	657.86853
Perturbation Northeast High	160,637.54976	13.44217 [18]	3.90000	248.88795	127.76742	0	64.71315	311.94222	137.96497	672.96693
Perturbation Southeast High	160,335.51918	13.44217 [18]	3.90000	248.88795	127.76742	200.00000	64.50899	312.14638	137.52973	673.40218
Perturbation Midwest High	159,957.67236	13.44217 [18]	3.90000	248.88795	127.76742	200.00000	64.79074	311.86463	138.13040	672.80151
Perturbation Southwest High	159,586.26455	13.44217 [18]	3.90000	248.88795	127.76742	400.00000	66.24158	310.41379	141.28865	669.64325
Perturbation West High	158,281.68652	13.44217 [18]	3.90000	248.88795	127.76742	100.00000	72.12176	304.53361	153.68493	657.24698
Stress California High	156,416.99958	13.44217 [18]	3.90000	248.88795	127.76742	100.00000	82.61389	294.04148	176.15132	634.78058
Stress Northeast High	162,336.30623	13.44217 [18]	3.90000	248.88795	127.76742	100.00000	61.37871	315.27666	130.85613	680.07578
Stress Southeast High	161,430.20821	13.44217 [18]	3.90000	248.88795	127.76742	200.00000	60.76625	315.88912	129.55039	681.38151
Stress Midwest High	160,296.67267	13.44217 [18]	3.90000	248.88795	127.76742	250.00000	61.61149	315.04388	131.35240	679.57951
Stress Southwest High	159,182.07871	13.44217 [18]	3.90000	248.88795	127.76742	200.00000	65.96400	310.69137	140.82716	670.10475
Stress West High	155,272.60747	13.44217 [18]	3.90000	254.22385	122.43152	0	83.79668	292.85869	178.01599	632.91592
Random Variation 1 High	159,703.50416	13.44217 [18]	3.90000	248.88795	127.76742	100.00000	66.53881	310.11656	142.06211	668.86980
Random Variation 2 High	159,732.05211	13.44217 [18]	3.90000	248.88795	127.76742	200.00000	66.25921	310.39615	140.97363	669.95827
Random Variation 3 High	159,586.49315	13.44217 [18]	3.90000	248.88795	127.76742	100.00000	67.31756	309.33781	143.37028	667.56162

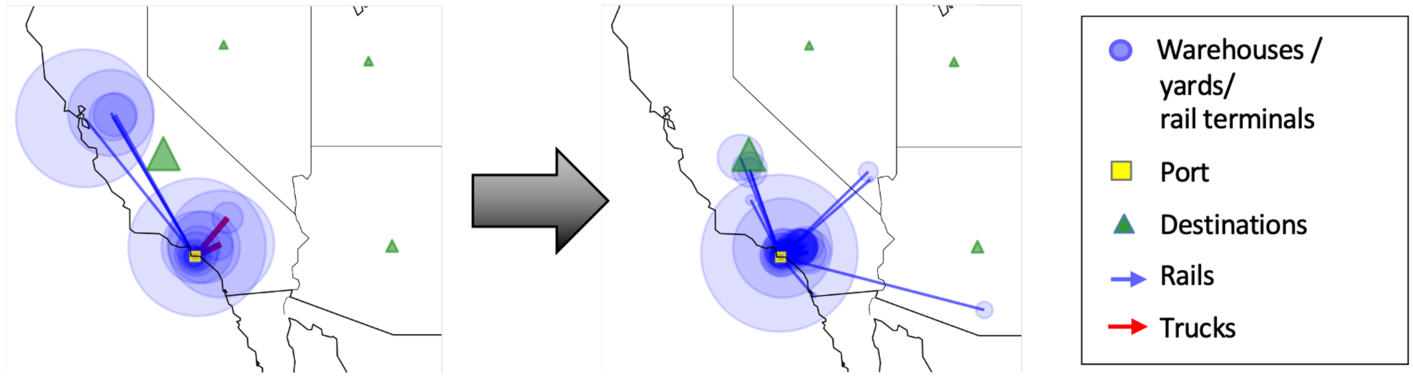

Figure 2.4: Flow of goods from the SPPC to warehouses: The left subfigure illustrates the flow in the current system, while the right subfigure depicts the flow in the proposed system. Blue lines represent rail transport, and red lines indicate truck transport. Warehouses are shown as circles, with larger circles denoting warehouses or clusters handling higher freight volumes. In each state, the destination is marked by a triangle.

Table 2.8: Freight volumes handled in intermediate warehouses across each state, along with total annual ton-miles transported by truck and rail, and the corresponding percentage changes

Scenarios	Freight Volumes Handled in Intermediate Warehouses by State (million tons)					Annual ton-mile (million ton-miles)					
	Current System	Proposed System				Current System	Proposed System		Current System	Proposed System	
	CA	CA	Change(%)	AZ	NV	By Trucks	By Trucks	Change(%)	By Rails	By Rails	Change(%)
Stochastic	376.65537	373.16878	(0.92567)	1.32771	2.15887	6,338.67262	6,216.51144	(1.92724)	207,547.54496	198,131.21609	(4.53695)
Deterministic											
Baseline Low	1.52812	1.52812	0	0	0	3,628.43520	3,628.43520	0	128,503.20568	128,503.20568	0
Perturbation CA Low	1.52812	1.52812	0	0	0	3,881.30291	3,881.30291	0	124,841.31919	124,841.31919	0
Perturbation Northeast Low	1.52812	1.52812	0	0	0	3,537.12614	3,537.12614	0	127,192.21902	127,192.21902	0
Perturbation Southeast Low	1.52812	1.52812	0	0	0	3,525.96380	3,525.96380	0	131,125.37794	131,125.37794	0
Perturbation Midwest Low	1.52812	1.52812	0	0	0	3,541.36860	3,541.36860	0	126,897.27505	126,897.27505	0
Perturbation Southwest Low	1.52812	1.52812	0	0	0	3,650.60801	3,650.60801	0	128,054.99472	128,054.99472	0
Perturbation West Low	1.52812	1.52812	0	0	0	3,908.89457	3,908.89457	0	124,056.33745	124,056.33745	0
Stress California Lo	1.52812	1.52812	0	0	0	4,440.68259	4,377.90812	-1.41362	119,869.77642	120,206.30306	0.28074
Stress Northeast Low	1.52812	1.52812	0	0	0	3,354.81217	3,354.81217	0	130,914.68429	130,914.68429	0
Stress Southeast Low	1.52812	1.52812	0	0	0	3,321.32515	3,321.32515	0	132,993.29644	132,993.29644	0
Stress Midwest Low	1.52812	1.52812	0	0	0	3,367.53956	3,367.53956	0	127,344.94117	127,344.94117	0
Stress Southwest Low	1.52812	1.52812	0	0	0	3,695.06766	3,695.06766	0	128,197.77625	128,197.77625	0
Stress West Low	1.52812	1.52812	0	0	0	4,523.45755	4,462.65260	-1.34421	116,744.03653	117,071.28769	0.28032
Random Variation 1 Low	1.52812	1.52812	0	0	0	3,759.83250	3,759.83250	0	127,998.50680	127,998.50680	0
Random Variation 2 Low	1.52812	1.52812	0	0	0	3,832.69655	3,832.69655	0	130,284.16869	130,284.16869	0
Random Variation 3 Low	1.52812	1.52812	0	0	0	3,690.93949	3,690.93949	0	127,999.68021	127,999.68021	0
Baseline Mid	140.46080	140.46080	0	0	0	5,175.42743	4,649.01162	-10.17145	156,970.30510	157,826.29502	0.54532
Perturbation CA Mid	140.46080	140.46080	0	0	0	5,491.23250	4,959.53548	-9.68265	154,264.06132	155,122.75618	0.55664
Perturbation Northeast Mid	140.46080	140.46080	0	0	0	5,060.20743	4,535.38777	-10.37150	159,402.88271	160,259.44554	0.53736
Perturbation Southeast Mid	140.46080	140.46080	0	0	0	5,046.11716	4,521.49294	-10.39659	158,512.00061	159,371.23602	0.54206
Perturbation Midwest Mid	140.46080	140.46080	0	0	0	5,065.56272	4,540.66876	-10.36201	157,419.59290	158,276.08197	0.54408
Perturbation Southwest Mid	140.46080	140.46080	0	0	0	5,203.06435	4,677.40400	-10.10290	156,112.14251	156,970.62969	0.54992
Perturbation West Mid	140.46080	140.46080	0	0	0	5,529.66839	4,995.92073	-9.65244	153,036.55445	153,893.09595	0.55970

Table 2.8 Continued

Scenarios	Freight Volumes Handled in Intermediate Warehouses by State (million tons)					Annual ton-mile (million ton-miles)					
	Current System	Proposed System				Current System	Proposed System		Current System	Proposed System	
	CA	CA	Change(%)	AZ	NV	By Trucks	By Trucks	Change(%)	By Rails	By Rails	Change(%)
Stress California Mid	140.46080	140.46080	0	0	0	6,125.83099	5,585.82657	-8.81520	148,850.09333	149,696.02944	0.56831
Stress Northeast Mid	140.46080	140.46080	0	0	0	4,830.07160	4,371.67086	-9.49056	164,267.80582	164,688.71054	0.25623
Stress Southeast Mid	140.46080	140.46080	0	0	0	4,787.80076	4,329.36132	-9.57516	161,595.16780	162,013.13785	0.25865
Stress Midwest Mid	140.46080	140.46080	0	0	0	4,846.13744	4,387.75363	-9.45875	158,317.92801	158,738.61867	0.26573
Stress Southwest Mid	140.46080	140.46080	0	0	0	5,258.45221	4,759.80298	-9.48281	154,395.77276	155,067.45903	0.43504
Stress West Mid	140.46080	140.46080	0	0	0	6,241.13868	5,694.73771	-8.75483	145,167.61190	146,008.89451	0.57953
Random Variation 1 Mid	140.46080	140.46080	0	0	0	5,474.88439	4,944.65060	-9.68484	155,693.50239	156,546.98552	0.54818
Random Variation 2 Mid	140.46080	140.46080	0	0	0	5,267.79027	4,786.20430	-9.14209	160,624.10588	161,295.55214	0.41802
Random Variation 3 Mid	140.46080	140.46080	0	0	0	5,180.81321	4,654.31426	-10.16248	159,974.35115	160,830.37087	0.53510
Baseline High	376.65537	373.16878	-0.92567	1.32771	2.15887	6,255.06043	6,126.87719	-2.04927	207,364.11237	197,988.00058	-4.52157
Perturbation CA High	376.65537	373.16878	-0.92567	1.32771	2.15887	6,633.18365	6,511.36773	-1.83646	203,933.87822	194,618.77730	-4.56771
Perturbation Northeast High	376.65537	373.16878	-0.92567	1.32771	2.15887	6,117.55942	5,985.31696	-2.16169	210,401.29074	201,028.06303	-4.45493
Perturbation Southeast High	376.65537	373.16878	-0.92567	1.32771	2.15887	6,100.74079	5,968.00127	-2.17579	209,351.85168	199,913.59405	-4.50832
Perturbation Midwest High	376.65537	373.16878	-0.92567	1.32771	2.15887	6,123.95166	5,991.89812	-2.15635	207,918.39461	198,543.90406	-4.50874
Perturbation Southwest High	376.65537	373.16878	-0.92567	1.32771	2.15887	6,272.56788	6,161.21542	-1.77523	206,360.03685	196,913.59826	-4.57765
Perturbation West High	376.65537	373.16878	-0.92567	1.32771	2.15887	6,695.53241	6,561.61262	-2.00014	202,315.45574	193,081.28583	-4.56424
Stress California High	376.65537	374.49649	-0.57317	-	2.15887	7,392.41844	7,320.89749	-0.96749	197,071.92947	187,995.08976	-4.60585
Stress Northeast High	376.65537	373.16878	-0.92567	1.32771	2.15887	5,842.86154	5,702.50065	-2.40226	216,475.41535	207,107.95582	-4.32726
Stress Southeast High	376.65537	373.16878	-0.92567	1.32771	2.15887	5,792.40565	5,650.55358	-2.44893	213,327.10645	203,764.55715	-4.48258
Stress Midwest High	376.65537	373.16878	-0.92567	1.32771	2.15887	5,862.03827	5,722.24413	-2.38474	209,026.71858	199,655.47050	-4.48328
Stress Southwest High	376.65537	373.16878	-0.92567	1.32771	2.15887	6,307.69679	6,230.00591	-1.23168	204,351.84122	194,764.74903	-4.69146
Stress West High	376.65537	374.49649	-0.57317	-	2.15887	7,579.46472	7,475.21721	-1.37539	192,216.70120	183,350.52369	-4.61259
Random Variation 1 High	376.65537	373.16878	-0.92567	1.32771	2.15887	6,333.02725	6,213.08203	-1.89396	207,625.25258	198,235.29236	-4.52255
Random Variation 2 High	376.65537	373.16878	-0.92567	1.32771	2.15887	6,196.99050	6,065.61645	-2.11997	209,742.27368	200,329.62769	-4.48772
Random Variation 3 High	376.65537	373.16878	-0.92567	1.32771	2.15887	6,338.67262	6,216.51144	-1.92724	207,547.54496	198,131.21609	-4.53695

Cost comparison

The proposed system outperforms the current system in terms of cost efficiency. For the baseline scenario, the objective value for the proposed system (here-and-now) is \$127,732.56 million compared to \$129,343.86 million for the current system—a cost reduction of approximately \$1,611.3 millions over a 10-year period. This improvement arises from the introduction of intermodal and track setup options, which increase logistic flexibility, decrease the dependency on truck-based transportation, and enhance the profitability of rail transport over shorter distances.

Notably, the intermodal and track setup costs in the proposed system are modest relative to the overall savings. For instance, in the "here-and-now" configuration, these costs amount to \$14.71 million and \$3.90 million, respectively, representing a small fraction of the total change in objective value. This underscores the importance of strategic infrastructure investments in optimizing freight operations. By incorporating demand uncertainty, the model enables flexible decision-making, allowing for the identification of cost-effective transportation strategies that adapt to varying demand patterns. In low-demand scenarios, the use of on-dock facilities alone is often sufficient to manage inbound freight to all destinations, with little to no additional flow requiring off-dock warehouses. This is likely due to the lower cost of direct transportation compared to using intermediate facilities, therefore, the system utilizes all available capacity at the on-dock terminal, and any excess flow is directed through intermediate warehouses. For mid-demand scenarios, upgrading existing off-dock warehouses into intermodal facilities capable of accommodating trains can result in substantial cost savings. In high-demand scenarios, while the total costs may be higher compared to the stochastic programming results of the current system, a comparison of deterministic high-demand scenarios between the proposed and current systems consistently shows that the proposed system is more cost-effective. This underscores the model robustness to variations ranging from light to significant changes at the state level, regional level, and in random fluctuations.

Warehouse analysis

There are 88 potential existing warehouse locations that could be upgraded into intermodal facilities with rail access. Among these, 33 warehouses currently lack rail access; however, 21 of these 33 warehouses have unused or inactive rail tracks adjacent to the facilities, eliminating the need for track setup costs during the upgrade process.

In all scenarios, if the model selects facilities for upgrades, they are all located in California.The stochastic programming of the proposed system selects the highest number of upgrades, with 20 facilities, followed by all deterministic results under the high-demand scenarios, which select 18 facilities. In the low- and mid-demand scenarios, fewer than 18 facilities are upgraded, but the selected facilities remain a subset of those chosen in the high-demand scenario, rather than introducing new ones. Among these 18 facilities, 13 already have inactive rail tracks adjacent to the warehouses, so no additional track construction costs are assumed. For the remaining five facilities without direct track access, the nearest rail tracks are located between 0.075 and 0.4 miles away, resulting in estimated track construction costs ranging from $300,000 to $1,600,000, assuming a track construction cost of $4 million per mile. All 18 selected facilities have relatively large capacities, capable of handling between 300,000 tons and approximately three million tons of freight annually. This suggests that smaller warehouses were not selected, likely because the cost of upgrading them with intermodal equipment and rail track construction would not be economically viable.

When examining the flow of tonnage by truck and rail from the port to the warehouses, we observe that the flows are generally consistent within each demand range. Specifically, the scenarios within the low-demand, medium-demand, and high-demand ranges are similar to each other, with many scenarios showing the same flow patterns. In fact, the flow is identical across all high-demand scenarios, except for the "Stress West Hi" scenario, which utilizes more trucks to transport freight to warehouses in California. Notably, both the "Stress West Hi" and "Stress CA Hi" scenarios differ from the other high-demand scenarios because they do not involve any freight flowing to warehouses in Arizona, whereas the other high-demand scenarios allocate 1.32771 million tons to Arizona.

It is important to note that these observations are based on the assumption that all warehouses allocate 40% of their capacity to serve the targeted inbound freight. The impacts of varying this warehouse allocation assumption on costs and freight flows will be discussed further in Section 2.7.2

Freight flow analysis

In the proposed system, freight volumes from ports to distribution centers shift from truck to rail transport. The current system handles \$264.997 million tons moved by trucks and \$111.658 million tons by rail, whereas the proposed system reduces truck dependence to \$248.888 million tons and increases rail usage to \$127.767 million tons. This increased reliance on rail highlights improved cost efficiency and enhanced environmental sustainability, aligning with modern logistics trends. The environmental and social impacts of these changes will be discussed in greater detail in the following section.

Freight movements between warehouses by rails are observed exclusively in the proposed system, highlighting the increased flexibility provided by intermodal options in the proposed system. These options minimize the reliance on truck transport by utilizing rail to directly move freight from ports to warehouses, with cargo being dropped off at multiple warehouse locations along the way. The highest total freight transported by rail, visiting multiple warehouses, can reach up to 400 million tons in the "Perturbation Southwest Hi" scenario. In the stochastic programming of the current system and the proposed system (the first two scenarios in **Table 2.7**), the specific realization of the second stage scenarios remains uncertain by nature. To provide a concrete example of how the system responds under uncertainty, we present the flows, which are second-stage decision variables, corresponding to a representative scenario – "Random Variation 3 Hi" scenario (the final scenario in Table 2.6). This scenario was selected because the random variations it incorporates fall within a range that aligns with fluctuations in GDP, as previously discussed during scenario generation. We chose the high-demand case because it most clearly illustrates the impact of such changes.

Flows from warehouses to destinations and from the port to destinations are predefined by mode based on the distance between location pairs. Distances greater than 500 miles are assigned to rail, while those less than or equal to 500 miles are served by trucks. These two types of flows exhibit minimal differences between the current and proposed systems, primarily because the analysis focuses on warehouses located within California, Arizona, Utah, and Nevada—states within the same region. Beyond this rationale, the model consistently selects warehouses in California. Consequently, the distances from these warehouses to destinations, which include one location in each U.S. state, remain similar, resulting in no significant change in the transport mode used. Rail accounts for a larger share of long-haul transport for both types of flows: from warehouses to destinations and from the port to destinations.

The freight flow from the port to destinations remains consistent across both the current and proposed systems, with 143.37 million tons transported by trucks and 667.56 million tons by rail. As mentioned earlier, even when more freight is directed from the port to warehouses, the direct flow from the port to destinations remains unchanged between the two systems. This is because if on-dock facilities alone can efficiently handle inbound freight to all destinations, the associated costs will be lower than those incurred by using intermediate warehouses, with only the excess flow routed through these facilities. These flows, compared under the stochastic modeling of both systems, are derived from the "Random Variation 3 Hi" scenario within high-demand conditions. In the deterministic modeling of all mid- and high-demand scenarios, the tonnage transported by each mode varies, but the total freight flow from the port to destinations consistently remains 810.9319 million tons, regardless of the mode. For low-demand scenarios, the flow remains consistent at 751.4027 million tons. The primary difference across demand ranges lies in the total amount of freight transported, reflecting variations in demand patterns.

In the current system, the total trucked tonnage over 10 years amounts to 475.279 million tons. This total comprises transportation along all truck-utilized connections in the network: 264.997 million tons from the port to warehouses, 66.912 million tons from warehouses to destinations, and 143.370 million tons from the port to destinations. In contrast, the proposed system reduces the total trucked tonnage to 459.576 million tons. The revised total includes 248.888 million tons from the port to warehouses, 67.318 million tons from warehouses to destinations, and 143.370 million tons from the port to destinations, eliminating truck transport between warehouses. Although the total tonnage in the proposed system is reduced by only 3.304%, this equates to a significant difference of 15.703 million tons, which translates to approximately 981,437 fewer truck trips over a 10-year period, assuming each truck carries a load of 16 tons.

In **Table 2.8**, we calculated the ton-miles for trucks and rail over a 10-year analysis period. The results show that truck ton-miles are reduced by 1.93% and rail ton-miles by 4.54%. This indicates that utilizing intermediate warehouses as container classification hubs and increasing rail usage for shorter distances can reduce total ton-miles, contributing to more efficient freight transportation. As mentioned, the flows between each location pair for the current and proposed systems are decision variables in the second stage of the stochastic programming. Therefore, to observe the flow changes, we need to display them for one scenario. We selected the Random Variation under high-demand scenario to illustrate the changes in the stochastic modeling of both systems. Therefore, when comparing the annual million ton-miles across all deterministic modeling scenarios with the current system flow, it is not particularly meaningful to focus on the exact numerical changes. Instead, it is more meaningful to examine the pattern of how the changes vary between scenarios within the same demand level (i.e., low, mid, and high).

Examining the deterministic modeling of the scenarios reveals that, across all demand levels, the scenarios with the lowest reduction in annual truck ton-miles are the Stress_CA scenario (which involves a 30% increase in demand in California), followed by the Perturbation_CA scenario (with a 10% increase in demand in California), and then the Stress_West scenario (which involves a 30% increase in demand in the West region). This is primarily due to the higher volume of short-distance shipments to California in these scenarios.

Environmental and social impacts

We also calculated the environmental impact costs, which include greenhouse gas emissions, criteria pollutants, and toxic releases as defined in Chapter 1. The environmental cost per ton-mile in 2020 dollars is $0.03974 for trucks and $0.01673 for rails. The social cost per ton-mile in 2020 dollars is $0.07219 for trucks and $0.00823 for rails. By multiplying these costs with the ton-miles for each mode, we compared the these impacts of the proposed system with the current system. in **Table 2.9** summarized the environmental and social impacts of the current and proposed system.

Under the same stochastic setting, the proposed system yields savings of $162.39 million in environmental impacts and $86.36 million in social impacts. However, when comparing the deterministic models of the proposed and current systems, minimal differences are observed under low-demand scenarios, except for the Stress California and Stress West scenarios, where environmental impacts worsen. This occurs because when freight demand is concentrated in California, shorter distances favor increased truck utilization. Nevertheless, social impact savings in these two scenarios under low demand remain slightly positive, accumulating approximately $1.7 million over ten years.

For medium-demand scenarios, environmental savings range from $6.5 million to $8.6 million, while social impact savings range from $29.2 million to $32.5 million. Similar to the low-demand case, stressing California and the western region by 30%

Table 2.9: The environmental and social impacts of the current and proposed system with respect to the environmental and social impacts

Scenarios	Environmental Impacts (M$)					Social Impacts (M$)				
	Current System		Proposed System			Current System		Proposed System		
	By Trucks	By Rails	By Trucks	By Rails	Saving	By Trucks	By Rails	By Trucks	By Rails	Saving
Stochastic	251.90015	3,472.38081	247.04544	3,314.84062	162.39490	457.5876725	1709.052384	448.7688783	1631.513527	86.35765
Deterministic										
Baseline Lo	144.19476	2,149.92697	144.19476	2,149.92697	0	261.93611	1058.16096	261.93611	1,058.16096	0
Perturbation California Lo	154.24377	2,088.66166	154.24377	2,088.66166	0	280.19058	1028.00712	280.19058	1,028.00712	0
Perturbation Northeast Lo	140.56612	2,127.99347	140.56612	2,127.99347	0	255.34452	1047.36563	255.34452	1,047.36563	0
Perturbation Southeast Lo	140.12252	2,193.79731	140.12252	2,193.79731	0	254.53871	1079.75327	254.53871	1,079.75327	0
Perturbation Midwest Lo	140.73471	2,123.05890	140.73471	2,123.05890	0	255.65078	1044.93691	255.65078	1,044.93691	0
Perturbation Southwest Lo	145.07591	2,142.42816	145.07591	2,142.42816	0	263.53676	1054.47017	263.53676	1,054.47017	0
Perturbation West Lo	155.34027	2,075.52850	155.34027	2,075.52850	0	282.18242	1021.54318	282.18242	1,021.54318	0
Stress California Lo	176.47363	2,005.48511	173.97896	2,011.11538	-3.13560	320.57210	987.06890	316.04042	989.84003	1.76055
Stress Northeast Lo	133.32092	2,190.27229	133.32092	2,190.27229	0	242.18331	1078.01831	242.18331	1,078.01831	0
Stress Southeast Lo	131.99014	2,225.04858	131.99014	2,225.04858	0	239.76588	1095.13466	239.76588	1,095.13466	0
Stress Midwest Lo	133.82671	2,130.54859	133.82671	2,130.54859	0	243.10209	1048.62322	243.10209	1,048.62322	0
Stress Southwest Lo	146.84274	2,144.81698	146.84274	2,144.81698	0	266.74629	1055.64590	266.74629	1,055.64590	0
Stress West Lo	179.76313	1,953.18982	177.34673	1,958.66490	-3.05868	326.54761	961.32996	322.15811	964.02472	1.69475
Random Variation 1 Lo	149.41651	2,141.48309	149.41651	2,141.48309	0	271.42165	1054.00501	271.42165	1,054.00501	0
Random Variation 2 Lo	152.31214	2,179.72343	152.31214	2,179.72343	0	276.68170	1072.82632	276.68170	1,072.82632	0
Random Variation 3 Lo	146.67869	2,141.50272	146.67869	2,141.50272	0	266.44828	1054.01468	266.44828	1,054.01468	0
Baseline Mid	205.67254	2,626.19668	184.75267	2,640.51785	6.59871	373.61320	1292.57358	335.61134	1,299.62224	30.95321
Perturbation California Mid	218.22270	2,580.91979	197.09295	2,595.28621	6.76333	396.41112	1270.28899	358.02800	1,277.35992	31.31218
Perturbation Northeast Mid	201.09368	2,666.89500	180.23724	2,681.22575	6.52569	365.29549	1312.60467	327.40885	1,319.65804	30.83326
Perturbation Southeast Mid	200.53373	2,651.99007	179.68505	2,666.36554	6.47321	364.27832	1305.26869	326.40579	1,312.34407	30.79715
Perturbation Midwest Mid	201.30650	2,633.71351	180.44710	2,648.04303	6.52988	365.68209	1296.27325	327.79009	1,303.32602	30.83924
Perturbation Southwest Mid	206.77084	2,611.83917	185.88099	2,626.20211	6.52690	375.60831	1285.50704	337.66098	1,292.57626	30.87811
Perturbation West Mid	219.75015	2,560.38294	198.53891	2,574.71334	6.88085	399.18580	1260.18107	360.65465	1,267.23427	31.47795

Table 2.9 Continued

Scenarios	Environmental Impacts (M$)					Social Impacts (M$)				
	Current System		Proposed System			Current System		Proposed System		
	By Trucks	By Rails	By Trucks	By Rails	Saving	By Trucks	By Rails	By Trucks	By Rails	Saving
Stress California Mid	243.44178	2,490.34122	221.98189	2,504.49418	7.30692	442.22267	1225.70762	403.23985	1,232.67349	32.01696
Stress Northeast Mid	191.94803	2,748.28775	173.73109	2,755.32971	11.17498	348.68203	1352.66493	315.59016	1,356.13087	29.62593
Stress Southeast Mid	190.26818	2,703.57310	172.04970	2,710.56596	11.22562	345.63050	1330.65706	312.53584	1,334.09884	29.65288
Stress Midwest Mid	192.58649	2,648.74313	174.37023	2,655.78151	11.17789	349.84182	1303.67060	316.75117	1,307.13478	29.62647
Stress Southwest Mid	208.97197	2,583.12339	189.15554	2,594.36106	8.57875	379.60675	1271.37357	343.60935	1,276.90458	30.46639
Stress West Mid	248.02413	2,428.73135	226.31004	2,442.80646	7.63898	450.54671	1195.38419	411.10212	1,202.31174	32.51704
Random Variation 1 Mid	217.57302	2,604.83510	196.50143	2,619.11432	6.79237	395.23095	1282.05974	356.95347	1,289.08776	31.24947
Random Variation 2 Mid	209.34306	2,687.32671	190.20474	2,698.56037	7.90467	380.28086	1322.66084	345.51525	1,328.18988	29.23658
Random Variation 3 Mid	205.88658	2,676.45597	184.96340	2,690.77764	6.60151	374.00200	1317.31043	335.99414	1,324.35934	30.95896
Baseline Hi	248.57738	3,469.31188	243.48335	3,312.44454	161.96136	451.55172	1707.54191	442.29820	1,630.33422	86.46121
Perturbation California Hi	263.60407	3,411.92224	258.76308	3,256.07565	160.68758	478.84837	1679.29561	470.05450	1,602.59031	85.49916
Perturbation Northeast Hi	243.11306	3,520.12549	237.85772	3,363.30641	162.07443	441.62555	1732.55158	432.07899	1,655.36764	86.73050
Perturbation Southeast Hi	242.44469	3,502.56782	237.16959	3,344.66075	163.18217	440.41141	1723.90997	430.82897	1,646.19054	87.30187
Perturbation Midwest Hi	243.36709	3,478.58532	238.11926	3,321.74510	162.08805	442.08700	1712.10615	432.55408	1,634.91181	86.72726
Perturbation Southwest Hi	249.27313	3,452.51316	244.84796	3,294.46922	162.46911	452.81558	1699.27384	444.77707	1,621.48704	85.82531
Perturbation West Hi	266.08183	3,384.84517	260.75983	3,230.35260	159.81457	483.34932	1665.96869	473.68167	1,589.92982	85.70651
Stress California Hi	293.77622	3,297.11819	290.93396	3,145.25783	154.70261	533.65740	1622.79082	528.49431	1,548.04749	79.90641
Stress Northeast Hi	232.19651	3,621.74883	226.61854	3,465.02625	162.30055	421.79516	1782.56902	411.66253	1,705.43258	87.26907
Stress Southeast Hi	230.19138	3,569.07594	224.55415	3,409.08941	165.62377	418.15275	1756.64424	407.91248	1,677.90133	88.98319
Stress Midwest Hi	232.95860	3,497.12817	227.40315	3,340.34220	162.34141	423.17952	1721.23265	413.08781	1,644.06502	87.25935
Stress Southwest Hi	250.66916	3,418.91498	247.58171	3,258.51783	163.48460	455.35153	1682.73733	449.74304	1,603.79232	84.55350
Stress West Hi	301.20948	3,215.88764	297.06666	3,067.55177	152.47868	547.16024	1582.81039	539.63463	1,509.80176	80.53424
Random Variation 1 Hi	251.67580	3,473.68090	246.90915	3,316.58187	161.86568	457.18013	1709.69227	448.52131	1,632.37054	85.98055
Random Variation 2 Hi	246.26967	3,509.09978	241.04884	3,351.62121	162.69940	447.35966	1727.12490	437.87580	1,649.61637	86.99240
Random Variation 3 Hi	251.90015	3,472.38081	247.04544	3,314.84062	162.39490	457.58767	1709.05238	448.76888	1,631.51353	86.35765

results in lower environmental savings compared to other regions but shows slight improvements in social impact savings. Across three random variations in demand allocation, the savings remain consistent with the baseline and all perturbation cases.

At a larger scale, under high-demand scenarios, savings increase significantly, with environmental impact reductions ranging from \$152.5 million to \$165.6 million and social impact savings between \$79.9 million and \$89 million. However, within these high-demand scenarios, stressing California and the western region by 30% yields the lowest environmental and social savings. Again, this is due to shorter travel distances increasing truck utilization while reducing rail usage.

The value of information and the stochastic solution

To evaluate the impact of accounting for uncertainty, we calculated both the Expected Value of Perfect Information (EVPI) and the Value of the Stochastic Solution (VSS). These metrics provide insights into the potential benefits of obtaining perfect information and the cost implications of disregarding uncertainty.

Expected Value of Perfect Information (EVPI): The EVPI, calculated as \$9,346,444 represents the maximum amount that would be justified to pay for perfect information on inbound freight demand. This value underscores the potential cost savings that could be achieved if all uncertainty were eliminated, allowing the model to operate with complete knowledge of future demand. In practical terms, this EVPI highlights the maximum amount we should be willing to pay for perfect information on inbound freight demand, which can be the value of investing in technologies or methodologies that can enhance the accuracy of demand forecasting and reduce uncertainty.

Value of the Stochastic Solution (VSS): The VSS, calculated as \$41,899,283 highlights the benefits of explicitly modeling uncertainty within the two-stage stochastic framework rather than using a deterministic approach. It indicates the significant cost incurred when uncertainty is ignored in decision-making. This value demonstrates that the deterministic approach, which does not account for demand variability, leads to substantially higher transportation costs compared to the stochastic model. The large positive VSS emphasizes the importance of explicitly addressing uncertainty in the decision-making process, as doing so yields substantial cost savings. These results suggest that the flexibility and robustness provided by the stochastic approach are essential in managing transportation costs effectively under uncertain demand conditions.

In summary, the EVPI and VSS together highlight the critical role of uncertainty modeling in transportation cost optimization. The EVPI of \$9,346,444 suggests that obtaining perfect information has substantial value, while the VSS of \$41,899,283 demonstrates the considerable cost benefits of incorporating uncertainty into the decision-making framework. These findings strongly support the adoption of stochastic programming to manage demand variability and optimize transportation systems in uncertain environments.

2.7.2 Sensitivity analysis

As detailed in Section 2.6.3 on scenario definitions and generation, we conduct a sensitivity analysis of the model with respect to various parameters, including warehouse capacities and loading and unloading (L&UL) costs at both the port and warehouses, with incremental variations of 10% up to ±30%. Additionally, we examine the intermodal installation cost (IIC), which is particularly relevant for intermediate warehouses lacking direct railroad access. The installation costs are categorized into four levels: low (\$100,000–\$500,000), base case (\$500,000–\$1,000,000), high (\$1,000,000–\$1,500,000), and very high (\$1,500,000–\$2,000,000). These costs may encompass activating unused tracks or acquiring intermodal handling equipment such as cranes or container handlers.

Table 2.10 illustrates the impact of varying each factor on the system's performance, measured through costs and freight flows. Additionally, **Table 2.11** presents changes in ton-miles by each mode and details the amount of freight handled by warehouses in each state.

Table 2.10: Sensitivity analysis results for factors influencing costs and freight flows across location pairs

Scenario	Cost (millions of dollars)			Freight Flow (millions of tons)						
	Total Cost	Intermodal Setup Cost	Track Setup Cost	Port to Whs		Whs to Whs	Whs to Dest.		Port to Dest.	
				By Trucks	By Rails	By Rails	By Trucks	By Rails	By Trucks	By Rails
Current system	129,343.85918	Not allowed	Not allowed	264.99693	111.65843	-	66.91156	309.74381	143.37028	667.56162
Proposed system	127,732.56109	14.71711 [20]	3.90000	248.88795	127.76742	-	67.31756	309.33781	143.37028	667.56162
Installation cost $100K-500K	127,723.41494	5.57096 [20]	3.90000	248.88795	127.76742	-	67.31756	309.33781	143.37028	667.56162
Installation cost $1M-1.5 M	127,738.93830	10.48398 [9]	2.80000	267.52409	109.13127	-	67.16270	309.49267	143.37028	667.56162
Installation cost $1.5M-2 M	127,740.01122	15554976 [9]	3.20000	264.11602	112.53935	-	67.26718	309.38819	143.37028	667.56162
Port L&UL - 30%	127,614.27848	16.83723 [23]	5.90000	119.63664	257.01873	41.18607	67.38650	309.26887	143.37028	667.56162
Port L&UL - 20%	127,660.07233	14.39473 [19]	5.90000	126.03874	250.61663	40.60786	67.35386	309.30151	143.37028	667.56162
Port L&UL - 10%	127,700.66266	9.37344 [13]	5.20000	139.70083	236.95454	-	67.28525	309.37012	143.37028	667.56162
Port L&UL + 10%	127,750.57846	14.71711 [20]	3.90000	249.57316	127.08221	-	67.31038	309.34499	143.37028	667.56162
Port L&UL + 20%	127,764.03483	11.85978 [16]	3.50000	264.16005	112.49532	-	67.19492	309.46045	143.37028	667.56162
Port L&UL + 30%	127,778.32974	11.23780 [15]	3.50000	281.21167	95.44370	-	67.08005	309.57531	143.37028	667.56162
Whs L&UL $300/ TEU	126,045.06957	16.79912 [23]	8.70000	0	376.65537	-	51.50978	325.14559	143.37028	667.56162
Whs L&UL $600/ TEU	126,989.48320	16.79912 [23]	8.70000	49.98014	326.67523	-	59.02334	317.63203	143.37028	667.56162
Whs L&UL $1200/ TEU	127,839.85916	6.64171 [9]	3.20000	346.89834	29.75702	-	67.07167	309.58369	143.37028	667.56162
Whs Capacity - 30%	127,892.82538	14.16338 [19]	3.90000	231.68566	144.96970	-	59.74349	316.91188	143.37028	667.56162
Whs Capacity - 20%	127,823.01130	14.71711 [20]	3.90000	245.45202	131.20335	-	63.52189	313.13348	143.37028	667.56162
Whs Capacity - 10%	127,770.10992	14.71711 [20]	3.90000	250.30607	126.34930	-	66.06251	310.59286	143.37028	667.56162
Whs Capacity + 10%	127,707.26590	12.65624 [17]	3.90000	246.68511	129.97026	5.77520	67.47856	309.17681	143.37028	667.56162
Whs Capacity + 20%	127,691.02315	12.65624 [17]	3.90000	247.03141	129.62396	10.78048	67.42947	309.22590	143.37028	667.56162
Whs Capacity + 30%	127,677.88560	13.44217 [18]	3.90000	250.38221	126.27315	-	67.35029	309.30508	143.37028	667.56162

Table 2.11: Freight volumes handled in intermediate warehouses across each state, along with total annual ton-miles transported by truck and rail, and the corresponding percentage changes

Factor	Freight Volumes Handled in Intermediate Warehouses by State (millions of tons)								Annual ton-mile (million of ton-miles)			
	CA	Change(%)	UT	Change(%)	AZ	Change(%)	NV	Change(%)	By Trucks	Change(%)	By Rails	Change(%)
Current system	376.655368	-	0	-	0	-	0	-	6,338.67262	0.000	207,547.54496	0.000
Proposed system	373.168782	-0.925670068	0	-	1.327712	-	2.158873	-	6,216.51144	-1.927	198,131.21609	-4.537
Installation cost $100K-500K	373.168782	-0.925670068	0	-	1.327712	-	2.158873	-	6,216.51144	-1.927	198,131.21609	-4.537
Installation cost $1M-1.5 M	372.246261	-1.170594494	0	-	1.81097	-	2.598136	-	6,239.43236	-1.566	198,150.66196	-4.528
Installation cost $1.5M-2 M	373.004657	-0.969244384	0	-	1.491837	-	2.158873	-	6,222.22085	-1.837	198,140.77191	-4.532
Port L&UL - 30%	366.377374	-2.728752826	0	-	1.327712	-	8.950281	-	6,216.09226	-1.934	198,272.81216	-4.469
Port L&UL - 20%	369.930472	-1.785424176	0	-	1.327712	-	5.397183	-	6,216.09226	-1.934	198,265.53290	-4.472
Port L&UL - 10%	373.004657	-0.969244384	0	-	1.491837	-	2.158873	-	6,208.63732	-2.051	198,279.76746	-4.465
Port L&UL + 10%	373.168782	-0.925670068	0	-	1.327712	-	2.158873	-	6,216.51144	-1.927	198,131.21609	-4.537
Port L&UL + 20%	373.168782	-0.925670068	0	-	1.327712	-	2.158873	-	6,216.51144	-1.927	198,126.83743	-4.539
Port L&UL + 30%	374.248219	-0.639085276	0	-	1.327712	-	1.079436	-	6,220.96657	-1.857	198,119.58411	-4.543
Whs L&UL $300/ TEU	260.128312	-30.93731456	0	-	105.732688	-	10.794366	-	4,961.25320	-21.730	203,748.28203	-1.831
Whs L&UL $600/ TEU	309.732061	-17.76778262	0	-	56.12894	-	10.794366	-	5,557.96011	-12.317	210,677.12234	1.508
Whs L&UL $1200/ TEU	375.575931	-0.286584791	0	-	0	-	1.079436	-	6,428.10012	1.411	197,591.67210	-4.797
Whs Capacity - 30%	320.569508	-14.89049799	0	-	49.994768	-	6.09109	-	6,124.60192	-3.377	197,929.96535	-4.634
Whs Capacity - 20%	346.73244	-7.94437848	0	-	25.60518	-	4.317746	-	6,180.90286	-2.489	197,904.19213	-4.646
Whs Capacity - 10%	364.03202	-3.351431859	0	-	9.292867	-	3.33048	-	6,218.54485	-1.895	197,902.07979	-4.647
Whs Capacity + 10%	375.643303	-0.268697883	0	-	0	-	1.012064	-	5,977.29081	-5.701	199,415.29647	-3.918
Whs Capacity + 20%	376.655368	0	0	-	0	-	0	-	5,738.07017	-9.475	200,699.37684	-3.300
Whs Capacity + 30%	376.655368	0	0	-	0	-	0	-	5,498.84954	-13.249	201,983.45722	-2.681

For the stress test on each region (Northeast, Southeast, Midwest, Southwest, and West), a stress scenario involves a 30% increase in demand allocated to states within that region. For example, the demand in one region is increased by 30%, while the reduced demand is redistributed to other regions to ensure that the total annual demand remains consistent across all demand levels.

Cost comparison

For the sensitivity analysis of intermodal installation costs (IIC), as discussed in the previous section, when comparing the base case of the proposed system to the current system, the savings amount to $1.611 billion over a 10-year period. If the installation cost decreases to $100,000 to $500,000 per warehouse, the savings increase to $1.620 billion. If the IIC rises to $1 million to $1.5 million, the savings remain around $1.605 billion. Even when the IIC reaches $1.5 million to $2 million per warehouse, the savings are still substantial, at $1.604 billion.

For L&UL costs of rail at intermediate facilities and destinations, we base our analysis on a starting rate of $900 per container, as discussed in Section 2.6.1, and introduce three additional scenarios: $600 per container (a 33% reduction) and $300 per container (a 66% reduction). These scenarios aligns with the Chargeable Events Demurrage published by Union Pacific Railroad (2024a), where charges can range from $105 to $3,150 Union Pacific Railroad (2024a), varying due to multiple factors such as freight type, L&UL locations, and other conditions. Note that in this instance, the term Chargeable Events Demurrage, as defined by Union Pacific, is calculated solely for the L&UL of rail cars (Union Pacific Railroad, 2024b). Assuming that congestion at these warehouses would be lower than at the port or rail terminals, we anticipate that the costs would be cheaper. If the L&UL cost is as low as $300 per container, the results show that this scenario yields the most cost-effective outcome across all tests in the sensitivity analysis. In contrast, if we assume that the system is new, meaning it may be less efficient despite reduced congestion due to adaptation time, and the L&UL cost increases to $1,200 per container, it results in the highest objective value among all sensitivity analysis scenarios. Since this parameter has a high degree of uncertainty and variability, it could have a significant impact on the performance of the proposed system.

For the sensitivity analysis of warehouse capacity allocation to handle our targeted inbound freight, the analysis focuses on warehouses that are not on-dock. This approach allows us to vary the capacity available at each warehouse and observe how these changes impact key metrics such as costs, freight flows, and other relevant outcomes. In terms of cost analysis, increasing warehouse capacity results in a negative variation, leading to a decrease in the objective value. Specifically, among six instances of varying warehouse capacity, the scenario with a 30% increase in capacity yields the lowest cost, while the scenario with a 30% decrease in capacity results in the highest cost.

Warehouse analysis

When we varied the parameters to assess their impact, we observed significant changes in the number of warehouses selected compared to the proposed system. This is particularly evident in the sensitivity analysis of warehouse L&UL costs. In the base case, we assume a cost of $900 per container, and the model selects 20 warehouses. However, this can drop to as few as 9 warehouses if the L&UL cost increases to $1200. Conversely, the number of warehouses can increase substantially to 23 warehouses if the L&UL cost decreases to as low as $300. We vary this cost because, as mentioned in the parameter justification section, L&UL costs depend on factors such as warehouse location, functionality, and the type of freight it serves. As a result, these costs can range widely, from $200 to over $1000. Since we do not know how the L&UL costs will be affected by the use of off-dock warehouses as intermodal facilities for container classification in our proposed system, we estimated the potential impact of these varying costs. Note that with an L&UL cost of $300 per container, this is the first scenario in which a warehouse outside of California—in Utah—is selected. This warehouse has a significantly larger capacity, capable of handling 317 million tons annually, which is substantially greater than the capacities of the selected warehouses in California.

A similar pattern is observed for IIC. In the proposed system (base case), with IIC ranging from \$500,000 to \$1 million per warehouse, the model selects 20 warehouses for upgrades. When the cost decreases to between \$100,000 and \$500,000, the number of selected warehouses remains at 20. However, as the cost increases to \$1 million to \$1.5 million, and further to \$1.5 million to \$2 million per facility, the model selects only 9 warehouses. In both higher-cost scenarios, all selected warehouses are located in California.

Next, we conduct a sensitivity analysis on the capacity allocation of warehouses used as intermediate facilities for our targeted inbound freight. In the base case, 40% of total warehouse capacity is allocated for this purpose. Intuitively, one might expect that increasing this allocation by 30% would reduce the number of warehouses needing upgrades, while decreasing the allocation would require more warehouses to be upgraded. However, our model results contradict this expectation. When we varied the base case by increasing or decreasing capacity allocation in increments of 10%, within a range of ±30%, we found that the number of upgraded warehouses remained relatively consistent. For instance, when the capacity allocation was reduced by 10% or 20%, the model still selected 20 warehouses for upgrades. This indicates that within this range of reduction, the warehouses are already operating at an optimal level, and the decrease in capacity is not significant enough to impact warehouse selection. However, there is a small trend suggesting that as warehouses are able to allocate more capacity to handle the targeted freight, fewer warehouses are needed. Conversely, with lower capacity allocation, more warehouses are required. This trend no longer holds when the capacity allocation is reduced by 30%. In this case, the model selects only 19 warehouses for upgrades, compared to 20 warehouses in the 10% and 20% reduction scenarios. This is likely because the investment in IIC and rail track construction becomes less justifiable for intermodal warehouses with such a significant capacity reduction.

As shown in **Table 2.11**, the volume of freight handled in warehouses across each state remains relatively unchanged between the current system and the base case of our proposed system. In the current system, all 376.655 million tons of freight moving to intermediate warehouses are processed within California. Under the proposed system, warehouse usage outside California increases slightly, with 2.16 million tons handled in Nevada and 1.33 million tons in Arizona over a ten-year period. This distribution remains largely consistent, even when the intermodal installation cost varies from $500,000 to $2,000,000 per warehouse upgrade.

The two primary factors influencing warehouse utilization across states are the cost of L&UL at warehouses supporting rail transport and the allocation of warehouse capacity dedicated to the proposed system's container classification. When L&UL costs reach $600 per container, freight flow shifts significantly, with 56.13 million tons handled in Arizona and 10.79 million tons in Nevada, reducing California's share to 309.73 million tons—a 17.77% decrease. This shift becomes even more pronounced when L&UL costs drop to $300 per container, with the model utilizing 105.73 million tons in Arizona and 10.79 million tons in Nevada, further reducing California's share to 260.13 million tons—a 30.93% decrease.

Warehouse capacity allocation also has a notable impact. If the allocation is reduced below the base case, meaning each warehouse can dedicate less than 40% of its capacity to inbound freight, the system increasingly relies on warehouses outside California, with Arizona seeing the most growth. If warehouse capacity allocation decreases by 10%, reducing available capacity from 40% to 36%, Arizona handles 9.29 million tons, while Nevada handles 3.33 million tons. When the allocation decreases by 20%, reducing available capacity to 32%, Arizona's share increases to 25.61 million tons, while Nevada handles 4.32 million tons. If warehouse allocation decreases by 30%, bringing the available capacity down to 28%, Arizona handles 49.99 million tons and an additional 6.09 million tons shift from California to Nevada. These results highlight the strong influence of warehouse capacity allocation and L&UL costs on the geographic distribution of freight within the proposed system. The visualization of this change is presented in **Figure 2.5**.

Freight flow analysis

When we adjust the intermodal installation cost (IIC), we observe an inverse relationship between IIC and the amount of freight transported by rail from SPPC to the warehouses. Higher IIC leads to a reduced reliance on rail and a greater dependence on trucks, as constructing rail access becomes more expensive.

Examining the port L&UL cost reveals a significant mode shift from truck to rail when the cost decreases from the base case of $200 per container by 10%, 20%, and 30%. In the base case, 248.89 million tons are transported by truck and 127.77 million tons by rail from SPPC to the warehouses. When the L&UL cost is reduced by 10%, truck transport decreases to 139.70 million tons, while rail transport increases to 236.95 million tons. The most pronounced shift occurs with a 30% reduction in L&UL cost, where truck transport drops to 119.64 million tons, while rail transport rises to 257.02 million tons.

A similar pattern emerges when analyzing the warehouse L&UL cost. If the new system incurs lower L&UL costs at selected warehouses for classification—compared to performing classification at the port or major railroad hubs—mode shifting becomes more pronounced. When the L&UL cost is $600 per container, freight movement from the port complex to warehouses is primarily handled by rail, with 326.68 million tons transported by rail and 49.98 million tons by truck. However, if the L&UL cost decreases to $300 per container, it becomes optimal to transport all freight by rail, entirely eliminating truck usage from SPPC to the warehouses. This reduction in cost streamlines rail transport, making it more economical and attractive even for shorter distances, further reinforcing the shift away from truck transport.

As discussed in the warehouse analysis, when we varied the base case by increasing or decreasing capacity allocation in increments of 10% within a range of ±30%, we observed that the number of upgraded warehouses and the tonnage transported from

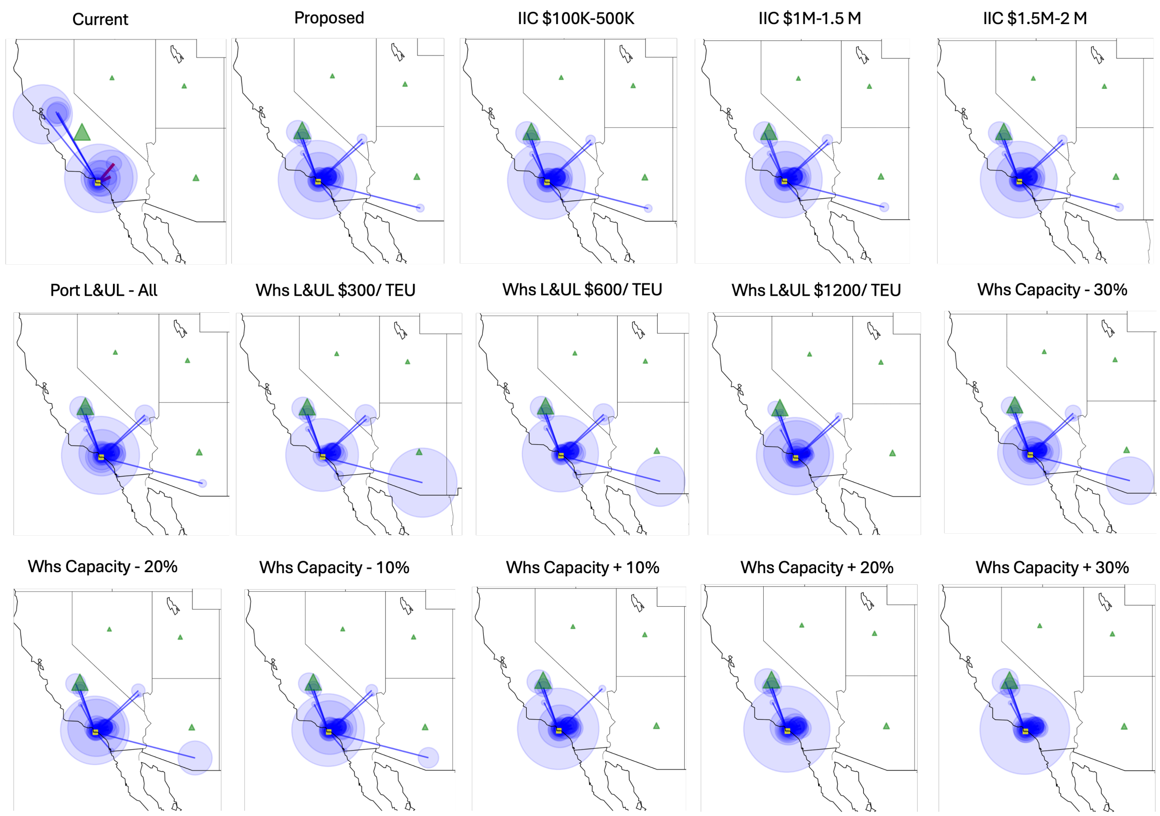

Figure 2.5: Changes in the use of intermediate warehouses across different sensitivity analysis scenarios.

SPPC to warehouses by mode remained relatively consistent, without a clear pattern in tonnage, as shown in **Table 2.10**. However, to better understand the impact on freight movement, we also examine the ton-mile changes for each mode, as presented in **Table 2.11**. This provides a clearer perspective on how warehouse capacity affects freight distribution. When warehouses have higher capacity, freight is more likely to be transported to nearby warehouses via trucks. Conversely, when warehouse capacity is more limited, freight must travel longer distances, leading to increased reliance on rail transport. Examining freight handled in warehouses by state reveals a notable shift in distribution when inbound warehouse capacity is reduced. Specifically, in a scenario where warehouse capacity is decreased by 30% compared to the base case, 6.09 million tons of freight are redirected from CA warehouses to facilities in NV and 49.99 million tons shift to AZ.

Environmental and social impacts

We also calculated the environmental impact costs, which include greenhouse gas emissions, criteria pollutants, and toxic releases as described in Rattanakunuprakarn et al. (2024). The environmental cost per ton-mile in 2020 dollars is $0.03974 for trucks and $0.01673 for rails. The social cost per ton-mile in 2020 dollars is $0.07219 for trucks and $0.00823 for rails. By multiplying these costs with the ton-miles for each mode, we compared the these impacts of the proposed system with the current system. in **Table 2.12** summarized the environmental and social impacts of the current and proposed system.

From the analysis, it is clear that the proposed system achieves environmental and social savings compared to the current system. The total environmental impact of the proposed system (base case) is reduced by approximately $162.39 million and the total social impact is reduced by approximately $86.36 millions over the 10-year analysis. These figures suggest that moving toward optimized warehouse allocation and intermodal transportation has clear benefits in reducing these impacts.

Table 2.12: The environmental impacts of the current and proposed system with respect to environmental and social impacts.

Factor	Environmental Impacts ($M)			Social impacts ($M)		
	By Trucks	By Rails	Saving($)	By Trucks	By Rails	Saving($)
Current system	251.90015	3,472.38081	-	457.58767	1709.05238	-
Proposed system	247.04544	3,314.84062	162.39490	448.76888	1631.51353	86.36
Installation cost $100K-500K	247.04544	3,314.84062	162.39490	448.76888	1,631.51353	86.35765
Installation cost $1M-1.5 M	247.95632	3,315.16596	161.15868	450.42354	1,631.67365	84.54287
Installation cost $1.5M-2 M	247.27233	3,315.00049	162.00813	449.18104	1,631.59221	85.86680
Port L&UL - 30%	247.02878	3,317.20959	160.04258	448.73862	1,632.67950	85.22194
Port L&UL - 20%	247.02878	3,317.08781	160.16437	448.73862	1,632.61956	85.28188
Port L&UL - 10%	246.73252	3,317.32596	160.22248	448.20045	1,632.73678	85.70283
Port L&UL + 10%	247.04544	3,314.84062	162.39490	448.76888	1,631.51353	86.35765
Port L&UL + 20%	247.04544	3,314.76736	162.46816	448.76888	1,631.47747	86.39371
Port L&UL + 30%	247.22248	3,314.64601	162.41246	449.09049	1,631.41774	86.13182
Whs L&UL $300/ TEU	197.16122	3,408.81712	118.30262	358.15200	1,677.76731	130.72074
Whs L&UL $600/ TEU	220.87447	3,524.74030	(21.33382)	401.22817	1,734.82292	30.58896
Whs L&UL $1200/ TEU	255.45401	3,305.81376	163.01318	464.04343	1,627.07065	75.52598
Whs Capacity - 30%	218.52540	3,379.29066	126.46489	396.96099	1,663.23485	106.44422
Whs Capacity - 20%	228.03208	3,357.80731	138.44156	414.23029	1,652.66107	99.74870
Whs Capacity - 10%	237.53876	3,336.32396	150.41823	431.49958	1,642.08730	93.05317
Whs Capacity + 10%	247.12624	3,311.00704	166.14766	448.91567	1,629.62670	88.09768
Whs Capacity + 20%	245.63034	3,311.04238	167.60822	446.19830	1,629.64410	90.79766
Whs Capacity + 30%	243.39293	3,311.47358	169.41444	442.13395	1,629.85633	94.64978

As previously discussed, reducing L&UL costs at the port improves rail utilization while decreasing truck usage. Given this change, it is reasonable to expect that lower L&UL costs would also improve environmental and social outcomes due to increased reliance on rails. This assumption holds true when port L&UL costs are reduced to \$300 per container, as the results show the most significant improvement in social impact among all sensitivity tests, with savings of \$130.72 million compared to the current system. These savings stem primarily from reduced congestion and improved safety. However, when L&UL cost is reduced to \$600 per container, the savings in social impacts decrease to \$30.59 million, even the negative savings of 21.33 million dollars in environmental impacts, the lowest among all sensitivity tests. This outcome suggests that at such a low rail L&UL cost, rail transport becomes highly competitive with trucking, potentially leading to longer overall freight travel distances to reach warehouses with rail access, offsetting some of the anticipated benefits.

When analyzing the impact of varying IIC, the resulting environmental and social savings remain marginal compared to the base case, as the annual ton-miles for each mode exhibit minimal change.

In contrast, variations in warehouse capacity have a more noticeable effect. As warehouse capacity decreases, total annual ton-miles across all modes increase, leading to reduced savings due to longer travel distances. However, this reduction remains relatively small. The lowest environmental savings in the warehouse capacity sensitivity analysis occur when the capacity is reduced by 30% from the base case, yielding savings of \$126.46 million compared to the current system. The lowest social savings occur when warehouse capacity is increased by 10%, with total savings of \$88.10 million. Conversely, when warehouses allocate 30% more capacity to manage the targeted inbound freight, the system achieves the highest environmental savings across all sensitivity analyses, reaching \$169.41 million over the 10-year period.

To summarize, charts illustrate the relationships between parameter variations and key metrics, including cost reductions, changes in truck and rail ton-miles, freight handled in warehouses across different states, and environmental and social impacts.

Figure 2.6 presents the cost reductions observed during the sensitivity analysis. The results indicate that the greatest cost reduction occurs when the L&UL cost for the proposed system, utilizing intermediate warehouses as classification facilities, is set at $300 per container. Under this scenario, the cost savings amount to $3,298.79 million compared to the current system. The second-largest reduction is achieved when the L&UL cost is $600 per container, leading to $2,354.38 million in cost savings relative to the existing system.

Regarding the impact on ton-miles, as shown in **Figure 2.7**, the results indicate that in nearly all parameter variations, the total ton-miles for both trucks and rail decrease. When warehouses allocate a larger portion of their capacity to handle the targeted inbound flow from the port, truck travel distances are further reduced. This effect is even more pronounced when the rail L&UL cost is lowered to $600 or $300 per container, compared to the base value of $900 per container, which aligns with costs at rail terminals. Lower rail L&UL costs encourage greater utilization of rail, leading to a significant modal shift from trucks to rail. Conversely, when the rail L&UL cost increases to $1,200 per container, freight shifts back to truck transport, making rail less cost-effective.

A similar trend is observed in **Figure 2.8**, where environmental and social cost savings are maximized when the L&UL cost is reduced to $600 or $300 per container. However, when the cost increases to $1,200 per container, environmental costs rise compared to the proposed system, primarily due to the shift back to truck transport.

As shown in **Figure 2.9**, reducing the L&UL cost to $600 or $300 per container causes the system to redistribute a portion of the freight handled in California warehouses to warehouses in Arizona and Nevada. Furthermore, if these warehouses allocate 10% to 30% less of their total capacity to managing the targeted inbound freight, the system increasingly relies on warehouses in Arizona and Nevada, further optimizing freight distribution.

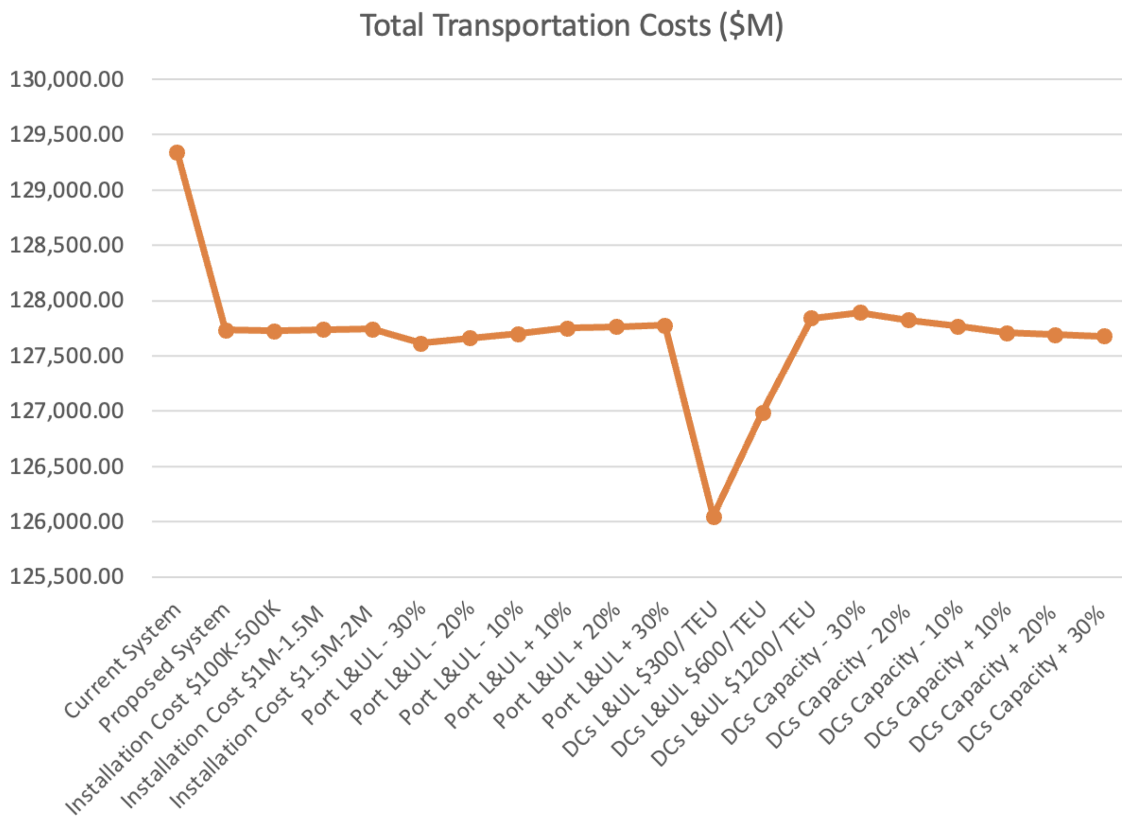

Figure 2.6: Impact of sensitivity analysis on transportation cost variations.

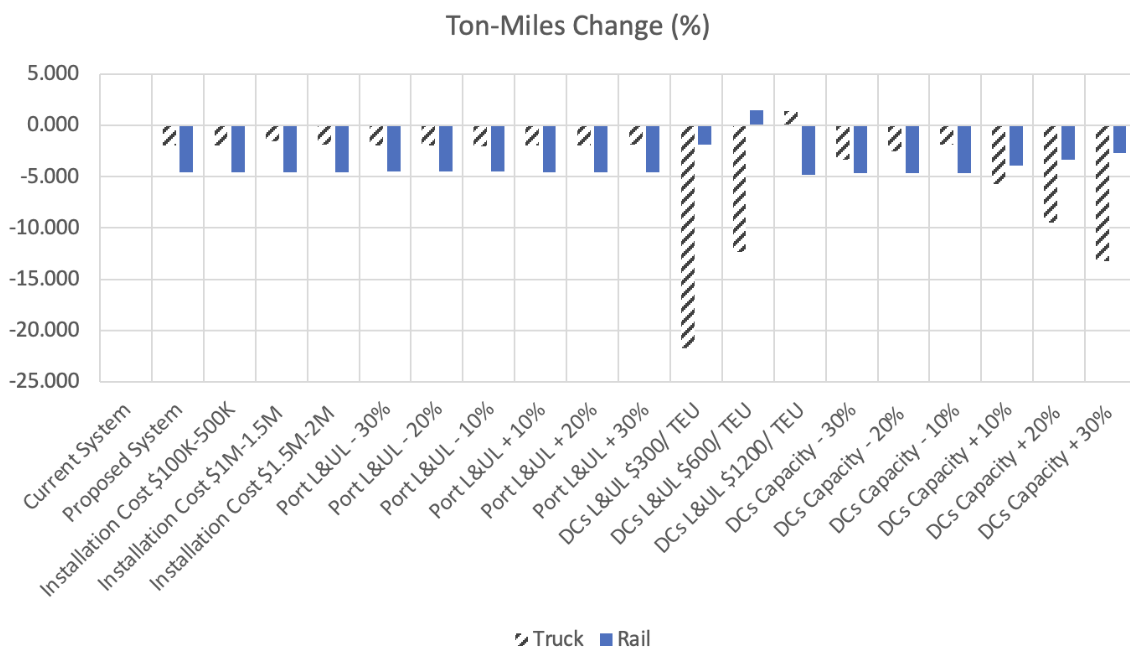

Figure 2.7: Impact of sensitivity analysis on ton-mile variations.

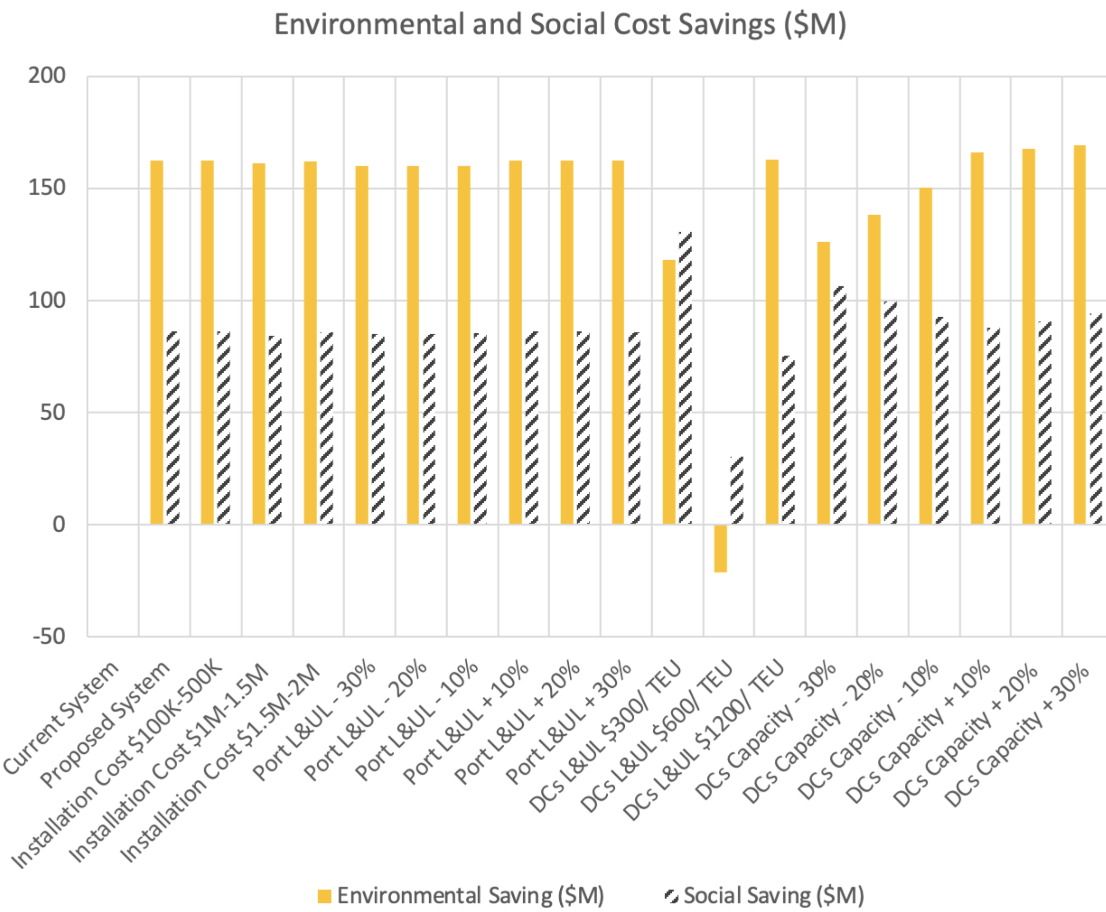

Figure 2.8: Impact of sensitivity analysis on environmental and social cost saving variations.

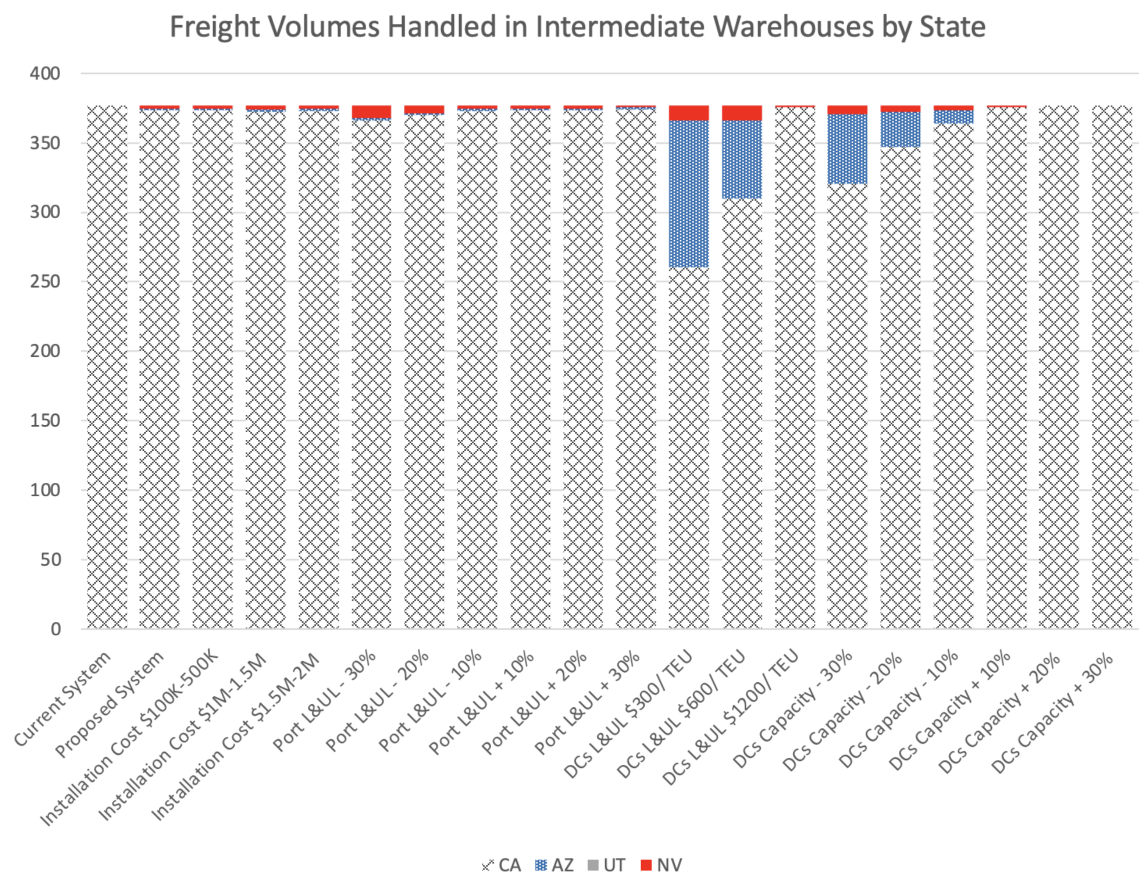

Figure 2.9: Impact of sensitivity analysis on the utilization of intermediate warehouses by state

2.8 Conclusion

This paper explores the application of two-stage stochastic programming to optimize warehouse selection and freight transportation within a supply chain management context, specifically focusing on the container inbound system. Unlike current operational practices, which primarily concentrate on sorting containers at the SPPC, our approach extends this process to include hinterland warehouses located farther from the SPPC. By incorporating uncertainties such as variations in demand levels and patterns across U.S. states, we developed a model that supports more informed decision-making in environments characterized by significant unpredictability. This methodology provides valuable insights into the trade-offs between different transportation modes and their impact on overall system performance. Our model demonstrates substantial potential for cost savings, with a projected reduction of \$1.611 billion over a 10-year period compared to the existing system. Computational results show that the proposed system not only reduces overall transportation costs and the number of trucks needed in the distribution network but also enhances the cost-effectiveness of rail transportation, particularly for shorter distances.

The analysis emphasizes that both warehouse capacity allocation and L&UL costs at warehouses significantly influence the geographic distribution of freight. Lower warehouse L&UL costs lead to a substantial shift of freight from California to neighboring states, particularly Arizona and Nevada. When the L&UL cost is \$600 per container, freight movement from the port complex to warehouses is primarily handled by rail, with 326.68 million tons transported by rail and 49.98 million tons by truck. Even more notably, if the L&UL cost decreases to \$300 per container, it becomes optimal to transport all freight by rail, completely eliminating truck usage from SPPC to the warehouses. This results in the most efficient total transportation costs across all scenarios, amounting to \$126,045.07 million. The cost reduction streamlines rail transport, making it more economical and appealing, even for shorter distances, and further reinforces the shift away from truck transport.

Similarly, reducing the percentage of warehouse capacity dedicated to the proposed system results in greater reliance on warehouses outside California, with Arizona experiencing the most significant increase in freight volume. These findings demonstrate that strategic adjustments in warehouse capacity and cost structures can optimize freight distribution while maintaining system efficiency across diverse condition.

The results demonstrate that the proposed system outperforms the current system in terms of environmental and social impacts, showing reductions in greenhouse gas emissions, pollutants, congestion, and safety risks. The sensitivity analysis identifies the key factors influencing these impacts of the proposed system, such as installation costs, L&UL costs at warehouses, and warehouse capacity. The proposed system remains robust, even with variations in key parameters, including intermodal installation costs (ranging from \$100,000 to \$2 million) and warehouse capacity allocations (fluctuating by $\pm$ 30%).

2.9 Future research

Future research could explore the incorporation of additional sources of uncertainty and the refinement of model parameters to enhance the system's robustness and applicability to real-world contexts. For example, scenario generation could be expanded to include disruptive events such as natural disasters or system outages, which would allow for the assessment of the framework's resilience under extreme conditions. Additionally, the current model assumes equal probability for all scenarios, an assumption that may not hold true in practice. Future studies could focus on developing methods to estimate the likelihood of each scenario based on historical data, expert judgment, or predictive analytics, thereby improving the realism and accuracy of the model's outcomes.

Moreover, the proposed supply chain system offers potential benefits that merit further investigation. These include the reduction of traffic congestion in and around port areas and neighboring communities, the mitigation of operational bottlenecks, the promotion of more balanced utilization of transportation resources, and the enhancement of overall freight throughput in the inbound supply chain. Quantifying and validating these advantages through empirical studies or simulation-based evaluations would be a valuable direction for future work.

Nonetheless, the proposed system also presents several challenges. One significant limitation is the restricted hinterland connectivity of rail, particularly in logistics centers lacking intermodal capabilities. Additionally, successful implementation of the system would require a modal shift from the current truck-dominant configuration to one that more fully integrates rail. The system also redefines the role of distribution centers—expanding beyond their traditional function of cargo transfer into domestic containers to encompass transloading, value-added services, and acting as intermediaries for railcar sorting and rail access.

Such a transformation necessitates increased coordination among multiple stakeholders. This includes private-sector entities such as warehouses and rail carriers, as well as public-sector actors such as highway authorities. To foster collaboration, a comprehensive review of strategic goals and relevant policies is essential. This would support efforts to increase stakeholder engagement, raise awareness, and facilitate alignment across sectors for effective implementation.

Chapter 3

Optimizing Inbound Port Container Dispatch via Rail: A Deep Reinforcement Learning Approach

Abstract

The selection of facilities for handling container shipments significantly impacts freight transportation performance. This study addresses the operational-level decision-making problem under uncertainty, where frequent scenario changes occur within short time intervals. We formulate the problem as a Markov Decision Process (MDP), focusing specifically on the container movement from SPPC to warehouses via rail. Then apply reinforcement learning (RL) techniques, including Deep Q-Networks (DQN) and Advantage Actor-Critic (A2C), to determine optimal warehouse selection policies. These methods effectively handle large state-action spaces and dynamic environments. We also compare the RL-based approaches with a baseline policy selection based on heuristics. Our findings confirm that the model can successfully learn and adapt policies for warehouse selection at an hourly decision-making interval. Among the methods tested, A2C performs consistently well across all problem size configurations and outperforms both DQN and heuristic-based policies. Evaluation results demonstrate its ability to adjust to fluctuating vessel arrivals and varying container distribution across transportation modes, validating the feasibility of RL-based approaches in optimizing freight transportation under uncertainty.

3.1 Introduction

The management of container logistics originating from ports is a crucial area of focus due to its direct impact on the efficiency and effectiveness of supply chain operations. In today's globally interconnected economy, the timely and cost-efficient movement of goods is imperative for businesses to maintain competitiveness. However, this field is confronted with escalating challenges stemming from the growing complexity and unpredictability of supply chain operations, including operational disruptions and fluctuating demand. There is a pressing need for robust and adaptable logistics strategies capable of effectively responding to changing conditions and mitigating risks.

Traditional models in logistics planning often assume deterministic demand and supply conditions, which fail to capture the inherent stochasticity present in real-world scenarios. As a result, such models are limited in their ability to provide robust decision-making frameworks under uncertainty. This dissertation addresses these limitations by developing a stochastic optimization model that explicitly incorporates demand variability and the impact of supply chain disruptions, such as vessel arrivals and varying amounts of containers assigned for truck and rail transport, on inland container flows. The proposed model integrates elements of reinforcement learning to dynamically optimize transportation decisions based on observed demand patterns, thereby offering a realistic and adaptable approach to intermodal freight management.

This research aims to expand the scope of the previous model in Chapter 2 by encompassing the operational dynamics of inbound freight container movement within the SPPC intermodal system. We approach the problem by formulating it as a Markov decision process, focusing specifically on the container movement from SPPC to warehouses via rail. This expansion incorporates various factors such as container movement, inventory level, operational timing, and lead time considerations. Our objective is to optimize container movement, streamline operations related to container sorting and storage at warehouses, and enhance system resilience by minimizing the total processing time across the system. Additionally, we seek to establish a daily operational-level policy for making train routing decisions.

Reinforcement learning is often preferred to stochastic programming, especially in dynamic or complex environments that demand continuous adaptive decision-making. For instance, in scenarios like optimizing routes in a dynamic supply chain or adjusting inventory levels in response to real-time demand, it offers a more flexible and scalable solution. In the context of this problem, deep reinforcement learning is particularly effective for environments with continuous or large state spaces. This capability enables it to manage complex decision-making tasks, such as determining when and where to assign rail transportation in a dynamic setting.

By exploring these operational intricacies, we provide valuable insights and practical guidance for container shipping planners, particularly for railroads and warehouses, to optimize their operations, improve efficiency, and adapt to dynamic decision-making in the face of uncertainty in container sorting processing time, including both processing time and storage time. This chapter contributes to the advancement of container logistics management, offering solutions to the real-world challenges faced by industry professionals.

This chapter is organized as follows: Section 3.2 provides a review of relevant literature. Section 3.3 describes the problem formulation as a Markov Decision Process (MDP), including the definitions of states, actions, transitions, and rewards. Section 3.4 presents the reinforcement learning algorithms—Deep Q-Network (DQN) and Advantage Actor-Critic (A2C)—as well as the heuristic-based policy used for comparison. Section 3.5 outlines the data collection process, model parameters, and underlying assumptions. Section 3.14 discusses the performance of the trained models, comparing both algorithms against the heuristic policy. Finally, Sections 3.7 and 3.8 provide the conclusion and future research directions, respectively.

3.2 Literature Review

Over the past few decades, extensive research has been dedicated to enhancing intermodal transportation systems, with a particular emphasis on optimizing port operations, which serve as critical hubs within global supply chains. Various methodological approaches have been explored to improve port logistics and operational efficiency. For instance, Gao and Sun (2023) proposed a nonlinear mixed-integer programming model to address ship routing, pickup-and-delivery scheduling between ports, speed optimization, and tidal berth time windows. Similarly, Zhang et al. (2023) developed a mixed-integer programming model aimed at minimizing the total driving distance of vehicles in daily yard allocation and manpower assignment operations. Beyond optimization models, researchers have also investigated the role of emerging technologies in improving port management, as seen in studies on blockchain applications and digital transformation in port operations (Molavi et al., 2020; Ahmad et al., 2021).

The inherent stochasticity of port and transportation systems has also been a focal point in the literature. Agra et al. (2015) applied a two-stage stochastic programming framework to an inventory routing problem, optimizing the distribution and inventory management of oil products between islands and ports. Similarly, Chen et al. (2023) addressed the dynamic container drayage booking and routing problem under uncertain demand using a multi-stage stochastic programming model, which optimally schedules tractors and trailers for container transportation. Bhurtyal et al. (2024) study how investments in port capacities, including handling equipment and storage infrastructure, can minimize expected total costs under uncertain commodity demand. In the context of disaster resilience, Peng et al. (2016) formulated a two-stage stochastic programming model to minimize post-disaster economic losses by determining which seaports should undergo retrofitting while incorporating shipping route design considerations. Further advancing the integration of stochastic programming and predictive analytics, Gumuskaya et al. (2021) enhanced periodic capacitated barge planning between an inland terminal and multiple container terminals by incorporating machine learning techniques into the scenario generation process, thereby improving predictions of barge arrival uncertainty.

These studies collectively highlight the diverse methodologies employed in port operation optimization, illustrating the importance of both deterministic and stochastic modeling approaches in addressing the complexities of intermodal logistics systems. However, micro-level planning with uncertainty scenarios faces limitations in handling large networks with many nodes, scenarios, and extended decision epochs. Several researchers have developed Markov Decision Processes (MDP) to address these limitations, leveraging its memoryless property. MDP enables the optimization of complex sequences of decisions over time.

In port operations, MDP has been widely applied to optimize container terminal efficiency. It has been used to minimize the total waiting time of quay cranes and vehicles during loading and unloading operations (Rida et al., 2011), estimate port capacity under various resource allocations, including quay cranes, yard cranes, and prime movers (Lee et al., 2014), and reduce the number of container relocations in empty yards, facilitating the selection of suitable handling equipment and yard configurations (Karakaya et al., 2021). To improve port resilience, MDPs have been employed in berth allocation problems, minimizing mean waiting times under disruptions in vessel arrivals and container handling (Lv et al., 2024). Furthermore, they optimize inter-terminal truck routing by addressing the multi-objective challenge of reducing both empty-truck trip costs and truck waiting times (Adi et al., 2021).

To solve MDPs with high-dimensional state and action spaces, Deep Q-Learning has become computationally more feasible than traditional Q-Learning. Yan et al. (2022) and Rolf et al. (2023) conducted comprehensive literature reviews on the application of reinforcement learning (RL) methodologies in logistics and supply chain management. Their work explores algorithms, key trends, challenges, and future research directions up to 2022, making them valuable references for further study in this field. For more recent papers, Ai et al. (2023) proposes a deep RL approach, Prioritized Experience Replay and Softmax strategy-based Dueling Double Deep Q-Network (PS-D3QN), which combines Double DQN and Dueling DQN to optimize berth and yard scheduling at a bulk cargo terminal, modeled as a MDP. Jin et al. (2023) introduced a self-attention-based Deep Reinforcement Learning (DRL) approach within an Actor–critic framework to minimize the number of blockages when retrieving the containers in maritime storage yards. Lv et al. (2024) utilized a Deep Q-Network (DQN) to solve the MDP formulation of the berth allocation problem, addressing uncertainties in vessel arrival and container handling times. Their approach aims to enhance port resilience by minimizing the mean waiting time. Similarly, Yan et al. (2024) proposed a DRL algorithm integrated with a beam search method to address the container relocation problem, aiming to minimize the number of relocations required to retrieve all containers from a bay. DRL approaches also applied to container shipping operations, including container delivery problems (Tomljenovic et al., 2024) and the empty container repositioning problem (Xu et al., 2024). Tomljenovic et al. (2024) investigated inland container delivery problems and fleet assignment problems, evaluating multiple reward functions and a combination of objectives. Their study sought to balance cost minimization with customer service maximization, offering insights into efficient container flow management. Meanwhile, Xu et al. (2024) examined the empty container repositioning problem in maritime logistics, proposing a reinforcement learning framework with a self-adaptive mechanism for adjusting multi-objective reward function weights. Their objective was to improve container utilization while reducing scheduling and repositioning costs, ultimately addressing resource shortages across various locations. Navigating Demand Uncertainty in Container Shipping, van Twiller et al. (2025), explores the use of DRL for optimizing storage management on vessels to enhance planning efficiency.

There is a significant body of research focused on improving operations for equipment, scheduling, and truck routing. However, most of this work has concentrated on the seaborne aspect, overlooking the critical role of the hinterland network in container transport. Additionally, the role of railroads in moving containers from ports to logistic centers or distribution centers has not been extensively studied. We aim to bridge this gap by examining the operations of port-hinterland facilities with a focus on rail transportation for inbound freight. Furthermore, our contribution lies in addressing the containerized freight movement problem with a dynamic decision-making model that accounts for uncertainty and unknown processing times, rather than treating it deterministically, as many other studies have done.

3.3 Problem Statement

3.3.1 Markov decision processes

This problem focuses on the operational level of container movement through Markov decision processes (MDPs), where the state space includes key variables such as inventory levels at each warehouse, transportation capacities, and the current demand for goods. The action space consists of decisions related to the allocation of containers for transportation via trucks and rails. The transition dynamics are modeled to reflect the changes in inventory and the fulfillment of demand based on the chosen actions. The detailed explanation of the components that define an MDP is provided as follows:

Decision epoch

The agent makes a decision at each time epoch because, in our problem, the state constantly changes as inventory levels are updated at every epoch. These updates occur when containers are dispatched from the port and warehouses, when new containers arrive at these locations, or when vessels arrive at the port. In our model, a decision epoch occurs every hour, ensuring that the agent responds promptly to changes in inventory levels.

States (S)

The state, denoted as a vector s, is defined as $s = (k, I^T, I^R)$, where $s \in S$. The variable k represents the number of containers currently at the port. The vector $I^T = \{I_j^T \mid j \in J\}$ represents the inventory of containers allocated for dispatch to destination by truck, where I_j^T denotes the truck inventory at each warehouse j. Similarly, $I^R = \{I_j^R \mid j \in J\}$ represents the inventory of containers allocated for dispatch to destination by rail, where I_j^R denotes the rail inventory at each warehouse j. Here, J is the set of warehouse locations, and j indexes each warehouse.

Actions (A)

In our model, the agent manages the dispatch of containers from the port to warehouses using a unit train during each epoch. The action space A consists of $|J|+1$ actions, where $a=0$ represents the 'wait' action, and $a=j$ corresponds to the action 'move to warehouse j', with $j \in J$ indexed from 1 to $|J|$.

$$A = \{0\} \cup \{a \mid a = j \text{ for } j \in J\},$$

At state s, the set of valid actions $A(s) \subseteq A$ contains all possible actions a_s that the agent can take. The availability of these actions depends on the port's inventory (k) and the state inventory levels (I_j^T, I_j^R). Specifically, the train will have the option to take the action $a_s = j$ only if both of the following conditions are met: (1) the port has enough inventory to fully load the train, and (2) warehouse j has sufficient available capacity to accommodate the containers being transported. If either of these conditions is not met—meaning that there is insufficient capacity at all warehouse locations or the port lacks the necessary inventory to fill a full train—then the only available action will be $a_s = \{0\}$. For example, if the port has enough containers to fill a full train and three warehouses (represented by indices 1, 2, and 3) each have sufficient capacity to receive the full load, then the action space would include three possible actions: $a_s = \{1, 2, 3\}$. The available capacity at warehouse j is calculated as the total capacity of the warehouse, (C_j), minus the current inventory levels for trucks and rail at the warehouse, $(I_j^T + I_j^R)$. This available capacity is considered sufficient to accommodate a full train if it exceeds the train's container-carrying capacity, denoted as μ_R, which is 240 TEUs for a single-stack configuration or 480 TEUs for a double-stack configuration. For simplicity, we assume each train services only one warehouse per route, and the agent determines the train's action for a single train at each decision epoch. These valid actions are defined as follows:

$$a_s \in A(s) = \{0\} \cup \{j \mid j \in J,\ C_j - I_j^T - I_j^R \geq \mu_R \text{ and } k \geq \mu_R\}.$$

The agent can take an action $a_s = j$ if and only if one or more warehouses $j \in J$ satisfy the condition $C_j - I_j^T - I_j^R \geq 480$, and the port's inventory satisfies $k \geq 480$. These conditions ensure that the chosen action is feasible, preventing the agent from deciding to move the train in either of the following cases: (1) there are insufficient containers at the port to load a full train, or (2) the destination warehouse j lacks sufficient capacity to accommodate the train. If both conditions are satisfied, the agent can choose an action to either wait ($a_s = 0$) or move to a warehouse $j (a_s = j)$.

Transition Probability (P)

The transition in each epoch is influenced by the following dynamics: the number of ships arriving at the port and the distribution of containers delivered to a specific warehouse j, transported by rail, into two inventory types I_j^T, I_j^R. The probability of transitioning from state s to s' given a valid action $a_s \in A_s$, is expressed as:

$$P(s'|s, a) = P((k', I'^T, I'^R)|(k, I^T, I^R), a)$$

The system includes two possible actions: $a = j$, where the agent chooses to move containers to warehouse j, and $a = 0$, where the agent waits at the port. For any action a, whether it is $a = 0$ or $a = j$ for some $j \in J$, the sum of transition probabilities over all possible next states s' must equal 1:

$$\sum_{\forall s'} P(s' \mid s, a) = 1 \quad \forall s,\, a \in \{0\} \cup J.$$

In the case of $a = j$, the transition probability $P(s' \mid s, a = j)$ considers two stochastic components: (1) the number of ship arrivals at the port, θ, modeled using a Poisson distribution with parameter λ, and (2) the distribution of containers arriving at warehouse j via rail, modeled using a Binomial distribution with parameters μ_R (the train's capacity for rail containers) and p (the probability of a container being assigned to rail inventory, I_j^R). The conditions for a valid state transition include updates to the port inventory k, rail inventory I_j^R, and truck inventory I_j^T. The updated number of containers at the port, k', accounts for the containers arriving from ships and those departing due to rail operations at each time epoch. Since each ship brings a fixed quantity of μ_S containers (the ship's container capacity), the total contribution of arriving containers is $\mu_S \cdot \theta$. The term $-\mu_R$ represents the number of containers deducted from the port inventory due to rail dispatch, where μ_R is the capacity of the train for containers.

For the updates to I_j^R and I_j^T, the allocation of containers to rail and truck inventories is determined after the train's arrival, with the total number of arriving containers defined by the train's capacity, μ_R. These containers are then allocated between rail inventory and truck inventory based on their intended destinations. Specifically, $\delta_j^R \sim \text{Binomial}(\mu_R, p)$ represents the number of containers assigned to rail inventory $I_j'^R$ at warehouse j. The remaining containers, $\mu_R - \delta_j^R$, are allocated to truck inventory $I_j'^T$. The parameter p reflects the average proportion of freight allocated to rail for long-distance transport from warehouse j to its destinations, while truck inventory primarily serves nearby destinations.

After allocation, the inventories I_j^R and I_j^T are reduced by their respective dispatch rates, w^R and w^T, which differ based on the mode of transportation. These dispatch rates are deterministic and represent the scheduled dispatch of containers from warehouse j to their final destinations. Specifically, w^R corresponds to the dispatch rate for containers in I_j^R that are designated for long-distance transport via rail, while w^T reflects the dispatch rate for containers in I_j^T that are transported locally via trucks.

For $a = 0$, the agent does not move containers to any warehouse by rails. The transition is influenced solely by the number of ship arrivals at the port, which increases the port inventory k proportionally to the number of container arrivals ($\mu_S \cdot \theta$). The rail and truck inventories, I_j^R and I_j^T, are reduced by the respective waiting rates w^R and w^T, reflecting scheduled operations.

In both cases, the probabilities for any state transition involving values of $\theta \notin \{0, 1, 2, 3\}$ are explicitly set to zero, ensuring that transitions outside the defined range of θ do not occur. This restriction reflects the intended constraint that at most 3 ships can arrive at the port in each epoch. Consequently, the probabilities for $\theta \in \{0, 1, 2, 3\}$ are normalized to ensure that the sum of probabilities for all feasible transitions equals 1. Specifically, this normalization divides the probabilities for $\theta = \{0, 1, 2, 3\}$ by their total sum, while the probabilities for other θ remain zero.

$$P_1(s'|s, a = j) = \begin{cases} \dfrac{\frac{e^{-\lambda}(\lambda)^{\theta}}{\theta!}\binom{\mu_R}{\delta_j^R}(p)^{\delta_j^R}(1-p)^{\mu_R-\delta_j^R}}{\sum_{\theta'=0}^{3}\frac{e^{-\lambda}\lambda^{\theta'}}{\theta'!}} & \text{if } k' = k + (\mu_S \cdot \theta) - \mu_R, \\ & I_j'^T = I_j^T + (\mu_R - \delta_j^R) - w^T, \\ & I_j'^R = I_j^R + \delta_j^R - w^R, \\ & I_j^T > w^T - (\mu_R - \delta_j^R), \\ & I_j^R > w^R - \delta_j^R, \quad w^R \leq \mu_R \\ & \theta \in \{0, 1, 2, 3\}, \\ & \delta_j^R \in \{0, 1, 2, \ldots, \mu_R\}, \\ \dfrac{\frac{e^{-\lambda}\lambda^{\theta}}{\theta!}\binom{\mu_R}{\delta_j^R}(p)^{\delta_j^R}(1-p)^{\mu_R-\delta_j^R}}{\sum_{\theta'=0}^{3}\frac{e^{-\lambda}\lambda^{\theta'}}{\theta'!}\sum_{\delta_j^{R'}=i_j^T-w^T+\mu_R}^{w^R-I_j^R}\binom{\mu_R}{\delta_j^{R'}}(p)^{\delta_j^{R'}}(1-p)^{\mu_R-\delta_j^{R'}}} & \\ & \text{if } k' = k + (\mu_S \cdot \theta) - \mu_R, \\ & I_j'^T = 0, I_j'^R = 0, \\ & I_j^T \leq w^T - (\mu_R - \delta_j^R), \\ & I_j^R \leq w^R - \delta_j^R, \quad w^R \leq \mu_R \\ & \theta \in \{0, 1, 2, 3\}, \\ & \delta_j^R \in \{I_j^T - w^T + \mu_R, 1, \ldots, w^R - I_j^R\}, \\ 0 & \text{otherwise.} \end{cases}$$

$$
P_2(s'|s,a=j) = \begin{cases}
\dfrac{\frac{e^{-\lambda}\lambda^{\theta}}{\theta!}\binom{\mu_R}{\delta_j^R}(p)^{\delta_j^R}(1-p)^{\mu_R-\delta_j^R}}{\sum_{\theta'=0}^{3}\frac{e^{-\lambda}\lambda^{\theta'}}{\theta'!}\sum_{\delta_j^{R'}=\psi}^{\mu_R}\binom{\mu_R}{\delta_j^{R'}}(p)^{\delta_j^{R'}}(1-p)^{\mu_R-\delta_j^{R'}}} & \text{if } k' = k + (\mu_S \cdot \theta) - \mu_R, \\
& \quad I_j'^T = 0, \\
& \quad I_j'^R = I_j^R + \delta_j^R - w^R, \\
& \quad I_j^T \leq w^T - (\mu_R - \delta_j^R), \\
& \quad I_j^R \geq w^R - \delta_j^R, \quad w^R \leq \mu_R \\
& \quad \theta \in \{0,1,2,3\}, \\
& \quad \psi = \max(w^R - I_j^R, I_j^T - w^T + \mu_R) \\
& \quad \delta_j^R \in \{\psi, \psi+1, \ldots, \mu_R\}, \\
\dfrac{\frac{e^{-\lambda}\lambda^{\theta}}{\theta!}\binom{\mu_R}{\delta_j^R}(p)^{\delta_j^R}(1-p)^{\mu_R-\delta_j^R}}{\sum_{\theta'=0}^{3}\frac{e^{-\lambda}\lambda^{\theta'}}{\theta'!}\sum_{\delta_j^{R'}=0}^{\phi}\binom{\mu_R}{\delta_j^{R'}}(p)^{\delta_j^{R'}}(1-p)^{\mu_R-\delta_j^{R'}}} & \text{if } k' = k + (\mu_S \cdot \theta) - \mu_R, \\
& \quad I_j'^T = I_j^T + (\mu_R - \delta_j^R) - w^T, \\
& \quad I_j'^R = 0, \\
& \quad I_j^T > w^T - (\mu_R - \delta_j^R), \\
& \quad I_j^R \leq w^R - \delta_j^R, \quad w^R \leq \mu_R \\
& \quad \theta \in \{0,1,2,3\}, \\
& \quad \phi = \min(w^R - I_j^R, i_j^T - w^T + \mu_R - 1) \\
& \quad \delta_j^R \in \{0, 1, \ldots, \phi\}, \\
0 & \text{otherwise.}
\end{cases}
$$

$$
P(s' \mid s, a=0) = \begin{cases}
\dfrac{\frac{e^{-\lambda}\lambda^{\theta}}{\theta!}}{\sum_{\theta'=0}^{3} \frac{e^{-\lambda}\lambda^{\theta'}}{\theta'!}} & \text{if } k' = k + (\mu_S \cdot \theta), \\
& I_j'^T = I_j^T - w^T, \\
& I_j'^R = I_j^R - w^R, \\
& I_j^T \geq w^T, \quad I_j^R \geq w^R, \\
& \theta \in \{0,1,2,3\}, \\
\dfrac{\frac{e^{-\lambda}\lambda^{\theta}}{\theta!}}{\sum_{\theta'=0}^{3} \frac{e^{-\lambda}\lambda^{\theta'}}{\theta'!}} & \text{if } k' = k + (\mu_S \cdot \theta) \\
& I_j'^T = 0, \quad I_j'^R = 0 \\
& I_j^T < w^T, \quad I_j^R < w^R, \\
& \theta \in \{0,1,2,3\}, \\
\dfrac{\frac{e^{-\lambda}\lambda^{\theta}}{\theta!}}{\sum_{\theta'=0}^{3} \frac{e^{-\lambda}\lambda^{\theta'}}{\theta'!}} & \text{if } k' = k + (\mu_S \cdot \theta), \\
& I_j'^T = 0, \quad I_j'^R = I_j^R - w^R, \\
& I_j^T < w^T, \quad I_j^R \geq w^R, \\
& \theta \in \{0,1,2,3\}, \\
\dfrac{\frac{e^{-\lambda}\lambda^{\theta}}{\theta!}}{\sum_{\theta'=0}^{3} \frac{e^{-\lambda}\lambda^{\theta'}}{\theta'!}} & \text{if } k' = k + (\mu_S \cdot \theta), \\
& I_j'^T = I_j^T - w^T, \\
& I_j'^R = 0 \\
& I_j^T \geq w^T, \quad I_j^R < w^R, \\
& \theta \in \{0,1,2,3\}, \\
0 & \text{otherwise.}
\end{cases}
$$

Here, "otherwise" indicates that if the specified conditions (e.g., constraints on k', $I_j'^R$, $I_j'^T$, or θ) are not satisfied, the probability of transitioning to the state s' is zero. In such a case, the model does not transition to the state described by s', and the current state remains unchanged.

Reward function (R)

In the MDP framework, the reward function is designed to guide the agent's learning by minimizing container dwell time (CDT). The reward at each epoch, denoted as $r(s)$, is computed based on the current state s prior to the state transition. Specifically, the reward reflects the total container dwell time, which is calculated by multiplying the sum of all container inventories in the system — including the port inventory k and the truck and rail inventories at each warehouse, i_j^T and i_j^R — by the time length of the epoch, Δt. The example of how to obtain CDT showed in **Figure 3.1** This reward structure incentivizes the agent to prioritize rail movement toward warehouses in a way that minimizes container accumulation over time. By doing so, the agent seeks to minimize the expected cumulative container dwell time experienced at the port and warehouses over the course of the decision process. The reward function is formally defined as:

$$r(s) = (k + I^T + I^R) \cdot \Delta t$$

In this section, the problem was formulated within the MDP framework, with detailed definitions of each component. The next section presents the methodology developed to solve the MDP and train the agent to minimize container dwell time throughout the system.

3.4 Methodology

In dynamic and complex environments where decisions are sequential and involve high-dimensional spaces, the challenge of modeling and solving problems becomes computationally intensive. This is especially true when the underlying probabilistic

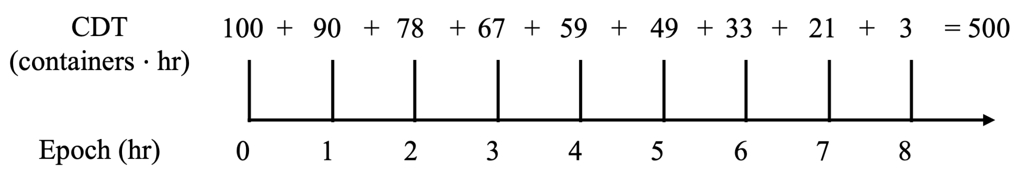

Figure 3.1: Reward structure

models of uncertainties are unknown, and environmental changes must be accounted for. Solving such problems over multiple time steps and scenarios can be infeasible. In these contexts, Q-learning provides a more practical solution. As a model-free reinforcement learning (RL) approach, Q-learning can adapt and learn directly from interactions with the environment, without requiring a predefined model of uncertainties.

For our problem, Q-learning is adopted to make sequential operational decisions, specifically for determining when and where rail transportation should be assigned to move containers from the SPPC to warehouses. The state and action spaces in our problem are quite large, leading to the following challenges in traditional Q-learning:

For 200 warehouses, this leads to a space dimension of 32,321,001, which is computationally prohibitive to store the Q-values for all state-action pairs using traditional Q-learning algorithms.

To address this complexity, we use more advanced approaches such as Deep Q-Networks (DQN) and Advantage Actor-Critic (A2C). Both of these reinforcement learning algorithms allow us to train agents to make optimal decisions in such large-scale sequential decision-making problems

3.4.1 Deep Q-Learning (DQN)

DQN is an extension of Q-learning that leverages neural networks as function approximators to estimate the Q-values for state-action pairs. Unlike traditional Q-learning, where each state-action pair is explicitly stored and updated, DQN uses a neural network to approximate the Q-values, significantly reducing the dimensionality of the state and action spaces. The neural network takes the current state s as input and outputs Q-values for each possible action a, allowing the agent to approximate the optimal action selection in a much more scalable way.

DQN introduces several key innovations to address the instability and divergence issues commonly encountered in standard Q-learning. One of the primary enhancements is the incorporation of experience replay, which enables the storage of past experiences and their random sampling during training. This mechanism reduces the correlation between consecutive updates, thereby preventing the model from overfitting to recent experiences and improving sample efficiency. Additionally, DQN employs a target network that is updated at a lower frequency than the policy network, ensuring more stable target values for Q-learning updates. By separating the target from the rapidly changing policy network, this approach mitigates the risk of divergence and enhances the overall stability of the learning process.

Algorithm 1 Deep Q-Network (DQN) with Experience Replay (Mnih et al., 2015)

```
Initialize replay memory D and target network update frequency C
Initialize policy network action-value function Q with random weights θ
Initialize target network action-value function Q̂ with weights θ⁻ = θ
for each episode do
    Initialize state s_0
    for each time step t do
        Select action a_t using ε-greedy policy:
            with probability ε, select a random action a_t
            otherwise, select a_t = arg max_a Q(s_t, a; θ)
        Execute the selected action a_t and observe reward r_t and next state s_{t+1}
        Store transition (s_t, a_t, r_t, s_{t+1}) in D
        Sample a random minibatch of transitions (s_j, a_j, r_j, s_{j+1}) from D
        Set target y_j = { r_j                                  if episode terminates at s_{j+1}
                         { r_j + γ max_{a'} Q̂(s_{j+1}, a'; θ⁻)   otherwise
        Update the policy network parameters θ by performing a gradient descent
    step to minimize the loss (y_j − Q(s_j, a_j; θ))^2
        Every C steps, update target network: θ⁻ ← θ
    end for
end for
```

The training process begins by initializing a replay memory D to store experience tuples and setting a target network update frequency C. The policy network, responsible for approximating the action-value function $Q(s, a; \theta)$, is initialized with random weights θ, while the target network, $\hat{Q}(s, a; \theta^-)$, is initialized with weights identical to the policy network ($\theta^- = \theta$).

During each episode, the algorithm starts from an initial state s_0 and follows a time-stepped process to interact with the environment. At each time step t, the agent selects an action a_t using an ϵ-greedy policy, where, with probability ϵ, a random action is chosen to encourage exploration, and otherwise, the action that maximizes the predicted Q-value is selected. The chosen action a_t is executed, leading to an observed reward r_t and a transition to the next state s_{t+1}. This transition tuple (s_t, a_t, r_t, s_{t+1}) is then stored in the replay memory D, which allows the model to break temporal correlations and improve learning stability.

To update the policy network, a minibatch of experience samples is randomly drawn from D. For each sampled transition, the target value y_j is computed using the Bellman equation. If the episode terminates at s_{j+1}, the target is simply the immediate reward r_j. Otherwise, the target includes the discounted maximum Q-value from the target network, incorporating future reward estimates. The policy network is then updated by performing a gradient descent step to minimize the loss between the predicted Q-value and the computed target. Every C steps, the target network is synchronized with the policy network by updating $\theta^- \leftarrow \theta$, ensuring stability in learning.

3.4.2 Advantage Actor-Critic (A2C)

A2C, on the other hand, is a different reinforcement learning technique that combines both value-based and policy-based methods. While Q-learning (and DQN) estimates the value of state-action pairs, A2C uses a different approach to learn the optimal policy. It employs two components: the actor and the critic networks.

The actor is responsible for selecting actions based on the current policy, which is typically represented as a probability distribution over actions. It updates the policy based on feedback from the critic. This is the part of the model that decides which action to take given a state. It directly learns the policy, which is the probability distribution over actions for each state. The goal of the actor is to learn the optimal policy that maximizes the expected cumulative reward.

The critic evaluates the actions taken by the actor by estimating the value function $V(s)$, which represents the expected return (reward) from a given state. The critic's feedback helps guide the actor in improving its decision-making process.

The key advantage of A2C over Q-learning (and DQN) is that it focuses on learning policies directly, rather than learning the value of state-action pairs. As a result, A2C does not explicitly store Q-values for every state-action pair. Training in A2C occurs by updating the actor's policy parameters using the advantage function to reduce variance in policy gradient updates, while the critic updates its value function using temporal difference learning. The algorithm operates synchronously, meaning multiple agents interact with the environment and update their parameters collectively, leading to improved sample efficiency.

This enhances the stability and efficiency of the learning process. The advantage function $A(s, a)$ is defined as the difference between the state-action value function $Q(s, a)$, which represents the expected return of taking action a in state s, and the state value function $V(s)$, which represents the expected return starting from state s. Mathematically, this is given by:

$$A(s, a) = Q(s, a) - V(s)$$

This function measures how much better or worse an action is compared to the average action for a given state. By using the advantage, A2C mitigates the problem of high variance often found in policy gradient methods, leading to more stable and efficient training.

The loss function in the A2C algorithm consists of two primary components: the policy loss (actor loss) and the value loss (critic loss).

The policy loss is designed to optimize the policy by encouraging actions that result in higher expected rewards. It is formulated as:

$$L_{\text{policy}} = -\mathbb{E}\left[\log \pi_\theta(a_t|s_t)A_t\right]$$

where $\pi_\theta(a_t|s_t)$ represents the probability of selecting action a_t given state s_t, which is parameterized by θ. The term A_t denotes the advantage function, typically computed as the difference between the cumulative reward R_t and the estimated state-value function $V(s_t)$, i.e., $A_t = R_t - V(s_t)$. The expectation is taken over the state-action distribution under the current policy. Since the goal is to maximize the advantage, the loss function is negated, ensuring that actions leading to positive advantages are reinforced.

The value loss is responsible for training the critic to estimate the state-value function accurately. It is expressed as a mean squared error (MSE) between the predicted value function and the actual return:

$$L_{\text{value}} = \mathbb{E}\left[(R_t - V_\phi(s_t))^2\right]$$

where $V_\phi(s_t)$ is the critic's estimate of the state-value function, parameterized by ϕ, and R_t is the actual return, computed using bootstrapped estimates from the sampled trajectories. This loss function ensures that the critic learns to approximate the true value function, thereby providing more accurate advantage estimates for the actor.

This formulation enables the A2C algorithm to jointly optimize both the policy and value function, ensuring stable and efficient learning in reinforcement learning environments.

3.4.3 Heuristic-based policies

The heuristic method is designed to serve as a baseline for comparison with the DRL. The state transtion function still the same as DRL based on ship arrivals, inventory movements, and warehouse processing, however, the action selection rule is different.

Algorithm 2 Advantage Actor-Critic (A2C) Algorithm (Mnih et al., 2016)

Initialize actor network $\pi_\theta(a|s)$ with random weights θ and learning rate α_π
Initialize critic network $V_\phi(s)$ with random weights ϕ and learning rate α_v
for each episode **do**
  Initialize environment and observe initial state s_0
  for each time step t **do**
    Sample action $a_t \sim \pi_\theta(a_t|s_t)$
    Execute action a_t, observe reward r_t and next state s_{t+1}
    Compute TD target: $R_t = r_t + \gamma V_\phi(s_{t+1})$
    Compute advantage estimate: $A_t = R_t - V_\phi(s_t)$
    Compute policy loss: $L_{\text{policy}} = -\log \pi_\theta(a_t|s_t) \cdot A_t$
    Compute value loss: $L_{\text{value}} = (R_t - V_\phi(s_t))^2$
    Update actor parameters: $\theta \leftarrow \theta - \alpha_\pi \nabla_\theta L_{\text{policy}}$
    Update critic parameters: $\phi \leftarrow \phi - \alpha_v \nabla_\phi L_{\text{value}}$
    Update state: $s_t \leftarrow s_{t+1}$
  end for
end for

At each time period, the action is selected according to a rule-based approach. If the port inventory k is greater than or equal to the rail capacity, the model selects the warehouse with the highest available capacity to receive the shipment. The available capacity of the warehouses is calculated as the difference between the maximum capacity of the warehouse and the sum of its truck and rail inventories. If the port inventory is less than the rail capacity, or if no warehouse has sufficient availability to receive a train, no containers are moved and the action defaults to ‘wait’.

The simulation is run for a fixed number of time periods, using the same configuration as DQN and A2C. The cumulative rewards are then compared across the rule-based model, DQN, and A2C to evaluate their relative performance in managing the container flow system.

3.5 Modeling approach

3.5.1 Data collection and parameters justification

We collected data on warehouses in California, Nevada, Arizona, and Utah, including warehouse capacity (or estimated annual tonnage where capacity was not publicly available), annual lift, location, rail accessibility, and functionalities (on-dock, near-dock, and off-dock). For warehouses with unknown capacities, we estimated their capacities based on a proportional comparison to other warehouses with known capacities, using factors such as total space, storage space, or the number of tracks, depending on the available online data for each facility. In total, we identified 214 warehouses, of which 104 currently have rail accessibility. Our current practice model involves training the policy using these 104 warehouses.

For time related data we use in our research, we have three main parts: time associated with container vessel at the port (ship arrival rate), time associated with rail at the port (dispatch rate), and time associated with rails' and trucks' inventories at warehouses (waiting time). We estimated the ship arrival rate based on the total number of containers handled by the Port of Los Angeles in 2020, which was 8 million TEUs, divided by the ship's capacity of 20,000 TEUs (Gresser, 2024; The Maritime Executive, 2021). This calculation suggests that approximately 400 ship arrivals occurred in the port in 2020. In CY 2023, Vessel Arrivals (All Types) at POLA was 1,712, including container Vessels, Tank Vessels, Dry Bulk/General Cargo Vessels, RoRo Vessels, Reefer Vessels, and Cruise Vessels (POLA, 2024).

POLA published container vessels activity, including daily information of the number of veseels at anchor, at berth, Vessels Departed, Average Days at Berth, and Average Days at anchor + Berth. (POLA, 2025) we sum up the log of number of vessels departed from POLA in 2024, obtained total of 898 vessels in 2024, which is 2.45 vessels per day.

For railcar capacity, well cars can be double-stacked, allowing up to 10 TEUs per railcar (BNSF, 2024b). With an average train consisting of 77.1 railcars (Rattanakunuprakarn et al., 2024), a double-stacked train can carry approximately 770 TEUs, while a single-stacked train can carry about 385 TEUs.

3.5.2 Model assumptions

The assumptions made in this model are grounded in historical data observed on a real scale. To ensure that the model remains representative across different sizes, we scale our parameters proportionally to align with historical data. For example, as we vary the model size from a small configuration with 15 warehouses to a large configuration with 104 warehouses, each parameter is adjusted to reflect the historical proportions accurately. The parameters and data used in this research are as follows:

- **Warehouse Inventory Capacity:** Each warehouse has a specific capacity, adjusted based on the size of the model, to ensure that smaller and larger models retain realistic storage limits comparable to actual historical distributions.

- **Transportation Schedules and Capacities:** Truck and rail schedules, along with their respective carrying capacities, are based on historical averages but scaled proportionally for the size of the model. This ensures realistic arrival intervals and volume flows across varying warehouse counts.

- **Port Inventory Levels and Ship Arrivals:** Inventory levels at the port and ship arrival rates are modeled using a Poisson distribution, with a maximum of three ship arrivals per time period. This keeps arrival patterns consistent with observed operational data.

- **Reduction Schedules:** Inventory reductions at warehouses and the port, which correspond to dispatches via trains and trucks, follow predetermined schedules that reflect observed dispatch frequencies and volumes.

- **Container allocation:** When a train arrives at warehouse j, the containers are divided into two inventory categories: those designated for outbound shipment by truck (i_j^T) and those by rail (i_j^R). This assignment follows a Binomial distribution, with a success probability of 0.7 for each container being allocated to long-distance rail shipment (i_j^R).

These assumptions allow the model to replicate realistic supply chain operations, maintaining fidelity to observed historical trends while adapting to different model sizes. Each parameter is chosen carefully to ensure that the model remains adaptable and accurately reflects real-world dynamics.

3.6 Results and discussion

This section presents the implementation details, experimental setup, and analysis of results obtained from our trained model.

3.6.1 Experimental setup

For our DQN and A2C implementation, we used PyTorch 2.5.0 as the primary framework to develop and train the model, utilizing its neural network modules and optimization routines. To enhance the performance of the algorithms, hyperparameter tuning is conducted. Parameters and network architecture such as the learning rate, discount factor, number of episodes, and the frequency of target network updates are systematically adjusted. Final parameter and model's hyperparameter values are shown in **Tables 3.1** to **Tables 3.13**, corresponding to different problem sizes with configurations of 5 warehouses, 15 warehouses, 55 warehouses, and 104 warehouses, respectively.

Table 3.1: Parameters for 5-Warehouse Configuration

Parameter	**Value**	**Parameter**	**Value**
No. warehouses	5	Ship capacity	150 containers
Warehouse capacity	range [10, 40]	Rail capacity	16 containers
Truck capacity	1 container	Container allocation	Binomial distribution, p = 0.7 for being assigned to i_j^R
Inventory reduction schedules	Trucks: 3-8 TEUs/hr, Rails: 30-60 TEUs/ 4 hrs	Ship arrival time	Poisson distribution, lambda = 1/5

Table 3.2: Parameters for 15-Warehouse Configuration

Parameter	**Value**	**Parameter**	**Value**
No. warehouses	15	Ship capacity	300 containers
Warehouse capacity	range [99, 553]	Rail capacity	100 containers
Truck capacity	1 container	Container allocation	Binomial distribution, p = 0.7 for being assigned to i_j^R
Inventory reduction schedules	Trucks: 3-8 TEUs/hr, Rails: 30-60 TEUs/ 4 hrs	Ship arrival time	Poisson distribution, lambda = 1/5

Table 3.3: Parameters for 30-Warehouse Configuration

Parameter	**Value**	**Parameter**	**Value**
No. warehouses	30	Ship capacity	1000 containers
Warehouse capacity	range [100, 600]	Rail capacity	200 containers
Truck capacity	1 container	Container allocation	Binomial distribution, p = 0.7 for being assigned to i_j^R
Inventory reduction schedules	Trucks: 3-5 TEUs/hr, Rails: 20 TEUs/ 4 hrs	Ship arrival time	Poisson distribution, lambda = 1/5

Table 3.4: Parameters for 55-Warehouse Configuration

Parameter	**Value**	**Parameter**	**Value**
No. warehouses	55	Ship capacity	1000 containers
Warehouse capacity	range (119, 166,926)	Rail capacity	200 containers
Truck capacity	1 container	Container allocation	Binomial distribution, p = 0.7 for being assigned to i_j^R
Inventory reduction schedules	Trucks: 3-10 TEUs/hr, Rails: 40-100 TEUs/ 4 hrs	Ship arrival time	Poisson distribution, lambda = 1/5

Table 3.5: Parameters for 104-Warehouse Configuration

Parameter	Value	Parameter	Value
No. warehouses	104	Ship capacity	1000 containers
Warehouse capacity	range (841, 1171691)	Rail capacity	200 containers
Truck capacity	1 container	Container allocation	Binomial distribution, p = 0.7 for being assigned to i_j^R
Inventory reduction schedules	Trucks: 3-10 TEUs/hr, Rails: 40-100 TEUs/ 4 hrs	Ship arrival time	Poisson distribution, lambda = 1/5

Table 3.6: Hyperparameters for DQN for 5-Warehouse Configuration

Parameter	Value	Parameter	Value
Time horizon	168 hrs	Episodes	400,000
Number of hidden layers	2	Neurons per hidden layer	[50], [50]
Learning rate	1×10^{-2}	Learning frequency	1 hour
Discount factor	1.0	Learning step	70
Epsilon initial and final	1.0 to 0	Decay rate	Exponential
Memory size	15,000	Sample episodes	800

Table 3.7: Hyperparameters for DQN for 15-Warehouse Configuration

Parameter	Value	Parameter	Value
Time horizon	168 hrs	Episodes	400,000
Number of hidden layers	2	Neurons per hidden layer	[100], [50]
Learning rate	1×10^{-5}	Learning frequency	1 hour
Discount factor	1.0	Learning step	40
Epsilon initial and final	1.0 to 0	Decay rate	Exponential
Memory size	20,000	Sample episodes	800

Table 3.8: Hyperparameters for DQN for 30-Warehouse Configuration

Parameter	Value	Parameter	Value
Time horizon	168 hrs	Episodes	400,000
Number of hidden layers	2	Neurons per hidden layer	[500], [500]
Learning rate	1×10^{-3}	Learning frequency	1 hour
Discount factor	1.0	Learning step	70
Epsilon initial and final	1.0 to 0	Decay rate	Exponential
Memory size	20,000	Sample episodes	2,000

Table 3.9: Hyperparameters for A2C for 5-Warehouse Configuration

Parameter	**Value**	**Parameter**	**Value**
Time horizon	168 hrs	Episodes	400,000
Actor's hidden layers	[80, 80]	Critic's hidden layers	[80, 80]
Actor's learning rate	1×10^{-3}	Critic's learning rate	1×10^{-3}
Discount factor	1.0	Learning step	1

Table 3.10: Hyperparameters for A2C for 15-Warehouse Configuration

Parameter	**Value**	**Parameter**	**Value**
Time horizon	168 hrs	Episodes	400,000
Actor's hidden layers	[1000]	Critic's hidden layers	[100, 50]
Actor's learning rate	1×10^{-8}	Critic's learning rate	1×10^{-5}
Discount factor	1.0	Learning step	1

Table 3.11: Hyperparameters for A2C for 30-Warehouse Configuration

Parameter	**Value**	**Parameter**	**Value**
Time horizon	168 hrs	Episodes	400,000
Actor's hidden layers	[1000]	Critic's hidden layers	[100,50]
Actor's learning rate	1×10^{-7}	Critic's learning rate	1×10^{-3}
Discount factor	1.0	Learning step	1

Table 3.12: Hyperparameters for A2C for 55-Warehouse Configuration

Parameter	**Value**	**Parameter**	**Value**
Time horizon	168 hrs	Episodes	500,000
Actor's hidden layers	[1000]	Critic's hidden layers	[100,50]
Actor's learning rate	1×10^{-7}	Critic's learning rate	1×10^{-3}
Discount factor	1.0	Learning step	1

Table 3.13: Hyperparameters for A2C for 104-Warehouse Configuration

Parameter	**Value**	**Parameter**	**Value**
Time horizon	168 hrs	Episodes	600,000
Actor's hidden layers	[1000]	Critic's hidden layers	[100,50]
Actor's learning rate	1×10^{-7}	Critic's learning rate	1×10^{-3}
Discount factor	1.0	Learning step	1

3.6.2 Performance Evaluation

The performance of the DQN algorithm is evaluated using key metrics, including total transportation costs, average delivery time, and inventory turnover rates. These metrics provide insights into the agent's effectiveness in optimizing logistics operations. A comparison is made with baseline policies, demonstrating the advantages of using DQN for this application.

DQN

To assess convergence during model training, both loss and reward metrics were monitored and evaluate using graphs for all four warehouse configurations. Upon completing the training, model performance was evaluated by conducting 10,000 simulations on randomly generated state samples to estimate the cumulative reward, denoted as G.

For the five-warehouse configuration as shown in **Figure 3.2**, the evaluation yielded a mean cumulative reward of -1,897,866.63, with a 95% confidence interval of (-1,906,218.05, -1,889,515.22). The observed cumulative rewards ranged from a minimum of -3,522,101 to a maximum of -326,919. Notably, the mean cumulative reward was consistent with the final performance range observed during training, indicating that the model effectively captured the system dynamics and converged to a stable policy.

Similarly, the results for the fifteen-warehouse configuration are presented in **Figure 3.3**. The model was trained for 400,000 iterations, requiring a total runtime of 14,836.85 seconds. The evaluation results showed a mean cumulative reward of -193,562.14, with a 95% confidence interval of (-194,143.26, -192,981.02). The cumulative rewards varied between -495,000 and -123,986. The consistency between the evaluation results and the training performance further demonstrates the model's ability to learn and generalize the policy within the larger system configuration.

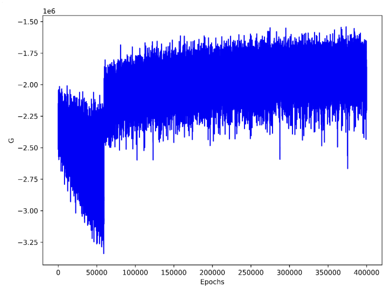

(a) Cumulative reward

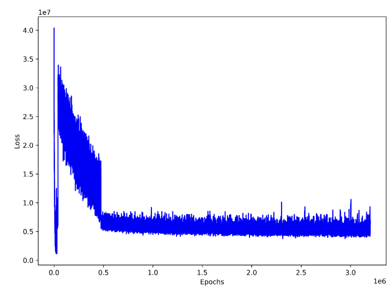

(b) Loss

Figure 3.2: Cumulative reward and loss of DQN with 5 warehouses

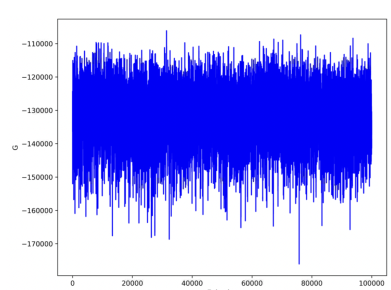

(a) Cumulative reward

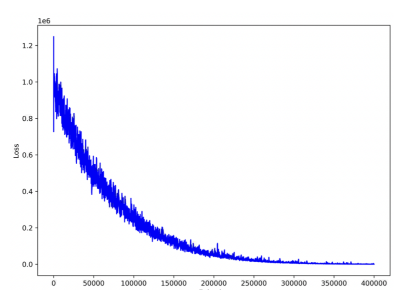

(b) Loss

Figure 3.3: Cumulative reward and loss of DQN with 15 warehouses

For the thirty-warehouse configuration as illustrated in **Figure 3.4**, the model was evaluated after 400,000 iterations, with a total runtime of 372,853.41 seconds. The mean cumulative reward was -4,224,506.56, with a 95% confidence interval of (-4,235,633.61, -4,213,379.51). The observed cumulative rewards varied from a minimum of -6,957,951 to a maximum of -2,454,812.

A2C

Just as with the DQN model, the training of the A2C model involved careful tuning of key parameters, including the number of hidden layers, the number of episodes, and the discount factor, as described in Section 3.6.1. Once the model was trained, its performance was rigorously validated through 10,000 simulations using randomly generated state samples.

As the number of warehouses increased, the complexity of the problem grew substantially, resulting in longer training times. It is important to note that the cumulative rewards reported for each problem size are not directly comparable across configurations, as each represents a distinct problem scale. Therefore, comparisons should focus primarily on training time and model behavior relative to the complexity of each scenario.

In the case of five warehouses, as displayed in **Figure 3.5**, the model achieved a mean cumulative reward of -102,615.28, with a 95% confidence interval ranging from -103,364.81 to -101,865.75. The observed rewards varied considerably, from a minimum of -293,681 to a maximum of -8,719. Training this configuration required 17,118.84 seconds for 400,000 iterations.

Expanding the system to fifteen warehouses, as shown in **Figure 3.6**, introduced additional complexity. However, the model remained stable, achieving a mean cumulative reward of -90,571.22. The 95% confidence interval ranged from -90,810.28 to -90,332.15, with individual rewards between -155,265 and -40,843. The total training time for this configuration was 18,574.73 seconds for 400,000 iterations.

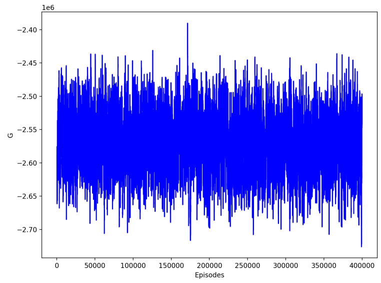

(a) Cumulative reward

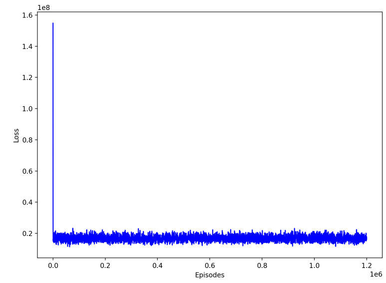

(b) Loss

Figure 3.4: Cumulative reward and loss of DQN with 30 warehouses

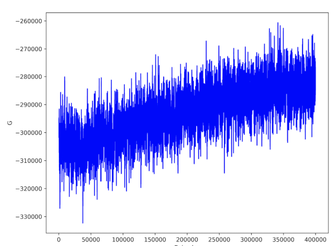

(a) Cumulative reward

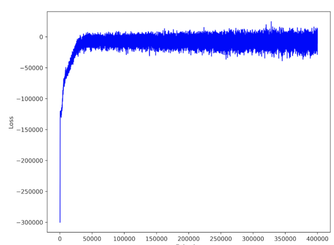

(b) Actor loss

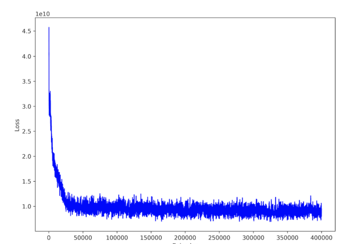

(c) Critic loss

Figure 3.5: Cumulative reward, actor loss, and critic loss of A2C with 5 warehouses

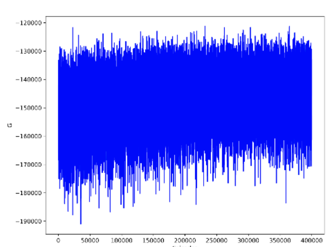

(a) Cumulative reward

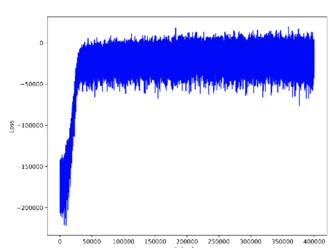

(b) Actor loss

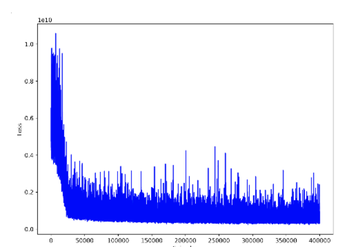

(c) Critic loss

Figure 3.6: Cumulative reward, actor loss, and critic loss of A2C with 15 warehouses

With thirty warehouses, as shown in **Figure 3.7**, the model faced increased computational challenges. However, it maintained stability while adapting to the added complexity.The mean cumulative reward decreased to -1,634,893.64, with a 95% confidence interval spanning from -1,640,042.53 to -1,629,744.75. Observed rewards ranged from a minimum of -2,846,788 to a maximum of -796,800. Training for this configuration required 23,779.39 seconds for 400,000 iterations.

The model training loss and G for the fifty-five warehouse scenario are presented in **Figure 3.8**. The model reported a mean cumulative reward of -18,503,265.14, with a 95% confidence interval between -18,588,898.70 and -18,417,631.58. The minimum and maximum observed rewards were -31,387,114 and -5,467,497, respectively. The training time for this configuration was increased to 38,796.85 seconds.

For the 104-warehouse configuration, the graphs of loss and G are shown in **Figure 3.9**. The model obtained a mean cumulative reward of -140,617,558.52, with a 95% confidence interval ranging from -141,221,452.98 to -140,013,664.07. The range of observed rewards extended from a minimum of -228,704,891 to a maximum of -48,810,617. Training this largest configuration required 66,668.23 seconds.

The results are analyzed and compared, as shown in **Table 3.14**, to evaluate the agent's ability to generalize its learned policy to unseen scenarios under different configurations and methodologies. The analysis focuses on the agent's effectiveness in reducing CDT (i.e., minimizing G) and the duration required for model training.

These findings highlight the impact of increasing system complexity on model performance in optimizing container flow across various warehouse configurations. A2C demonstrates stable convergence during training and performs well when evaluated on new simulation samples. In contrast, DQN struggles to adapt to our problem setting, even under the smallest configuration.

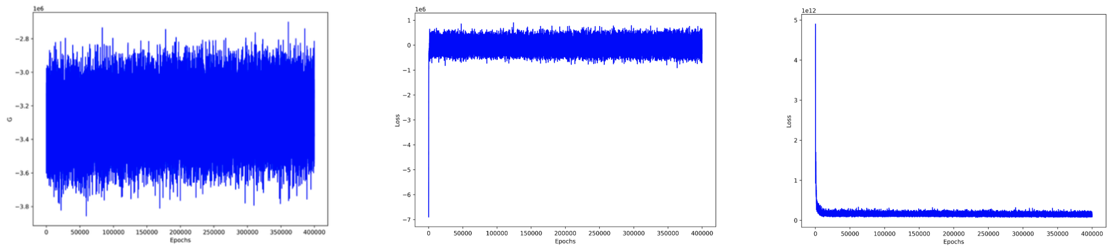

(a) Cumulative reward　**(b)** Actor loss　**(c)** Critic loss

Figure 3.7: Cumulative reward, actor loss, and critic loss of A2C with 30 warehouses

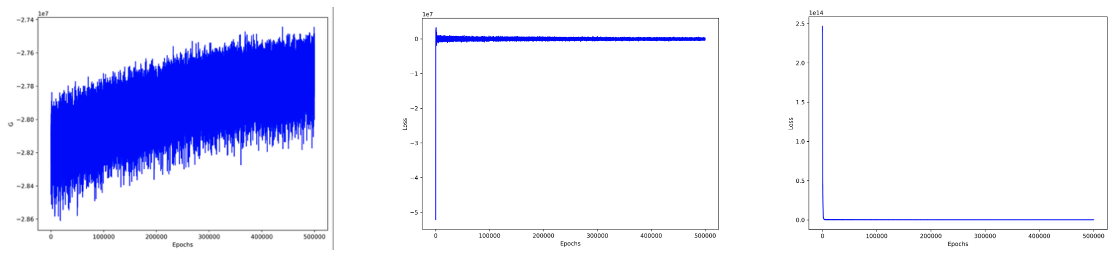

(a) Cumulative reward　**(b)** Actor loss　**(c)** Critic loss

Figure 3.8: Cumulative reward, actor loss, and critic loss of A2C with 55 warehouses

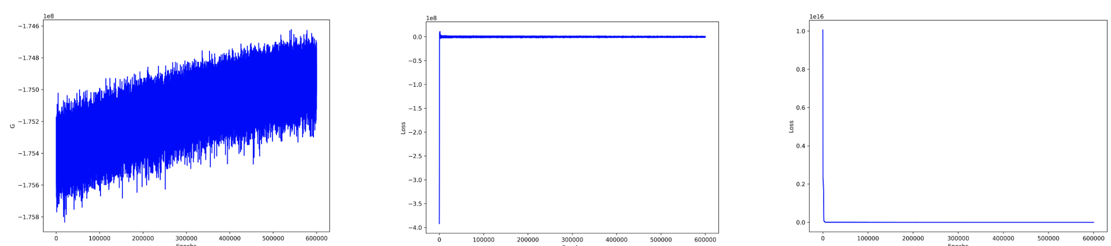

(a) Cumulative reward　**(b)** Actor loss　**(c)** Critic loss

Figure 3.9: Cumulative reward, actor loss, and critic loss of A2C with 104 warehouses

Table 3.14: Computational Results for Algorithms Across Warehouse Configurations with Uniform Epochs and Episodes per Configuration

Whs	Dimention (space)			Itr	G or CDT (hr.)			Traning time (s.)		
	S	A	$P(s' \mid s, a)$		DQN	A2C	Heuristic	DQN	A2C	Heuristic
5	11	6	726	400,000	1,897,867	102,615	244,235	10,483	17,119	-
15	31	16	15,376	400,000	193,562	90,571	180,025	14,837	18,575	-
30	61	31	115,351	400,000	4,224,507	1,634,893	3,102,145	372,853	23,780	-
55	111	56	689,976	500,000	-	18,503,265	30,150,849	-	38,797	-
104	209	105	4,586,505	600,000	-	140,617,559	227,747,345	-	66,668	-

3.7 Conclusion

This study investigates the operational dynamics of inbound container flow following a vessel's arrival at the port. The primary focus is on optimizing train dispatch from the port to warehouses on an hourly basis, taking into account warehouse capacity, existing inventory levels, and vessel arrivals at any given time. The objective is to develop an intelligent agent capable of determining the optimal warehouse allocation for each time period, ensuring that cargo from arriving vehicles is efficiently distributed to minimize container handling time.

To evaluate the effectiveness of different reinforcement learning approaches, we trained and validated models across five distinct warehouse configurations: 5, 15, 30, 55, and 104 warehouses. The results indicate that the A2C algorithm consistently performs well across all scenarios, whereas the DQN model exhibits strong performance only in the smallest configuration. This suggests that A2C is more robust and scalable in complex logistical environments.

Consequently, the A2C algorithm proves to be a viable solution for real-time decision-making in rail dispatch operations. By continuously receiving updates on inventory levels, the agent can dynamically adjust its decisions to accommodate fluctuations in demand and capacity. This adaptability demonstrates the algorithm's potential for practical implementation in large-scale logistics and supply chain management, enabling more efficient and responsive container transportation systems.

3.8 Research Plan

To maintain the simplicity of the model, we currently ignore lead time, including the travel time between the port and warehouses. However, incorporating a spatial assessment of warehouse locations would provide a more comprehensive understanding of how warehouse placement influences the agent's decision-making process.

In real-world logistics operations, train departures from the port are not solely dictated by inventory levels at the port and warehouses. Additional constraints, such as vehicle availability, waiting times, queue lengths, and the processing time required for loading and unloading containers, play significant roles in scheduling departures. At present, our model assumes that rail transport is always available to move inventory out of the port at each time epoch. A more realistic approach would involve considering the scheduled arrivals of trains at the port and integrating this aspect into the decision-making framework.

Additionally, we currently assume that each train serves only one warehouse per route and that the agent determines the action for a single train at each decision epoch. Increasing flexibility by allowing trains to stop at multiple warehouses per route and dispatching multiple trains from the port within each time period could enhance the model's realism. However, such modifications would significantly increase the model's complexity.

Each additional factor introduced into the model would necessitate the inclusion of corresponding variables in the state representation. Future extensions of this research will focus on systematically incorporating these complexities to enhance the model's realism and applicability to real-world freight transportation systems.

For the algorithm fine-tuning, a grid search approach, which is a machine learning technique that systematically evaluates every possible combination of hyperparameters, can be employed to identify the optimal set of parameters, ensuring that you explore all potential configurations. By doing so, it helps to determine which combination leads to the best performance, allowing the agent to converge to a more robust policy. This ensures that the agent converges effectively to a robust policy.

Bibliography

Adi, T. N., Bae, H., and Iskandar, Y. A. (2021). Interterminal truck routing optimization using cooperative multiagent deep reinforcement learning. *Processes*, 9(10):1728. 135

Agra, A., Christiansen, M., Delgado, A., and Hvattum, L. M. (2015). A maritime inventory routing problem with stochastic sailing and port times. *Computers & Operations Research*, 61:18–30. 134

Ahmad, R. W., Hasan, H., Jayaraman, R., Salah, K., and Omar, M. (2021). Blockchain applications and architectures for port operations and logistics management. *Research in Transportation Business & Management*, 41:100620. 134

Ai, T., Huang, L., Song, R., Huang, H., Jiao, F., and Ma, W. (2023). An improved deep reinforcement learning approach: A case study for optimisation of berth and yard scheduling for bulk cargo terminal. *Advances in Production Engineering & Management*, 18(3). 135

American Council for an Energy-Efficient Economy (2021). Maximizing truck load factor. Retrieved April 5, 2022. 184

American Trucking Associations (2022). Driver Shortage Update 2022. https://ata.msgfocus.com/files/amf_highroad_solution/project_2358/ATA_Driver_Shortage_Report_2022_Executive_Summary.October22.pdf, accessed 24th November 2023. 61

Association of American Railroads (2021). Railroad facts 2021. Retrieved May 2022. 13, 185, 187

Aulsebrook, A. E., Connelly, F., Johnsson, R. D., Jones, T. M., Mulder, R. A., Hall, M. L., Vyssotski, A. L., and Lesku, J. A. (2020). White and amber light at night disrupt sleep physiology in birds. *Current Biology*, 30(18):3657–3663. 49

Azimi, M., Fayek, E. K., Qi, Y., et al. (2021). Analysis of intermodal vessel-to-rail connectivity. Technical report, University of North Carolina at Charlotte. Center for Advanced Multimodal Mobility Solutions and Education. 81

Bhagavathula, R., Gibbons, R., and Kassing, A. (2021). Roadway lighting's effect on pedestrian safety at intersection and midblock crosswalks. Technical report, Illinois Center for Transportation. 49

Bhurtyal, S., Hernandez, S., Eksioglu, S., and Yves, M. (2024). A two-stage stochastic optimization model for port infrastructure planning. *Maritime Economics & Logistics*, 26(2):185–211. 134

Biggar, K. (2023). Dwell Time 'Back to Normal' at San Pedro Ports. `https://splash247.com/dwell-time-back-to-normal-at-san-pedro-ports/`, accessed 15th December 2023. 77

Blaze, J. (2020). Commentary: Do you want to build a freight railroad? Retrieved March 23, 2022. 16

BNSF (2024a). Intermodal rules and policies guide. Retrieved February 13, 2024. 78

BNSF (2024b). Three-pack and five-pack well cars. `https://www.bnsf.com/about-bnsf/virtual-train-tour/flatbed.html`, Retrieved November 9, 2024. 153

BNSF (2024c). Weekly surface transportation board update. Retrieved February 20, 2024. 78

Bohmhold, A. and Weiss, J. (2015). Smart roadside initiative macro benefit analysis user's guide for the benefit-cost analysis tool. Retrieved August 3, 2021. 7

Boyes, D. H., Evans, D. M., Fox, R., Parsons, M. S., and Pocock, M. J. (2021). Street lighting has detrimental impacts on local insect populations. *Science Advances*, 7(35):eabi8322. 49

Bureau of Transportation Statistics (2021a). Estimated u.s. average vehicle emissions rates per vehicle by vehicle type using gasoline and diesel. Retrieved July 15, 2022. 30, 31

Bureau of Transportation Statistics (2021b). Hazardous materials fatalities, injuries, accidents, and property damage data. Retrieved March 30, 2022. 33, 34, 182

Bureau of Transportation Statistics (2022a). Freight analysis framework. Retrieved May 14, 2022. 13, 26, 28, 34, 72, 85, 182

Bureau of Transportation Statistics (2022b). U.s. ton-miles of freight. Retrieved April 24, 2022. 13, 41, 182

Bureau of Transportation Statistics (2022c). U.s. vehicle-miles. Retrieved April 24, 2022. 26, 28

Bureau of Transportation Statistics (2024). 2024 port performance freight statistics program: Annual report to congress. 76

Cao, P., Zheng, Y., Yuen, K. F., and Ji, Y. (2023). Inter-terminal transportation for an offshore port integrating an inland container depot. *Transportation Research Part E: Logistics and Transportation Review*, 178:103282. 67

Carrington, D. (2020). Car tyres are major source of ocean microplastics – study. *Guardian News and Media*. 48

Chambers, M., Goworowska, J., Rick, C., Sedor, J., et al. (2015). Freight facts and figures 2015. 184

Chen, K., Lu, Q., Xin, X., Yang, Z., Zhu, L., and Xu, Q. (2022). Optimization of empty container allocation for inland freight stations considering stochastic demand. *Ocean & Coastal Management*, 230:106366. 67

Chen, R., Jia, S., and Meng, Q. (2023). Dynamic container drayage booking and routing decision support approach for e-commerce platforms. *Transportation Research Part E: Logistics and Transportation Review*, 177:103220. 134

Chesner, W., Collins, R., MacKay, M., and Emery, J. (2008). User guidelines for waste and byproduct materials in pavement construction. 53, 55

Costello, B. (2022). Economics and industry data. Accessed on May 29, 2023. 2

CSX (2023). Intermodal 101. `https://www.intermodal.com/index.cfm/resource-center/information-kits/intermodal-101-part-two-the-benefits-of-intermodal-rail-shipping/`, accessed 11th March 2024. 61

Dharmadhikari, N., Lee, E., and Kayabas, P. (2016). The lifecycle benefit–cost analysis for a rural bridge construction to support energy transportation. *Infrastructures*, 1(1):2. 7, 9

Evangeliou, N., Grythe, H., Klimont, Z., Heyes, C., Eckhardt, S., Lopez-Aparicio, S., and Stohl, A. (2020). Atmospheric transport is a major pathway of microplastics to remote regions. *Nature communications*, 11(1):3381. 47, 48

Fayek, E. K. (2021). Vessel-to-rail intermodal connectivity analysis for the port of houston. Master's thesis, Texas Southern University. 80, 81

Federal Aviation Administration (2021). Final eis document. Retrieved August 4, 2021. 49, 50

Federal Highway Administration (2000). Our nation's highways—2000. 12

Federal Highway Administration (2020). National highway construction cost index (nhcci) 2.0. Retrieved May 11, 2022. 14

Federal Railroad Administration (1990). Benefit-cost methodology for the local rail freight assistance program. Technical report, Federal Railroad Administration. 7

Federal Railroad Association (2016). Benefit-cost analysis guidance for rail projects. 7

Gallaway, T., Olsen, R. N., and Mitchell, D. M. (2010). The economics of global light pollution. *Ecological economics*, 69(3):658–665. 48

Gao, Y. and Sun, Z. (2023). Tramp ship routing and speed optimization with tidal berth time windows. *Transportation Research Part E: Logistics and Transportation Review*, 178:103268. 133

Goodchild, A., Wygonik, E., McMullen, B. S., and Holder, D. (2014). Multimodal freight project prioritization. Technical report, Oregon. Dept. of Transportation. Research Section. 6, 7

Gorman, M. F. (2008). Evaluating the public investment mix in us freight transportation infrastructure. *Transportation Research Part A: Policy and Practice*, 42(1):1–14. 41

Goßmann, I., Halbach, M., and Scholz-Böttcher, B. M. (2021). Car and truck tire wear particles in complex environmental samples–a quantitative comparison with "traditional" microplastic polymer mass loads. *Science of the total environment*, 773:145667. 48

Gren, M. and Jägerbrand, A. (2019). Calculating the costs of animal-vehicle accidents involving ungulate in sweden. *Transportation research part D: transport and environment*, 70:112–122. 52

Gresser, E. (May 22, 2024). Trade fact of the week: A new container ship launches every day. Retrieved November 9, 2024. 152

Gühnemann, A., Laird, J. J., and Pearman, A. D. (2012). Combining cost-benefit and multi-criteria analysis to prioritise a national road infrastructure programme. *Transport Policy*, 23:15–24. 7

Gumuskaya, V., van Jaarsveld, W., Dijkman, R., Grefen, P., and Veenstra, A. (2021). Integrating stochastic programs and decision trees in capacitated barge planning with uncertain container arrivals. *Transportation Research Part C: Emerging Technologies*, 132:103383. 134

Halim, R. A., Kwakkel, J. H., and Tavasszy, L. A. (2016). A strategic model of port-hinterland freight distribution networks. *Transportation Research Part E: Logistics and Transportation Review*, 95:368–384. 67

Harmon, T., Bahar, G. B., and Gross, F. B. (2018). Crash costs for highway safety analysis. Technical report, U.S. Federal Highway Administration. Office of Safety. 35, 39

Hasnat, M. M., Bardaka, E., Findley, D., and Goode, L. (2021). North carolina highway cost allocation and revenue attribution study. Technical report, North Carolina State University. Research and Development Unit. 12, 14, 21

Hecht, J. and Andrew, D. (1997). The environmental effects of freight. Technical report, Organization for Economic Co-operation and Development. 51, 54

Hooper, A. (2018). Cost of congestion to the trucking industry: 2018 update. 40, 41

Hu, Y. and Zhang, X. (2020). Analysis of the advantageous railway transportation distance compared with truck-only transportation. In *4th International Conference on Informatization in Education, Management and Business (IEMB 2020), Suzhou, China*. 81

IntelliTrans (2020). IntelliTrans Rail 101: Chapter 3. `https://blog.intellitrans.com/intellitrans-rail-101-chapter-3`, accessed 6th February 2024. 65

Interagency Working Group (2021). Technical support document: social cost of carbon, methane, and nitrous oxide interim estimates under executive order 13990. Technical report, Tech. rep., White House. 29

Jin, X., Duan, Z., Song, W., and Li, Q. (2023). Container stacking optimization based on deep reinforcement learning. *Engineering Applications of Artificial Intelligence*, 123:106508. 135

Jula, P. and Leachman, R. C. (2011). A supply-chain optimization model of the allocation of containerized imports from asia to the united states. *Transportation Research Part E: Logistics and Transportation Review*, 47(5):609–622. 66

Karakaya, E., Vinel, A., and Smith, A. E. (2021). Relocations in container depots for different handling equipment types: Markov models. *Computers & Industrial Engineering*, 157:107311. 135

Khattak, A. J., Noltenius, M. S., Cherry, C., Greene, D., Zhang, M., and Arvin, R. (2018). Green generates green. 7

Korytárová, J. and Papežíková, P. (2015). Assessment of large-scale projects based on cba. *Procedia Computer Science*, 64:736–743. 7, 9

Kruse, C. J., Farzaneh, R., Glover, B., Warner, J. E., Steadman, M., Jaikumar, R., and Lee, D. (2022). A modal comparison of domestic freight transportation effects on the general public: 2001–2019. 17, 30, 31, 39

Kuschel, G. (2022). Public health risks associated with transport emissions in nz. 33

LaRocco, L. A. (2023). West Coast port labor issues continue as some Los Angeles, Long Beach rail shipments get temporarily paused.

https://www.cnbc.com/2023/06/06/west-coast-port-labor-issues-continue-as-some-los-angeles-bound-rail-shipments-get-paused.html, accessed 7th February 2024. 62

Larson, W. (2015). *New estimates of value of land of the United States*. BEA. 11, 12

Lawson, J. (2007). The environmental footprint of surface freight transportation. *Transportation Research Board Special Report*, 291. 52

Lee, B. K., Lee, L. H., and Chew, E. P. (2014). Analysis on container port capacity: A markovian modeling approach. *OR spectrum*, 36:425–454. 135

Lee, J. (2015). Economic valuation of marine litter and microplastic pollution in the marine environment: An initial assessment of the case of the united kingdom. *SOAS-CeFiMS: London, UK*, pages 1–16. 48

Lee, M. and Jin, X. (2020). Incorporating reliability measures into the freight project prioritization decision support system. Technical report, Florida. Department of Transportation. 6, 7

Lee, Y., Yang, J., Lim, Y., and Kim, C. (2021). Economic damage cost of premature death due to fine particulate matter in seoul, korea. *Environmental Science and Pollution Research*, 28:51702–51713. 31

Leleur, S., Petersen, N. B., and Barfod, M. B. (2007). The cosima approach to transport decision making–combining cost-benefit and multi-criteria analysis for comprehensive project appraisal. *Improving Public Investment Management for Large-Scale Government Projects: Focusing on the Feasibility Studies–Lessons and Challenges*, pages 100–122. 8, 9

Leslie, A. and Murray, D. (2021). An analysis of the operational costs of trucking: 2021 update. 18, 26, 27

Link, H., Nash, C., Ricci, A., and Shires, J. (2016). A generalized approach for measuring the marginal social costs of road transport in europe. *International Journal of Sustainable Transportation*, 10(2):105–119. 3

Litman, T. (2020). Transportation cost and benefit analysis ii – noise costs. *Victoria Transport Policy Institute*. 51

Liu, X., Xu, J., Li, M., Wei, L., and Ru, H. (2019). General-logistic-based speed-density relationship model incorporating the effect of heavy vehicles. *Mathematical Problems in Engineering*, 2019. 184

Los Angeles Harbor Department (2023). Demurrage rates chart. Retrieved January 16, 2024. 77

Lv, Y., Zou, M., Li, J., and Liu, J. (2024). Dynamic berth allocation under uncertainties based on deep reinforcement learning towards resilient ports. *Ocean & Coastal Management*, 252:107113. 135

Macgregor, C. J., Evans, D. M., Fox, R., and Pocock, M. J. (2017). The dark side of street lighting: impacts on moths and evidence for the disruption of nocturnal pollen transport. *Global Change Biology*, 23(2):697–707. 49

Maricopa Association of Governments (2019). Adot roadway maintenance costs. 20

Mascoop, D. R. (2017). High-speed rail and local land development: case studies in london and las vegas. Master's thesis, Massachusetts Institute of Technology. 8

McKenzie, L. (2023). Understanding Port Operations And Logistics. `https://www.supplychainflow.com/port-operations-and-logistics/#mcetoc_1fe90qhhe1bq`, accessed 2th February 2024. 61

Mnih, V., Badia, A. P., Mirza, M., Graves, A., Lillicrap, T., Harley, T., Silver, D., and Kavukcuoglu, K. (2016). Asynchronous methods for deep reinforcement learning. In *International conference on machine learning*, pages 1928–1937. PmLR. 151

Mnih, V., Kavukcuoglu, K., Silver, D., Rusu, A. A., Veness, J., Bellemare, M. G., Graves, A., Riedmiller, M., Fidjeland, A. K., Ostrovski, G., et al. (2015). Human-level control through deep reinforcement learning. *nature*, 518(7540):529–533. 147

Molavi, A., Shi, J., Wu, Y., and Lim, G. J. (2020). Enabling smart ports through the integration of microgrids: A two-stage stochastic programming approach. *Applied Energy*, 258:114022. 134

Molnar, V., Fedorko, G., Honus, S., Girovska, L., and Lizbetin, J. (2018). Selection and allocation of a warehouse linked to reloading terminal and seaport. *NAŠE MORE: znanstveni časopis za more i pomorstvo*, 65(4 Special issue):169–173. 66

Musselman, J. A., West, R. C., and Director, P. (2020). Life cycle cost analysis–end of life considerations ncat report 20-05. 53

Narisada, K. and Schreuder, D. (2004). *Light pollution handbook*, volume 322. Springer Science & Business Media. 49

National Highway Traffic Safety Administration (2021). Traffic safety facts 2019: A compilation of motor vehicle crash data. *DOT HS*, 813141. 52

National Railroad Passenger Corporation (2016). National fact sheet fy 2016. Retrieved April 5, 2022. 41

National Railroad Passenger Corporation (2021). Amtrak host railroad report card 2020. Retrieved August 15, 2022. 41

Nolte, C. (2020). High-resolution land value maps reveal underestimation of conservation costs in the united states. *Proceedings of the National Academy of Sciences*, 117(47):29577–29583. 11

Osorio-Mora, A., Núñez-Cerda, F., Gatica, G., and Linfati, R. (2020). Multimodal capacitated hub location problems with multi-commodities: An application in freight transport. *Journal of Advanced Transportation*, 2020:1–9. 67

Peng, Y., Wang, W., Guo, Z., Song, X., and Zhang, Q. (2016). A stochastic seaport network retrofit management problem considering shipping routing design. *Ocean & Coastal Management*, 119:169–176. 134

POLA (2024). Facts and figures. `https://www.portoflosangeles.org/business/statistics/facts-and-figures`, accessed 1th February 2024. 61, 152

POLA (2025). Container vessel in port activity. `https://kentico.portoflosangeles.org/getmedia/d4f44790-0ed5-49c8-abfb-5c70386d7135/Port-of-Los-Angeles-Container-Vessel-Activity-Summary-2024`, accessed 18th February 2025. 152

Port Houston (2024a). Port houston finishes 2023 strong biggest december on record for loaded. Retrieved February 6, 2024. 80, 81

Port Houston (2024b). Port statistics. Retrieved February 5, 2024. 80

Port of Long Beach (2024). Port statistics - tonnage summary. Accessed on Jan 13, 2024. 74

Premack, R. (2022). Washington lawmakers still believe there's a truck driver shortage. Accessed on May 26, 2023. 4

Rahimi, M., Asef-Vaziri, A., Harrison, R., and Center, M. T. (2008). Integrating inland ports into the intermodal goods movement system for ports of los angeles and long beach. Technical report, METRANS Transportation Center (Calif.). 67

Rattanakunuprakarn, S., Jin, M., Sussman, M., and Felix, P. (2024). Comparative evaluation of highways and railroads using life-cycle benefit-cost analysis. *International Journal of Sustainable Transportation*. 74, 75, 80, 119, 153

Rezvani, A. Z., Peach, M., Thomas, A., Cruz, R., and Kemmsies, W. (2015). Benefit-cost methodology for highway-railway grade crossing safety protocols as applied to transportation infrastructure project prioritization processes. *Transportation Research Procedia*, 8:89–102. 8

Rida, M., Mouncif, H., and Boulmakoul, A. (2011). Application of markov decision processes for modeling and optimization of decision-making within a container port. In *Soft Computing in Industrial Applications*, pages 349–358, Berlin, Heidelberg. Springer Berlin Heidelberg. 135

Rodrigue, J.-P. (2020). Types of Intermodal Terminals. In *The Geography of Transport Systems (5th ed)*. Routledge. `https://transportgeography.org/contents/chapter6/function-of-transport-terminals/types-intermodal-terminals/`, accessed 7th February 2024. 65

Rodrigue, J.-P. (2024). Transportation Modes. In *The Geography of Transport Systems (6th ed)*. Routledge. 81

Rodrigue, J.-P., Notteboom, T., and Pallis, A. (2022). Chapter 3.4 – container terminal design and equipment. In *Port Economics, Management and Policy (1st ed)*. Routledge. `https://porteconomicsmanagement.org/pemp/contents/part3/container-terminal-design-equipment/`, accessed 5th February 2024. xi, 64, 65, 66

Rolf, B., Jackson, I., Müller, M., Lang, S., Reggelin, T., and Ivanov, D. (2023). A review on reinforcement learning algorithms and applications in supply chain management. *International Journal of Production Research*, 61(20):7151–7179. 135

Root, T. (2019). Tires: The plastic polluter you never thought about. *National Geographic*, 20. 47

RSI Logistics (2024). Comparing the costs of rail shipping vs truck. Retrieved May 25, 2024. 78

Sarmadi, K. (2021). *Robust optimisation of dry port network design in the container shipping industry under uncertainty*. PhD thesis, Newcastle University. 67

Seiler, A., Olsson, M., Rosell, C., and Van Der Grift, E. (2016). Saferoad safe roads for wildlife and people: Cost-benefit analyses for wildlife and traffic safety. Technical report, CEDR. 52

Shang, X., Yang, K., Jia, B., and Gao, Z. (2021). The stochastic multi-modal hub location problem with direct link strategy and multiple capacity levels for cargo delivery systems. *Transportmetrica A: Transport Science*, 17(4):380–410. 67

Shrestha, K. J., Uddin, M., and Adebiyi, J. (2021). Calculating road user cost for specific sections of highway for use in alternative contracting project. Technical report, Tennessee. Department of Transportation. 16, 35

Siciliano, G., Barontini, F., Islam, D. M. Z., Zunder, T. H., Mahler, S., and Grossoni, I. (2016). Adapted cost-benefit analysis methodology for innovative railway services. *European transport research review*, 8:1–14. 8, 36, 42, 50, 52

Silva, E., Marco, A., da Graça, J., Pérez, H., Abella, E., Patino-Martinez, J., Martins, S., and Almeida, C. (2017). Light pollution affects nesting behavior of loggerhead turtles and predation risk of nests and hatchlings. *Journal of Photochemistry and Photobiology B: Biology*, 173:240–249. 49

Solomon, T. and Singer, N. (2021). Freight activity in the u.s expected to grow fifty percent by 2050. Accessed on May 29, 2023. 4

Song, S. (2017). Transport emissions & social cost assessment: Methodology guide. 31, 33

Spasovic, L., Zhang, W., Besenski, D., and Pathak, C. (2018). Modeling the impacts of changes in freight demand, infrastructure improvements and policy measures on a metropolitan region. Technical report, Rutgers University. Center for Advanced Infrastructure and Transportation. 8

Sullivan, D. E. (2006). Materials in use in us interstate highways. 23

Surface Transportation Board (2022). Annual report financial data 2020. Retrieved May 13, 2022. 19, 22, 24, 27, 28, 79, 188

Svechkina, A., Portnov, B. A., and Trop, T. (2020). The impact of artificial light at night on human and ecosystem health: a systematic literature review. *Landscape Ecology*, 35:1725–1742. 49

The Maritime Executive (Aug 19, 2021). Yantian reports new teu record, while no updates from ningbo. Retrieved November 9, 2024. 152

Tolliver, D. D. and Lindamood, B. A. (1993). Chaffee junction to chaffee benefit cost analysis. 8

Tomljenovic, V., Merzifonluoglu, Y., and Spigler, G. (2024). Optimizing inland container shipping through reinforcement learning. *Annals of Operations Research*, 339(1):1025–1050. 136

Transportation for America (2019). Repair priorities. 23

Trumbull, N. and Bae, C. (2000). Transportation and water pollution. Retrieved , 2022. 56

Union Pacific Railroad (2024a). Accessorial charges. Retrieved January 28, 2024. 80, 113

Union Pacific Railroad (2024b). Chargeable events system (ces). Retrieved January 28, 2024. 80, 113

U.S. Bureau of Economic Analysis (2023). Gross domestic product by state and personal income by state, 3rd quarter 2023. Retrieved March 11, 2024. ix, 72, 73, 87

U.S. Bureau of Economic Analysis (2024). Gross domestic product by state and personal income by state, 2nd quarter 2024. Retrieved October 31, 2024. 87

U.S. Department of Transportation (2016). The value of travel time savings: Departmental guidance for conducting economic evaluations revision 2. 41

U.S. Energy Information Administration (2022). Gasoline and diesel fuel update. petroleum & other liquids. Retrieved May 13, 2022. 17

U.S. Environmental Protection Agency (2018). 2018 smartway logistics company partner tool: Technical documentation u.s. version 2.0.17. Technical report, U.S. Environmental Protection Agency. Retrieved April 24, 2022. 31

U.S. Environmental Protection Agency (2021). Emission factors for greenhouse gas inventories. 29

USDOT (2022). Benefit-cost analysis guidance for discretionary grant programs. Retrieved April 19, 2022. 10, 12, 23, 31, 38, 50

van Twiller, J., Adulyasak, Y., Delage, E., Grbic, D., and Jensen, R. M. (2025). Navigating demand uncertainty in container shipping: Deep reinforcement learning for enabling adaptive and feasible master stowage planning. *arXiv preprint arXiv:2502.12756*. 136

Vanek, F. (2019). Mode and commodity perspectives on us freight energy consumption and co2 emissions: Insights and directions for improvement. *International Journal of Sustainable Transportation*, 13(10):741–760. 58

Walls, J. and Smith, M. R. (2018). Life-cycle cost analysis in pavement design — interim technical bulletin. Technical report, Federal Highway Administration. 22, 23

Walther, C., Monse, J., and Haßheider, H. (2015). Revision of project evaluation as part of the german federal transport infrastructure plan. *Transportation Research Procedia*, 8:41–49. 8

Warehouse and Fulfillment (2024). Warehousing services costs, pricing, rates and fees. Retrieved March 8, 2024. 78

Western Overseas Corporation (2022). Weekly Vessels Anchored and at Terminals as of 1/21/2022. `https://www.westernoverseas.com/port-congestion-update-1-21-22/`, accessed 8th February 2024. 61

WSDOT (2002). Highway construction cost comparison survey: Final report. Technical report, Washington State Department of Transportation. 14

Xu, X., Huang, X., and Wang, L. (2024). Empty container repositioning problem using a reinforcement learning framework with multi-weight adaptive reward function. *Maritime Policy & Management*, 51(8):1742–1763. 136

Yan, Q., Song, R., Kim, K.-H., Wang, Y., and Feng, X. (2024). Optimizing container relocation operations by using deep reinforcement learning. *Maritime Policy & Management*, pages 1–23. 136

Yan, Y., Chow, A. H., Ho, C. P., Kuo, Y.-H., Wu, Q., and Ying, C. (2022). Reinforcement learning for logistics and supply chain management: Methodologies, state of the art, and future opportunities. *Transportation Research Part E: Logistics and Transportation Review*, 162:102712. 135

Zhang, D., Chen, F., and Mei, Z. (2023). Optimization on joint scheduling of yard allocation and transfer manpower assignment for automobile ro-ro terminal. *Transportation Research Part E: Logistics and Transportation Review*, 177:103256. 133

Zhang, H., Yang, K., Gao, Y., and Yang, L. (2022). Accelerating benders decomposition for stochastic incomplete multimodal hub location problem in many-to-many transportation and distribution systems. *International Journal of Production Economics*, 248:108493. 68

Appendix

A Appendix for Chapter 1: Freight Volume Calculation under Actual and Maximum Flows

In the United States, two primary sources of transportation data are the Bureau of Transportation Statistics (Bureau of Transportation Statistics, 2021b, 2022b) and the Freight Analysis Framework 4 (Bureau of Transportation Statistics, 2022a). These datasets were employed to convert the total values of specified metrics into dollars per ton-mile units. The numerical values in **Tables 15** and **16** pertain to the actual transportation scenario. Data for highways were gathered for the years 2016, 2018, 2019, and 2020, while railroad data is specifically from the year 2020. Both modes encompass metrics such as annual ton-miles, tons hauled, and vehicle miles.

In addition to acquiring historical freight traffic volumes, we have calculated average and maximum annual ton-miles for both highways and railroads using theoretical models. **Table 17** presents the parameters for both scenarios. In the maximum scenario, we assume that highways remain consistently busy 24 hours a day, with a load factor of 80%. The actual truckload is determined by multiplying the truckload by the load factor.

We utilize the following equation to calculate the average volume of trucks traversing a randomly selected point within the U.S. highway network throughout the year, commonly known as the average flow:

Table 15: Actual U.S. highway volumes by years.

Year	Freight Ton-Miles	Tons Hauled	Vehicle Miles
2016	2,060,780,000,000	11,595,143,427	287,895,000,000*
2018	2,033,921,000,000	11,920,161,455	304,864,000,000
2019	2,070,450,924,800	- *	300,051,000,000
2020	2,233,588,364,732	12,417,522,921	302,141,000,000

Note: * indicates that the data is not applied to the calculation.

Table 16: Actual U.S. railroad volumes in 2020.

Railroads	Freight Ton-Miles	Tons Hauled	Train Miles
Class I	1,439,814,000,000	1,389,076,087 *	381,000,000
BNSF	588,919,405,000	511,801,000	144,392,892*

Note: * indicates that the data is not applied to the calculation.

Table 17: Estimated highway freight operations.

Parameter	Average	Maximum	Parameter	Average	Maximum
Density	8.33	8.33	Truckload	25	25
Speed (mph)	55	55	Load factor	33.90%	80.00%
Operating hours	10	24	Actual load	8.475	20
Operating days	365	365			

$$\text{Hourly flow (vehicles/ hr)} = \text{density (vehicles/ mile)} \times \text{speed (mph)}$$

According to Table 4-2 in Freight Facts and Figures 2015, the average truck speed on interstates can be approximated at 55 mph (Chambers et al., 2015). Additionally, research conducted by Liu et al. (2019) on the speed-density relationship provides valuable insights. Under free-flow conditions, when the speed is 90 km/hour (approximately 56 mph), the density is estimated to be around 15 vehicles/km. Converting this to miles, the density is approximately 25 vehicles/mile. It is important to note that these vehicles refer to passenger cars, so a conversion is needed to obtain truck flow. Typically, one truck is equivalent to the traffic impact of three passenger cars. Therefore, at the speed of 55 mph, we derived the density of 8.33 trucks/ mile. Consequently, the average annual highway truck flow can be estimated as follows:

$$\begin{aligned}\text{Flow (vehicles/ year)} =& 8.33\text{(trucks/ mile)} \times 55\text{(mph)} \times 10\text{(working hr)} \times \\ & 365\text{(days/year)} \\ =& 1,672,917\text{(trucks/ year at a random location)}\end{aligned}$$

To calculate annual freight ton-miles from the estimated truck flow, we multiply the number of trucks per year by the length of the National Highway system, which is 161,188 miles. We also take into account a practical load of 8.475 tons. This figure is calculated based on the maximum load of 25 tons, adjusted for an average load factor of 57%. It also considers empty movements, which constitute approximately 20-35% of truck miles (American Council for an Energy-Efficient Economy, 2021). To put it simply, the actual load is approximately 33.90% of the maximum truckload. Consequently, we can determine the theoretically estimated annual average highway freight ton-miles as follows:

$$
\begin{aligned}
\text{Annual average highway ton-miles} =& 8.33(\text{trucks/ mile}) \times 55(\text{mph})\times \\
& 10(\text{working hr}) \times 365(\text{days/year})\times \\
& 161,188(\text{miles}) \times 8.475(\text{tons}) \\
=& 2,285,318,426,887(\text{ton-miles})
\end{aligned}
$$

When comparing this theoretical estimation with the actual ton-miles of 2,233,588,364,732 in 2020, the estimated ton-miles value is only 2.32% higher than the actual data. This slight difference falls within an acceptable range, validating our calculation procedure. If we assume that trucks consistently flow along the U.S. highways 24 hours a day with a higher load factor of 80%, we can calculate the estimated annual maximum highway ton-miles as follows:

$$
\begin{aligned}
\text{Annual maximum highway ton-miles} =& 8.33(\text{trucks/ mile}) \times 55(\text{mph})\times \\
& 24(\text{working hr}) \times 365(\text{days/year})\times \\
& 161,188(\text{miles}) \times 20(\text{tons}) \\
=& 12,943,396,400,000(\text{ton-miles})
\end{aligned}
$$

Similarly, we have estimated the average and maximum railroad ton-miles per year using the parameters listed in **Table 18**. According to the Railroad Facts 2021 published by the Association of American Railroads (Association of American Railroads, 2021), the average cargo weight per carload in 2020 was estimated to be 52.9 tons. For Class I railroads, the average number of cars per freight train was reported as 77.1 cars in the same year (Association of American Railroads, 2021). By multiplying these figures, we can calculate the cargo per trainload, which amounted to 4,079 tons. Note that these carload and trainload values already account for empty

Table 18: Estimated railroad freight operations.

Parameter	Avg	Max	Parameter	Avg	Max
Tons per Carload	52.9	110	Daily Trains	12	50
Cars per Train	77.1	130	Class I Miles	92,190	
Tons per Train	4,079	14,300	BNSF Miles	22,384	

freight cars. In terms of the daily train frequency at a randomly selected point within the U.S. railroad network, our estimates are grounded in consultations with experts in the field. We have considered an average of 12 trains per day, with a maximum limit set at 50 trains daily. The total U.S. miles of railroad is 136,729 miles for the freight rail network, including Class I, Regional, and Local railroads, with Class I railroads owning 92,190 miles of this network (Association of American Railroads, 2021). These miles of road represent the length of railways within the United States and exclude the extension of the Canadian Railroad. Additionally, "miles of road" refers to the total length of the railway system and does not specify the total length of tracks, as a unit of road may consist of multiple tracks. Yard tracks and sidings are also excluded from this number.

Assuming year-round operations for Class I railroads, we can estimate an annual flow of 4,380 trains at a random location. This calculation is derived by multiplying the daily rate of 12 trains by the total number of days in a year, resulting in 4,380 trains annually. When this figure is multiplied by the extent of Class I railroad road ownership, which spans 92,190 miles, the result is 403,792,200 train-miles per year. Then, we multiply the annual train-miles by the average load per train, set at 4,079 tons. The product of this calculation yields a total of 1,646,902,828,998 ton-miles of annual rail freight. The detailed calculation is as follows:

$$\begin{aligned}\text{Annual average Class I ton-miles} =& 4,380(\text{trains/ year}) \times 92,190(\text{miles}) \times \\ & 4,079(\text{tons/ train}) \\ =& 1,646,902,828,998(\text{ton-miles})\end{aligned}$$

When comparing this theoretically estimated annual freight ton-miles with the actual ton-miles from FAF in 2020, we observed that the estimated ton-miles are 14.38% higher than the actual data, which falls within an acceptable range. To derive the estimation for the maximum potential ton-miles, two assumptions were made.

Firstly, we assumed that the average cargo weight per carload is 110 tons. Secondly, we assumed that the average number of cars per freight train is 130. Multiplying these values, we calculated an average cargo load per train of 14,300 tons. Assuming that BNSF operates 365 days a year with 50 trains per day at a random location, the total number of trains per year would be 18,250. Based on these considerations, we computed the theoretically estimated annual maximum railroad ton-miles as follows:

$$\begin{aligned}\text{Annual maximum Class I} =& 18,250(\text{trains/ year}) \times 92,190(\text{miles}) \times \\ & 14,300(\text{tons/ train}) \\ =& 24,059,285,250,000(\text{ton-miles})\end{aligned}$$

By comparing the theoretically estimated annual freight ton-miles to the actual ton-miles in 2020, we observed a slight variance of only 1.85%, indicating the precision and dependability of our estimation. Since comprehensive expense data for Class I railroads is not publicly available, we have chosen to use BNSF as a representative for estimating certain costs and benefits. To calculate both the average and maximum flow of BNSF, we utilized the company's mileage data, which indicates that BNSF owns and operates a total of 22,384 miles of main track (Surface Transportation Board, 2022). This figure excludes yard tracks, sidings, and the Canadian Railroad extension. Assuming continuous operation throughout the year, we estimated the annual flow of BNSF at a random location by multiplying the average of 18 trains per day by 365, resulting in an estimated 6,570 trains per year at a random location. For the cargo load per train, we used the previously mentioned average trainload for Class I railroads, which stands at 4,079 tons. By multiplying these figures, we arrived at the following detailed calculation:

$$\begin{aligned}\text{Annual average BNSF ton-miles} =& 6,570(\text{trains/ year}) \times 22,384(\text{miles}) \times \\ & 4,079(\text{tons/ train}) \\ =& 599,809,191,739(\text{ton-miles})\end{aligned}$$

To estimate the maximum flow in ton-miles for BNSF, we will apply the same conditions used for Class I railroads, involving an average cargo weight per carload of 110 tons and an average number of cars per freight train of 130. When we multiply these values, we arrive at an average cargo load per train of 14,300 tons. Assuming BNSF's continuous operation 365 days a year with 50 trains per day at a random location, the total number of trains per year will amount to 18,250. Based on these parameters, we calculated the theoretically estimated annual maximum railroad ton-miles as follows:

$$\begin{aligned}\text{Maximum BNSF ton-miles} =& 18,250(\text{trains/ year}) \times 22,384(\text{miles}) \times \\ & 14,300(\text{tons/ train}) \\ =& 5,841,664,400,000(\text{ton-miles})\end{aligned}$$

B Appendix for Chapter 2: Demand Destribution by States

Table 19: Destinations with Alpha Values for Different Years

Destination	2025			2026		
	$\alpha_{\pm 5\%}$	$\alpha_{\pm 7\%}$	$\alpha_{\pm 10\%}$	$\alpha_{\pm 5\%}$	$\alpha_{\pm 7\%}$	$\alpha_{\pm 10\%}$
Alabama	0.010720288	0.011129384	0.010207793	0.011094614	0.010493225	0.01214487
Arizona	0.017819939	0.019125479	0.020470876	0.019638899	0.01865329	0.017809181
Arkansas	0.006189136	0.00663927	0.006353698	0.006804073	0.00648836	0.006396931
California	0.146344091	0.143140807	0.153175743	0.146426299	0.152999602	0.134711599
Colorado	0.019464065	0.017937529	0.019096243	0.019228382	0.018950887	0.018297543
Connecticut	0.013028624	0.013063648	0.011710318	0.013291928	0.012152574	0.014144976
Delaware	0.00360552	0.003672858	0.003680787	0.003718388	0.003588203	0.003652891
Washington DC	0.006785255	0.006248699	0.006802495	0.007062404	0.006838819	0.00692184
Florida	0.05536557	0.057842331	0.057004106	0.056764618	0.059335506	0.060038639
Georgia	0.030206882	0.030396187	0.027984504	0.02903794	0.028499125	0.028830329
Idaho	0.004381733	0.004352139	0.004250323	0.004512649	0.004461347	0.004278316
Illinois	0.038762863	0.03788606	0.043577607	0.040534197	0.039998225	0.040819013
Indiana	0.017472706	0.019558191	0.020037114	0.019060989	0.017576434	0.017888783
Iowa	0.009117714	0.008878673	0.009676723	0.009304176	0.008514456	0.01039726
Kansas	0.007802963	0.007703779	0.00774953	0.007959622	0.007945245	0.008730226
Kentucky	0.01041212	0.010161271	0.010742757	0.009995257	0.010551973	0.010210918
Louisiana	0.010927611	0.010595497	0.009754717	0.011419319	0.011111949	0.011256472
Maine	0.003441226	0.003298951	0.003378233	0.003731674	0.00316764	0.003522803
Maryland	0.019681926	0.02039831	0.020632652	0.018482942	0.019175582	0.020187376
Massachusetts	0.028642019	0.027762904	0.027293519	0.02730907	0.029494533	0.029777083
Michigan	0.023933002	0.023336128	0.026623667	0.02422434	0.023952557	0.024175236
Minnesota	0.017110799	0.017045901	0.019129243	0.017611312	0.0170172	0.01850639
Mississippi	0.00507601	0.005635239	0.004730804	0.005618966	0.005248519	0.005565159
Missouri	0.015536337	0.016165454	0.015663913	0.015852798	0.016022131	0.017345121
Montana	0.002410547	0.002377501	0.002725044	0.002829674	0.002321227	0.00298985
Nebraska	0.006138987	0.00637921	0.006018203	0.006499836	0.006538404	0.006473317
Nevada	0.008372686	0.008196912	0.007990349	0.008507464	0.009083403	0.008883323
New Hampshire	0.003990878	0.004388169	0.004382887	0.00433327	0.004190498	0.004570894
New Jersey	0.03047003	0.029288741	0.030013663	0.031593393	0.029267245	0.030465209
New Mexico	0.00475031	0.004678791	0.004749308	0.004749366	0.004751894	0.004940121
New York	0.084483819	0.085573072	0.074209956	0.077813167	0.08386425	0.075578394
North Carolina	0.028585403	0.029580557	0.028854961	0.028980985	0.027784884	0.02890954
North Dakota	0.002634821	0.002744098	0.002548912	0.002678911	0.002367041	0.002862374
Ohio	0.030310635	0.030849202	0.033376135	0.031637598	0.033027725	0.029375882
Oklahoma	0.009207648	0.008731516	0.009387755	0.00913269	0.009136587	0.008665641
Oregon	0.011892048	0.011113122	0.010791735	0.012598074	0.011220002	0.012570571
Pennsylvania	0.035779646	0.033971186	0.03841093	0.036182604	0.03781053	0.035274309
Rhode Island	0.002800511	0.002985349	0.003006053	0.003149202	0.002628649	0.003182663
South Carolina	0.011368607	0.012324087	0.011022716	0.012111246	0.011305156	0.012201814
South Dakota	0.002473677	0.002645471	0.002700947	0.002698666	0.002511025	0.00298121
Tennessee	0.019389982	0.018240366	0.020604522	0.020129403	0.019889757	0.019836321
Texas	0.09216888	0.094244446	0.081763136	0.087534524	0.084840561	0.094141319
Utah	0.009864573	0.010059652	0.009821062	0.010413355	0.010185753	0.009324546
Vermont	0.001636652	0.00170817	0.001492623	0.001915696	0.001507201	0.001874896
Virginia	0.027398136	0.028130475	0.024671393	0.025816584	0.025014006	0.027273148
Washington	0.030559659	0.028148462	0.032417124	0.029310759	0.027623471	0.029081014
West Virginia	0.003624227	0.003727635	0.003376417	0.003801889	0.003247394	0.003701175
Wisconsin	0.016031542	0.016136014	0.014226041	0.015003803	0.016070319	0.017173924
Wyoming	0.001827698	0.001803107	0.001710758	0.001892985	0.001575635	0.002059589

Table 19 Continued

Destination	2027			2028		
	$\alpha_{\pm 5\%}$	$\alpha_{\pm 7\%}$	$\alpha_{\pm 10\%}$	$\alpha_{\pm 5\%}$	$\alpha_{\pm 7\%}$	$\alpha_{\pm 10\%}$
Alabama	0.011610783	0.010681248	0.010108472	0.011393522	0.011661204	0.010298798
Arizona	0.01845344	0.018630213	0.01903606	0.019460701	0.019207045	0.0200681
Arkansas	0.006779741	0.006499745	0.006343446	0.006459486	0.006847602	0.006261507
California	0.141844612	0.147735097	0.132548941	0.139452578	0.145566261	0.150439875
Colorado	0.019351518	0.019172192	0.021164895	0.020238407	0.018605041	0.01887616
Connecticut	0.012897518	0.013663193	0.013243942	0.012754112	0.013838915	0.013520577
Delaware	0.003727674	0.0034413	0.003816923	0.003559163	0.00373665	0.003510008
Washington DC	0.007012717	0.006750684	0.006180628	0.006573182	0.007485583	0.006445056
Florida	0.057389657	0.057680732	0.050779632	0.058122804	0.053161358	0.05605583
Georgia	0.029472487	0.03100426	0.031957307	0.030992212	0.03010984	0.028727045
Idaho	0.004572967	0.004254672	0.004079123	0.004476623	0.004575067	0.004496625
Illinois	0.039567291	0.039823688	0.043308014	0.039792411	0.041336225	0.040880597
Indiana	0.01849961	0.017720929	0.01698651	0.017824235	0.017708148	0.018068224
Iowa	0.009208839	0.009069803	0.008883786	0.008944814	0.009878989	0.009398384
Kansas	0.008539107	0.008460791	0.007854529	0.008356013	0.008405905	0.008201237
Kentucky	0.01053794	0.009983617	0.010480389	0.009801175	0.010269661	0.01003548
Louisiana	0.010932076	0.010061169	0.011164567	0.010333765	0.010526743	0.010738404
Maine	0.003544977	0.00349927	0.003788134	0.003480918	0.003969153	0.003109621
Maryland	0.020126544	0.01783607	0.020000821	0.01927343	0.020378244	0.020603887
Massachusetts	0.028904861	0.028774456	0.029904878	0.026731228	0.028755946	0.028136892
Michigan	0.026093093	0.024470774	0.024560362	0.025764996	0.025957934	0.025596952
Minnesota	0.017981505	0.017616564	0.017998803	0.017560076	0.017967718	0.017327363
Mississippi	0.005279548	0.00555105	0.005039109	0.005336139	0.005846142	0.00564263
Missouri	0.016020592	0.01667926	0.016212539	0.015469458	0.016342981	0.016382366
Montana	0.002685323	0.002607719	0.002562775	0.002708515	0.002866586	0.002443303
Nebraska	0.006443823	0.006138883	0.006621834	0.006554259	0.006815616	0.005609698
Nevada	0.009105775	0.008398462	0.008983543	0.0091727	0.009112064	0.0079978
New Hampshire	0.004520713	0.00425595	0.004424721	0.004462518	0.004800924	0.004232256
New Jersey	0.031006499	0.031769484	0.029098291	0.029042394	0.029399611	0.030953365
New Mexico	0.004896046	0.004620541	0.004990716	0.004622268	0.004805793	0.004092742
New York	0.079391116	0.07700991	0.089069262	0.083975846	0.077326074	0.086230978
North Carolina	0.028537809	0.030121674	0.029602498	0.027781117	0.030156775	0.029818133
North Dakota	0.00265957	0.002625333	0.002786849	0.002742093	0.002840344	0.002658993
Ohio	0.032001661	0.029862225	0.031977643	0.033284355	0.031706079	0.029547522
Oklahoma	0.008941547	0.009113103	0.008730101	0.00920579	0.009747544	0.009176794
Oregon	0.01226629	0.011940447	0.011167768	0.012259272	0.011845218	0.010780899
Pennsylvania	0.037487282	0.035602707	0.033193951	0.035009648	0.03556246	0.03370835
Rhode Island	0.003001937	0.003065878	0.003077852	0.002990952	0.003278724	0.002680199
South Carolina	0.011957365	0.0121327	0.011499227	0.011289746	0.011800547	0.010883117
South Dakota	0.002725065	0.002777258	0.002812392	0.002739509	0.003126393	0.002659484
Tennessee	0.019452144	0.018360728	0.019478577	0.019360076	0.02054059	0.017247692
Texas	0.085620297	0.092443216	0.096631077	0.091870184	0.082992742	0.088494914
Utah	0.010413022	0.009905804	0.009259304	0.010467567	0.010764862	0.008936401
Vermont	0.001840456	0.00173794	0.001648972	0.001788019	0.002030148	0.001582603
Virginia	0.026006525	0.026170262	0.028528132	0.025579737	0.0263533	0.025471785
Washington	0.029438595	0.029750297	0.02828579	0.029532496	0.02858711	0.032282669
West Virginia	0.003759265	0.003413078	0.003339636	0.003818238	0.004029417	0.003402213
Wisconsin	0.015573759	0.01528535	0.014835462	0.015674636	0.01524522	0.014756307
Wyoming	0.001919022	0.001830275	0.001951822	0.001916619	0.002127508	0.001530165

Table 19 Continued

Destination	2029			2030		
	$\alpha_{\pm 5\%}$	$\alpha_{\pm 7\%}$	$\alpha_{\pm 10\%}$	$\alpha_{\pm 5\%}$	$\alpha_{\pm 7\%}$	$\alpha_{\pm 10\%}$
Alabama	0.010821367	0.010886699	0.010999068	0.011547423	0.010006583	0.011792784
Arizona	0.01907693	0.019806512	0.018256931	0.019010802	0.017692477	0.019077461
Arkansas	0.006066203	0.006186897	0.006049203	0.006696522	0.005909825	0.006198252
California	0.145940761	0.145947147	0.15370858	0.147086779	0.151523415	0.139297677
Colorado	0.018717021	0.01942628	0.020016789	0.020042177	0.020038863	0.02079896
Connecticut	0.012263944	0.013642011	0.012366926	0.012507427	0.012311575	0.012458115
Delaware	0.003213336	0.003580802	0.003733996	0.003506638	0.003393326	0.003589721
Washington DC	0.006876737	0.006902839	0.007355946	0.006999531	0.006200078	0.007542103
Florida	0.058731394	0.05669092	0.057717442	0.054839601	0.058444366	0.057586176
Georgia	0.031544274	0.028579407	0.032528238	0.031571176	0.032061485	0.028618348
Idaho	0.004343349	0.004394192	0.004048993	0.004464283	0.003916142	0.00412393
Illinois	0.040634329	0.040786716	0.036773359	0.039986128	0.040954653	0.043958299
Indiana	0.017552868	0.017394584	0.017244545	0.01888182	0.018658928	0.01883952
Iowa	0.008600435	0.008679782	0.009168977	0.009216396	0.008847291	0.008909441
Kansas	0.007790476	0.007733139	0.008707462	0.008632203	0.007801191	0.007921403
Kentucky	0.010389651	0.010592238	0.011028358	0.010357464	0.010321505	0.009848912
Louisiana	0.010600536	0.010667546	0.011685156	0.01079485	0.01088773	0.010738666
Maine	0.003389793	0.00326816	0.003386186	0.003561902	0.002957327	0.003669142
Maryland	0.019381075	0.01856315	0.018881994	0.019859377	0.019053446	0.019944248
Massachusetts	0.026719526	0.028935732	0.025268757	0.027183771	0.029585352	0.026032643
Michigan	0.024982052	0.024710887	0.024675491	0.024628201	0.025212514	0.023835165
Minnesota	0.01666045	0.018089969	0.016687309	0.017261873	0.017696772	0.019167752
Mississippi	0.005406856	0.005006119	0.005441979	0.005196501	0.004967171	0.005632272
Missouri	0.015203572	0.015418096	0.016582072	0.015923087	0.015520188	0.01697458
Montana	0.002448786	0.002521455	0.00262557	0.002760154	0.002210864	0.002592514
Nebraska	0.006357396	0.006117585	0.006182624	0.006525202	0.006454126	0.006116712
Nevada	0.008808283	0.009202588	0.008335745	0.009198261	0.008810896	0.009233039
New Hampshire	0.004052973	0.004496572	0.003882819	0.00451752	0.003955428	0.004047314
New Jersey	0.028658352	0.029765774	0.028168585	0.028658767	0.029942714	0.030195217
New Mexico	0.004621221	0.005040106	0.004680506	0.004876213	0.004170921	0.004914655
New York	0.0843107	0.081858869	0.074711702	0.083196228	0.084843409	0.078417217
North Carolina	0.029092148	0.028935365	0.030130264	0.028827146	0.026050742	0.026851174
North Dakota	0.002426353	0.002695065	0.002486962	0.002748476	0.002414217	0.002604549
Ohio	0.03180829	0.03262904	0.033375491	0.032395577	0.03172177	0.033104185
Oklahoma	0.008856039	0.008637102	0.009005176	0.008939396	0.00854319	0.009114021
Oregon	0.011742356	0.011871235	0.012731961	0.011458934	0.01182383	0.010904603
Pennsylvania	0.036699454	0.03531927	0.038398844	0.034687437	0.03362289	0.038890069
Rhode Island	0.002695866	0.002831032	0.002994702	0.00314282	0.002758326	0.003189319
South Carolina	0.010973888	0.01162409	0.011406981	0.011659682	0.011932212	0.012469782
South Dakota	0.002405779	0.002598745	0.002674047	0.002745811	0.002401562	0.003017098
Tennessee	0.019695778	0.019353714	0.018759592	0.019983813	0.019767605	0.018870602
Texas	0.09074749	0.091343815	0.090292796	0.086221977	0.091161869	0.090765255
Utah	0.010173524	0.009388185	0.009244685	0.009889778	0.009038486	0.009223753
Vermont	0.001518065	0.001585804	0.001712035	0.001748753	0.001501934	0.002042706
Virginia	0.027022313	0.027414327	0.024260349	0.025986692	0.024667442	0.025584708
Washington	0.029001808	0.028651215	0.030174586	0.029566696	0.027699981	0.028427939
West Virginia	0.003346812	0.003665177	0.003693736	0.003584047	0.003556892	0.003592595
Wisconsin	0.01604397	0.01466274	0.016009405	0.014965265	0.015538347	0.017098493
Wyoming	0.001585424	0.001901307	0.001747081	0.001959425	0.001448147	0.002176909

Table 19 Continued

Destination	2031			2032		
	$\alpha_{\pm 5\%}$	$\alpha_{\pm 7\%}$	$\alpha_{\pm 10\%}$	$\alpha_{\pm 5\%}$	$\alpha_{\pm 7\%}$	$\alpha_{\pm 10\%}$
Alabama	0.011336265	0.010101338	0.011168456	0.01049591	0.011214932	0.011303692
Arizona	0.018362464	0.017357294	0.018695468	0.01842191	0.018869592	0.017418293
Arkansas	0.006459386	0.006055179	0.00648536	0.00645228	0.006288297	0.006254425
California	0.141663494	0.155780997	0.132479832	0.141281986	0.136458807	0.139391668
Colorado	0.01993088	0.018098789	0.02018299	0.020033397	0.020072623	0.021576623
Connecticut	0.012696423	0.012789788	0.013798136	0.013053777	0.013654671	0.014051462
Delaware	0.003623176	0.003054598	0.003940814	0.003606517	0.003791196	0.00387481
Washington DC	0.006897841	0.006059142	0.007846379	0.006429477	0.006782567	0.007150669
Florida	0.058816446	0.058968993	0.052307613	0.058389575	0.058446622	0.051641177
Georgia	0.030375572	0.032170861	0.03268505	0.031496648	0.031225087	0.029433368
Idaho	0.00449977	0.004146272	0.004870027	0.004414493	0.004169918	0.005074723
Illinois	0.0410077	0.039896499	0.036645666	0.039003995	0.041596957	0.043839379
Indiana	0.018373118	0.019079554	0.017758247	0.018137412	0.017589991	0.020395292
Iowa	0.008872429	0.009103254	0.009810529	0.009202903	0.009778917	0.009596805
Kansas	0.008149072	0.007706845	0.009209316	0.00843868	0.008350771	0.009000291
Kentucky	0.010251818	0.00989832	0.010946079	0.009650262	0.0107555	0.010972438
Louisiana	0.010790237	0.009892462	0.012150032	0.010732745	0.011437925	0.010530429
Maine	0.003543276	0.003263296	0.003983222	0.003326783	0.003625016	0.003822249
Maryland	0.019634809	0.017968536	0.021144561	0.018365706	0.018937298	0.019194902
Massachusetts	0.028172506	0.029074034	0.029528307	0.028752345	0.026633567	0.028475901
Michigan	0.023965131	0.024383992	0.025724039	0.026068126	0.023427977	0.0268407
Minnesota	0.018243801	0.016385736	0.017814895	0.018329243	0.018697458	0.017290852
Mississippi	0.005460412	0.005243878	0.005565536	0.005144386	0.005139939	0.006288424
Missouri	0.015146619	0.014373693	0.016324537	0.014994973	0.015539496	0.016484457
Montana	0.002577961	0.002418774	0.00304379	0.002463542	0.002494256	0.002922188
Nebraska	0.006788251	0.005802176	0.00734015	0.006572228	0.006566723	0.006268143
Nevada	0.009226176	0.008008682	0.009482155	0.00867011	0.00866229	0.009161992
New Hampshire	0.00438575	0.003716079	0.00512366	0.004396087	0.004513392	0.004382989
New Jersey	0.030762467	0.031513229	0.03021108	0.030613269	0.030136572	0.027629793
New Mexico	0.004744043	0.004577562	0.004945558	0.004612456	0.004748864	0.005103217
New York	0.083669234	0.082908827	0.080226245	0.084474926	0.083255019	0.081831099
North Carolina	0.027322225	0.027896236	0.029753007	0.02720461	0.027711345	0.028861865
North Dakota	0.002816643	0.002273483	0.003371018	0.002691731	0.002641975	0.003135356
Ohio	0.031520966	0.032536024	0.032111612	0.032322611	0.031973336	0.02923851
Oklahoma	0.00882686	0.008862367	0.009281356	0.008710829	0.008605557	0.010246957
Oregon	0.011972582	0.011783641	0.011354545	0.011530452	0.011460748	0.012813673
Pennsylvania	0.034529587	0.034461219	0.035883955	0.03597265	0.034298335	0.037134155
Rhode Island	0.003070137	0.00266785	0.003656882	0.003095427	0.002820733	0.003248504
South Carolina	0.012211675	0.011962371	0.012015118	0.01194851	0.012134565	0.011007941
South Dakota	0.002669658	0.002257827	0.003049301	0.002618193	0.002755968	0.002947673
Tennessee	0.019093732	0.017922489	0.021363715	0.019194397	0.019309321	0.019300767
Texas	0.090202135	0.088871974	0.082763375	0.089668689	0.091800412	0.084434964
Utah	0.009894235	0.009520996	0.009627133	0.009636923	0.009706839	0.010154701
Vermont	0.001808532	0.001522113	0.002390056	0.001722218	0.001731024	0.002006398
Virginia	0.025678529	0.027295303	0.028591394	0.025615646	0.027506862	0.028300853
Washington	0.028367931	0.029996764	0.032381712	0.030438276	0.031267533	0.027336514
West Virginia	0.003752399	0.003183482	0.003823744	0.003698205	0.003458886	0.003811398
Wisconsin	0.015987882	0.015758313	0.014685237	0.016146231	0.016193525	0.016424511
Wyoming	0.001847763	0.001428867	0.002459108	0.001758255	0.001760797	0.002392807

Table 19 Continued

Destination	2033			2034		
	$\alpha_{\pm 5\%}$	$\alpha_{\pm 7\%}$	$\alpha_{\pm 10\%}$	$\alpha_{\pm 5\%}$	$\alpha_{\pm 7\%}$	$\alpha_{\pm 10\%}$
Alabama	0.010987924	0.011378923	0.012238698	0.010811307	0.010775663	0.011260861
Arizona	0.017759991	0.017857676	0.018512602	0.018992889	0.019697915	0.018060734
Arkansas	0.006044288	0.006599139	0.007140776	0.006425064	0.006936774	0.006213903
California	0.148067263	0.141262617	0.14186949	0.145899865	0.141334031	0.159090909
Colorado	0.018911738	0.020038193	0.019676015	0.01869929	0.018823038	0.017487171
Connecticut	0.012420051	0.013455083	0.012876883	0.013383239	0.012824284	0.013521423
Delaware	0.003455882	0.003713635	0.003589808	0.003800936	0.003951562	0.004006962
Washington DC	0.00666379	0.007414293	0.006405944	0.006689167	0.00722649	0.006598926
Florida	0.058754669	0.055402029	0.053287268	0.059038726	0.057666303	0.054126777
Georgia	0.029444725	0.030347842	0.032004003	0.029192623	0.030056081	0.02786676
Idaho	0.004139376	0.004506192	0.004206512	0.004552144	0.004425292	0.004308944
Illinois	0.039078788	0.040473999	0.037903729	0.040845555	0.038072908	0.0372526
Indiana	0.017687194	0.018831362	0.017464355	0.018242566	0.01996271	0.016908006
Iowa	0.008889929	0.009841736	0.01026533	0.008942841	0.009803589	0.0100471
Kansas	0.008329758	0.00790568	0.00828247	0.008412631	0.008307813	0.007867901
Kentucky	0.010007305	0.0103757	0.00962448	0.010198988	0.010125828	0.010646679
Louisiana	0.010349203	0.010408738	0.011914033	0.011289197	0.010960397	0.010119293
Maine	0.003185251	0.003560313	0.004046683	0.003427029	0.00398929	0.003372847
Maryland	0.019784015	0.018430054	0.017805052	0.018756997	0.018596596	0.018831092
Massachusetts	0.026799028	0.029109644	0.030525989	0.027918872	0.029404174	0.027731801
Michigan	0.025833914	0.025992949	0.023448597	0.025008924	0.025939789	0.023649739
Minnesota	0.016914901	0.017255761	0.016752784	0.017243959	0.017187215	0.018452166
Mississippi	0.005402073	0.005834177	0.005576854	0.005526265	0.005563181	0.005520166
Missouri	0.016028723	0.015237535	0.016548759	0.015345936	0.014936124	0.014325644
Montana	0.002538253	0.002886642	0.00289855	0.002694908	0.003045247	0.00287544
Nebraska	0.006626671	0.006871162	0.006557768	0.006545243	0.006961553	0.006720454
Nevada	0.008654506	0.00918566	0.008853294	0.009223547	0.009317553	0.008170956
New Hampshire	0.00399519	0.004707159	0.004496062	0.004383122	0.004857616	0.004211157
New Jersey	0.030647925	0.030349693	0.027685528	0.031356735	0.028630415	0.031064485
New Mexico	0.004597864	0.005189989	0.004688215	0.004900378	0.005027632	0.00508136
New York	0.080728021	0.08621343	0.084037993	0.080004424	0.07627488	0.077273486
North Carolina	0.029284076	0.028405751	0.026263434	0.029005977	0.026846996	0.029576041
North Dakota	0.002490682	0.002735239	0.002716651	0.002583891	0.002788951	0.002756491
Ohio	0.032842598	0.030622975	0.033763882	0.031804779	0.030248813	0.030122172
Oklahoma	0.008546536	0.009125916	0.009881593	0.009363533	0.009550971	0.00890448
Oregon	0.011645548	0.011663034	0.01270751	0.011358741	0.012157594	0.011418294
Pennsylvania	0.033963303	0.033608834	0.038192777	0.03488337	0.033608965	0.035917367
Rhode Island	0.002878686	0.003205471	0.003135505	0.003090468	0.003276884	0.003123641
South Carolina	0.012095329	0.012557877	0.01169989	0.011908042	0.011378964	0.010763222
South Dakota	0.002634917	0.00274726	0.002761523	0.002816665	0.003031715	0.002794376
Tennessee	0.018291929	0.019867392	0.019109554	0.019984917	0.020604412	0.018081194
Texas	0.092869107	0.083194461	0.089609042	0.087535878	0.091079185	0.096983409
Utah	0.010154319	0.010127712	0.009468499	0.009546128	0.010978919	0.009730234
Vermont	0.00158479	0.001880857	0.001985779	0.001692508	0.002097608	0.001873889
Virginia	0.02758107	0.028525181	0.025218891	0.026101904	0.028703096	0.025658693
Washington	0.029613876	0.029350903	0.030171625	0.029696718	0.029806948	0.028075888
West Virginia	0.003574636	0.003784668	0.004124373	0.003696798	0.004128005	0.003683401
Wisconsin	0.015550302	0.015846692	0.015977002	0.015288155	0.016785606	0.01577344
Wyoming	0.00167009	0.002112774	0.002027943	0.00188816	0.002244423	0.002098026

Vita

Sarita Rattanakunuprakarn was born and raised in Nakhon Pathom, Thailand. She grew up in a supportive family where education was always encouraged. She completed her Bachelor of Engineering in Industrial Engineering-Logistics at Kasetsart University. Her undergraduate years were filled with energy, friendships, and vibrant activity—an enriching time marked not only by fun, but by deep learning about others, herself, academic life, and how to embrace each moment with joy.

She was lucky to have an advisor, Miss Parinya Pattanawasanporn, who believed in her and encouraged her to apply for scholarships, which eventually gave her the opportunity to continue her studies in the United States. She moved to Orlando to pursue her Master of Science in Industrial Engineering at the University of Central Florida. Adjusting to a new country was not always easy, but having Dr. Ahmad Elshennawy as her advisor made the environment feel a lot more welcoming.

Later, she began her Ph.D. in Industrial Engineering at the University of Tennessee, Knoxville. This became the most challenging and stressful part of her academic life. She had the opportunity to work on several research projects with different people, which helped her grow both professionally and personally. Through all the challenges and fears, she learned to persevere and gradually developed the confidence and responsibility of someone ready to take on greater challenges.

As she writes this, she will soon return to Thailand to begin a new chapter as a lecturer at Burapha University. It is hard to put into words everything this journey has meant, but it has been full of moments that she will always carry with her.